

AFFIDAVIT

I declare that I have authored this thesis independently, that I have not used other than the declared sources/resources, and that I have explicitly indicated all material which has been quoted either literally or by content from the sources used. The text document uploaded to TUGRAZonline is identical to the present doctoral thesis.

Date

Signature

ACKNOWLEDGEMENTS

The process of earning a Ph.D. and writing a dissertation is long and sometimes arduous – and is certainly not done singlehandedly. Here, I would like to honor all people involved.

First and foremost, I would like to express my sincere thanks to my supervisor Univ.-Prof. Gabriele Berg for her constant confidence in me and my work. Without her expertise, help, advice and encouragement, the accomplishment of this thesis would not have been possible.

Special thanks go to my project leader Dr. Tomislav Cernava for his unfailing support throughout the last two years of my thesis; his guidance and feedback were essential to keep up my spirit and his innovative and out-of-the-box thinking mind was a driving force for the success of the project.

I thank Dr. Armin Erlacher for introducing me to the exciting world of microalgae and for encouraging me to advance my scientific career by doing a Ph.D. His visions led to the realization of this project and he deserves credit for its success.

I would like to express my gratitude to Barbara Fetz, whose training and teaching since the very first day in the lab laid the foundation for the success of my practical work.

I would also like to thank Univ.-Prof. Kai-Uwe Fröhlich for being part of my thesis committee and for succeeding to the task of examining my thesis.

Doing a Ph.D. shaped me professionally and personally. At the very beginning of my project I was lucky enough to meet who has become one of my very best friends, Birgit – and therefore I will be forever grateful. With all my heart I thank her for walking this journey with me side by side. Without her, I would not be who I am today.

My deepest thanks to my boyfriend, for never failing to cheer me up in frustrating moments, for always putting up with me when things didn't go as planned and for always believing in me.

Von ganzem Herzen möchte ich mich auch bei meiner Familie bedanken. Besonders meine Eltern haben mich in jeder Lebenssituation unterstützt, mir ihr Vertrauen geschenkt und mich stets ermutigt nicht aufzugeben. Danke Mama für die unzähligen Telefongespräche, in denen ich dir mein Herz ausschütten durfte. Danke Papa für die vielen Bergtouren auf denen ich dich begleiten durfte und aus denen ich immer wieder sehr viel Kraft schöpfen konnte.

My deepest thanks to BioFerm GmbH and BDI-BioLifeScience GmbH for enabling the project and for providing the necessary resources.

I especially want to honor Dr. Christina Donat and Dipl.-Ing. Christina Morauf (BioFerm); their expertise concerning methylobacteria and fascination about microalgae is highly appreciated and was essential for the accomplishment of this thesis. Special thanks also to Corinna Jäger, M.Sc. and Dr. Peter Pucher (BDI) for sharing their expertise from an industrial point of view.

This work has been supported by the Federal Ministry for Digitization and Business Location (BMDW), the Federal Ministry for Transport, Innovation and Technology (BMVIT), the Styrian Business Promotion Agency SFG, the Standortagentur Tirol, Government of Lower Austria and ZIT - Technology Agency of the City of Vienna through the COMET-Funding Program managed by the Austrian Research Promotion Agency FFG. The funding agencies had no influence on the conduct of this research.

ABSTRACT

Microalgae are a diverse group of single-celled organisms exhibiting versatile features including rapid growth, high lipid content and the accumulation of various highly valuable compounds. Due to their eclectic characteristics, they find broad application in industry, e.g. as source material for biofuel production, as animal feed, as pharmaceuticals or as sustainable alternative to synthetic fertilizers. In large-scale microalgae production systems, sterile operation is neither economically nor practically feasible; microorganisms generally spread in these cultivation processes and affect the biotechnological processes in various ways and possibly decrease productivity. On the contrary, a healthy co-occurring microbiome has considerable potential to provide stability, reproducibility and controllability of microalgae cultivation systems. However, current mass-cultivation technologies have failed to reach economic competitiveness in terms of biomass yields, contamination prevention and costs involved. To address all these challenges a polyphasic approach was conducted aiming to i) extend our knowledge concerning algae-bacteria co-evolution by investigating natural co-occurrences of algae, bacteria and fungi and thus harness the native algae microbiome for successful algal biotechnology, ii) to evaluate the potential of plant growth-promoting methylobacteria to promote microalgae growth and thereby improve biomass yields, and iii) to find a sustainable, nature-based alternative for bioreactor decontaminations in order to avoid the extensive use of hazardous detergents.

The microbiome is a crucial part of the native algal holobiont and is essential for modulating algal populations. In order to decipher evolutionary evolved co-occurrences, microalgae and their naturally associated microbiota were investigated. Seasonally occurring snowfields were studied by 16S and 18S rRNA gene amplicon sequencing, where distinct correlation patterns of microalgae and associated bacteria and basidiomycetous yeasts were discovered. Bacterial isolates were further screened for their growth-promoting potential on the industrially relevant microalgae *C. vulgaris*, resulting in the identification of nine promising strains, producing phytohormones, siderophores and N-acylhomoserine lactone. Moreover, in natural biofilms, microalgae have been found co-occurring with plant growth-promoting methylobacteria; therefore, their potential to enhance microalgae growth and thus improve biomass yields was evaluated. The growth of two industrially relevant microalgae could be significantly increased when co-cultured with methylobacteria up to 14-fold. The results suggest species-specific symbiotic algae-bacteria interactions, where physical proximity is essential for

a successful metabolite exchange. Complementary genome analyses indicate, that the growth-promoting effects are conceivably attributed to the production of vitamins, phytohormones and siderophores.

Additionally, the potential of natural compounds to replace hazardous chemicals for bioreactor decontaminations was evaluated. By applying the antimicrobial 5-isobutyl-2,3-dimethylpyrazine on three different microalgal genera, the algicidal effect of this naturally occurring volatile organic compound was demonstrated. Direct application of the decontaminant as well as passive treatment led to a significant reduction of viable cell count for all the investigated microalgal genera.

The undertaken polyphasic approach substantiates the tremendous potential of natural resources for sustainable algal biotechnology in various areas. The understanding of evolutionary evolved microbiome-algae associations and the identification of putative beneficiary constituents give rise to new co-inoculation strategies for microalgae cultivation systems; moreover, natural compounds harbor potential to replace conventional, ecologically harmful detergents and thus contribute to a sustainable algal biotechnology.

ZUSAMMENFASSUNG

Mikroalgen sind einzellige Organismen mit vielseitigen Eigenschaften wie schnelles Wachstum, hoher Lipidgehalt und die Akkumulierung wertvoller Substanzen. Deshalb finden sie Anwendung in der Industrie als Ausgangsmaterial für die Herstellung von Biokraftstoffen, als Tierfutter, Arzneimittel oder als Alternative zu synthetischen Düngemitteln. In Mikroalgenproduktionssystemen ist ein steriler Betrieb weder wirtschaftlich noch praktisch durchführbar; Mikroorganismen breiten sich in den Kulturen aus und beeinflussen die biotechnologischen Prozesse auf unterschiedliche Weise und können im schlimmsten Fall zu einem Zusammenbruch der Kultur führen. Ein gesundes Mikrobiom hingegen hat großes Potential Stabilität, Reproduzierbarkeit und Kontrollierbarkeit von Algenkulturen zu gewährleisten. Niedrige Erträge, Kontaminationen und hohe Produktionskosten stellen für Algenzüchter nach wie vor eine große Herausforderung dar. Ein vielschichtiger Ansatz zielte darauf ab, i) das Wissen über die Koevolution von Algen, Bakterien und Pilzen zu erweitern, um das native Algenmikrobiom biotechnologisch nutzen zu können, ii) das Potential pflanzenwachstumsfördernder Methylobakterien zur Förderung des Wachstums von Mikroalgen zu evaluieren um eine erhöhte Biomasseausbeute zu erreichen und iii) eine naturbasierte Alternative für die Dekontamination von Bioreaktoren zu finden, um den Einsatz von umweltschädlichen Reinigungsmitteln zu vermeiden.

Das Mikrobiom ist ein entscheidender Bestandteil des Holobionts Alge und ist für die Modulation von Algenpopulationen unerlässlich. Um das Wissen über Algen-Mikrobiom-Wechselwirkungen und Koevolution auszuweiten, wurden natürliche Assoziationen von Algen, Bakterien und Pilzen auf saisonal auftretenden Schneefeldern untersucht. Mittels 16S und 18S rRNA Genamplikonsequenzierung wurden eindeutige Korrelationsmuster von auftretende Mikroalgen, Bakterien und Basidiomyceten aufgezeigt. Bakterienisolate wurden anschließend durch Co-Kultivierungsexperimente auf ihr Potenzial hin untersucht, das Wachstum der industriell relevanten Mikroalge *C. vulgaris* zu fördern; dies führte zur Identifizierung von neun vielversprechenden Stämmen, die Phytohormone, Siderophore und N-Acylhomoserinlacton produzieren können.

Um Algenkultivierung wirtschaftlicher zu machen, wurde das Potenzial von pflanzenwachstumsfördernden Methylobakterien zur Steigerung des Mikroalgenwachstums evaluiert. Durch Co-Kultivierung konnte die Biomasseausbeute zwei industriell relevanter Mikroalgen um das bis zu 14-fache erhöht werden, wobei eine Spezies-spezifische, symbiotische Beziehung zwischen Algen und

Bakterien vermutet wird; essentiell für einen erfolgreichen Metabolitenaustausch ist dabei die räumliche Nähe beider Partner. Genomanalysen deuten darauf hin, dass die wachstumsfördernde Wirkung auf die Produktion von Vitaminen, Phytohormonen und Siderophoren zurückzuführen ist.

Darüber hinaus wurde das Potential von Naturstoffen als Reinigungsmittel für Bioreaktoren untersucht. Durch Anwendung der antimikrobiellen Substanz 5-Isobutyl-2,3-dimethylpyrazin auf drei verschiedene Mikroalgen wurde die algizide Wirkung dieser natürlich vorkommenden flüchtigen organischen Verbindung auf *Chlorella*, *Scenedesmus* und *Haematococcus* nachgewiesen. Die direkte Anwendung, sowie eine passive Behandlung führten bei allen untersuchten Mikroalgen zu einer signifikanten Verringerung der Lebendzellzahl.

Diese vielschichtigen Untersuchungsarbeiten untermauern das enorme Potential natürlicher Ressourcen für eine nachhaltige Algenbiotechnologie in verschiedenen Bereichen. Das Verständnis evolutionär entwickelter Mikrobiom-Algen-Assoziationen und die Identifizierung von kultivierbaren Algen-Symbionten führen zu neuen Co-Inokulationsstrategien für die Algenbiotechnologie. Darüber hinaus haben Naturstoffe großes Potential umweltschädliche Reinigungsmittel zu ersetzen und so zu einer nachhaltigen Algenbiotechnologie beizutragen.

LIST OF CONTENT

| | |
|---|------------|
| ACKNOWLEDGEMENTS | i |
| ABSTRACT | iii |
| ZUSAMMENFASSUNG | v |
| LIST OF CONTENT | vii |
| HARNESSING NATURE FOR SUSTAINABLE ALGAL BIOTECHNOLOGY | 1 |
| Background | 1 |
| Objectives | 5 |
| CHAPTER 1 | |
| THE MICROBIOME OF ALPINE SNOW ALGAE SHOWS A SPECIFIC INTER-KINGDOM CONNECTIVITY AND ALGAE-BACTERIA INTERACTIONS WITH SUPPORTIVE CAPACITIES | 9 |
| Abstract | 9 |
| Introduction | 11 |
| Material and Methods | 13 |
| Results | 19 |
| Discussion | 28 |
| Supplementary Material | 33 |
| CHAPTER 2 | |
| PLANT GROWTH-PROMOTING METHYLOBACTERIA INCREASE THE BIOMASS OF BIOTECHNOLOGICALLY RELEVANT MICROALGAE | 39 |
| Abstract | 39 |
| Introduction | 41 |
| Materials and Methods | 43 |
| Results | 48 |
| Discussion | 54 |
| Supplementary Material | 57 |

LIST OF CONTENT

| | |
|--|------------|
| CHAPTER 3 | |
| A NOVEL, NATURE-BASED ALTERNATIVE FOR PHOTOBIOREACTOR DECONTAMINATIONS | 63 |
| Abstract | 63 |
| Introduction..... | 65 |
| Materials and Methods..... | 67 |
| Results | 70 |
| Discussion..... | 76 |
| Supplementary Material | 79 |
| ADDITIONAL PUBLICATION 1 | |
| THE TEA LEAF MICROBIOME SHOWS SPECIFIC RESPONSES TO CHEMICAL PESTICIDES AND BIOCONTROL APPLICATIONS | 83 |
| ADDITIONAL PUBLICATION 2 | |
| <i>NICOTIANA TABACUM</i> SEED ENDOPHYTES SHARE A COMMON CORE STRUCTURE AND GENOTYPE-SPECIFIC SIGNATURES IN DIVERGING CULTIVARS FROM ASIA AND THE AMERICAS | 85 |
| REFERENCES | 87 |
| CURRICULUM VITAE | 101 |

HARNESSING NATURE FOR SUSTAINABLE ALGAL BIOTECHNOLOGY

Background

In the last decades, the extensive application potential of microalgae in several sectors of industry has been increasingly realized. Microalgae are a versatile group of single-celled, photosynthetic organisms exhibiting a variety of features including high lipid and protein content and the ability to accumulate highly valuable compounds. Therefore they find application as feedstock for biofuels, as animal feed, as bioremediators and as source material for carotenoids and antioxidants (Gupta *et al.*, 2019; Mata *et al.*, 2010; Pulz and Gross, 2004; Wijffels and Barbosa, 2010).

While the production of microalgae for bulk production is usually based on open pond systems, the production of highly valuable compounds for the food and pharmaceutical industry takes place in closed photobioreactors. While open pond systems allow easy handling and cleaning, their limitations include little control over contaminations, dependency on sunlight, evaporation losses and the requirement of large land areas (Ugwu *et al.*, 2008). Although closed photobioreactors allow better controllability of culture condition including e.g. pH-value, temperature, CO₂ availability and light intensity, their construction requires sophisticated materials and thereby increases production and maintenance expenses. Current microalgal mass-cultivation technologies – independent from cultivation strategy – have failed to reach economic competitiveness in terms of contamination prevention, biomass yields and costs involved. One of the major constraints for successful algae mass-cultivations are biological pollutants, such as weedy microalgae competing for light, nutrients and space, parasitic fungi and bacteria, zooplankton grazers and protists preying on algae (Bínová *et al.*, 1998; Borowitzka, 2013; Letcher *et al.*, 2013; Wang *et al.*, 2016b). Fulbright and colleagues investigated the co-occurring bacterial community over the scale-up process of an industrial algae cultivation system and could reveal major shifts in the microbial community composition, whereas hardly any links between the abundant microbiome and cultivation success rate could be made (Fulbright *et al.*, 2018). Several bacterial and fungal enzymes such as glucosidases, chitinases or cellulases have been described to be involved in the lysis of algal cells, and thus impede satisfactory yields (Afi *et al.*, 1996; Arora *et al.*, 2012; Nikolaeva *et al.*, 1999). Additionally, the competition for available nutrients by bacteria, fungi or weedy algae also hamper growth rates of the desired microalgae, which after several generations might even lead to outcompetition (Cole, 1982; Kazamia *et al.*, 2012a). All those findings reinforce the need to understand algae-bacteria interactions in order to identify and minimize

detrimental bacteria; unpredictable, co-occurring microbial communities affect stability, reproducibility and controllability of microalgae cultivation systems. Those unwanted co-occurring microorganisms are not only responsible for dramatic decreases in biomass yields, but can lead to a complete collapse of the culture, forcing the growers to an early harvest of the product and a subsequent costly decontamination procedures of the photobioreactors (Ma *et al.*, 2017). *In situ* steam-sterilization fails due to the fact, that cultivation takes place in semi-closed photobioreactors, leaving the application of chemicals and detergents as only option. Those cleaning procedures commonly include rinsing the reactors with sodium hypochlorite or the application of hydrogen peroxide, both unstable, highly reactive chemicals, negatively affecting the process environment and hazardous not only for humans but also the environment (Johnston *et al.*, 2005; Klapes and Vesley, 1990).

Not only contaminating microorganisms and associated costs hinder algae-derived biofuels and bioproducts from being sustainable and economically viable competitors to non-sustainable alternatives, but also slow growth rates and consequently insufficient and uneconomical yields. A variety of abiotic parameters have a great influence and impact on the overall yield of biomass and metabolites; light, temperature, pH-value, mixing and the availability of nutrients are major factors to consider when culturing microalgae. For maintaining a healthy algae culture a range of micro- and macronutrients is essential. Nutrient deficiency greatly affects growth rates as well as the synthesis and accumulation of carbohydrates, carotenoids and lipids in microalgae (Khan *et al.*, 2018). Besides those inorganic nutrients more than half of 306 otherwise autotrophic algal species surveyed, required an external supply of vitamin B₁₂, indicating the widespread vitamin auxotrophy within the algal kingdom (Croft *et al.*, 2005). In natural ecosystems algae and bacteria support each through mutualistic relationships, where the bacteria provide the essential micro- and macronutrients and the algae in return release dissolved organic matter, allowing heterotrophic bacteria to co-exist in their surroundings. Croft and colleagues, for example, demonstrated that the essential vitamins required by the algae are acquired through a symbiotic relationship with bacteria (Croft *et al.*, 2005). Kazamia and co-workers showed similar interactions, when the vitamin B₁₂-dependent microalga *Lobomonas rostrata* was able to grow in a vitamin depleted medium when co-cultured with *Rhizobium* (Kazamia *et al.*, 2012b). Amin and colleagues describe a “carbon for iron mutualism” where algae assimilate iron complexed in bacterial siderophores and in return provided the for the bacteria essential dissolved organic carbon (Amin *et al.*, 2009, 2012a, 2015). Moreover, the nitrogen (N) released by bacteria as an integrative part of siderophores, provides requisite nitrogen that is essential for growth and replication in microalgae (Villa *et al.*, 2014). In aquatic environments N is one of the major limiting nutrients. Although elemental nitrogen is abundant, most algae are not able to assimilate N in its unmineralized form and are therefore dependent on nitrogen-fixing microorganisms to transform inaccessible N

sources into forms usable for algae. In this context, Calatrava and co-workers could show a mutualistic relationship between *Chlamydomonas reinhardtii* and methylobacteria; the bacteria facilitate algae growth by mineralizing certain amino acids and thereby produce ammonium assimilable by *Chlamydomonas* (Calatrava *et al.*, 2018). Additionally, the growth of the microalgae *C. vulgaris* could be enhanced through co-cultivation with the nitrogen-fixing *Bacillus pumilus* (Hernandez *et al.*, 2009). Several studies also suggest the involvement of auxins, in particular indole-3-acetic acid (IAA), in microalgal growth promotion (de-Bashan *et al.*, 2008; Bajguz and Piotrowska-Niczyporuk, 2014; Ozioko *et al.*, 2015; Liu *et al.*, 2016; Yu *et al.*, 2017). Also the involvement of N-acylhomoserine lactone (AHL) in microalgal growth-promotion is hypothesized, since Rivas and colleagues could identify two AHL producing bacterial species significantly increasing the growth of *Botryococcus braunii*. They suggest, that biofilm forming bacteria adhering to the algae's surface enhance the bioavailability of essential metabolites, attributable to close physical proximity between producer and consumer (Rivas *et al.*, 2010).

Until today, it is still unclear, whether these symbiotic relationships are species-specific (Grossart *et al.*, 2005; Rooney-Varga *et al.*, 2005; Sapp *et al.*, 2007a; Schäfer *et al.*, 2000), or whether these interactions are determined by abiotic, environmental conditions (Eigemann *et al.*, 2013; Sapp *et al.*, 2007b). However, similarities between abundant bacterial taxa in the plant rhizosphere and the planktonic equivalent – the phycosphere – suggests the co-evolution of algae-bacteria associations (Goecke *et al.*, 2013; Ramanan *et al.*, 2015; Seymour *et al.*, 2017). The necessity of these inter-kingdom relationships becomes explicit when attempting to remove bacteria and fungi from microalgae; microbiota deprived algae mostly show poorer growth or abnormal cell morphologies compared to original strains, underlining the importance of the algal microbiome as an indispensable part of the alga holobiont (Hom *et al.*, 2015).

CHALLENGES ADDRESSED WITHIN THIS PROJECT

- Contaminations with unwanted microorganisms such as weedy microalgae competing for light, nutrients and space, parasitic fungi and bacteria, zooplankton grazers and protists preying on algae
- Insufficient algal biomass yields to reach economic competitiveness
- Usage of commonly used, hazardous chemicals for photobioreactor cleaning procedures

Objectives

In order to address these challenges a polyphasic approach was conducted aiming i) to extend the knowledge concerning algae-bacteria co-evolution with the goal to track down sophisticated natural algae-bacteria interactions allowing the design of synthetic microbial communities to be included in a probiotic cultivation supplement, ii) to evaluate the potential of prominent plant growth-promoting methylobacteria to induce and promote microalgae growth and thereby improve biomass yields, and iii) to find a sustainable, nature-based alternative for bioreactor decontaminations in order to avoid the extensive use of hazardous hydrogen peroxide and sodium hypochlorite.

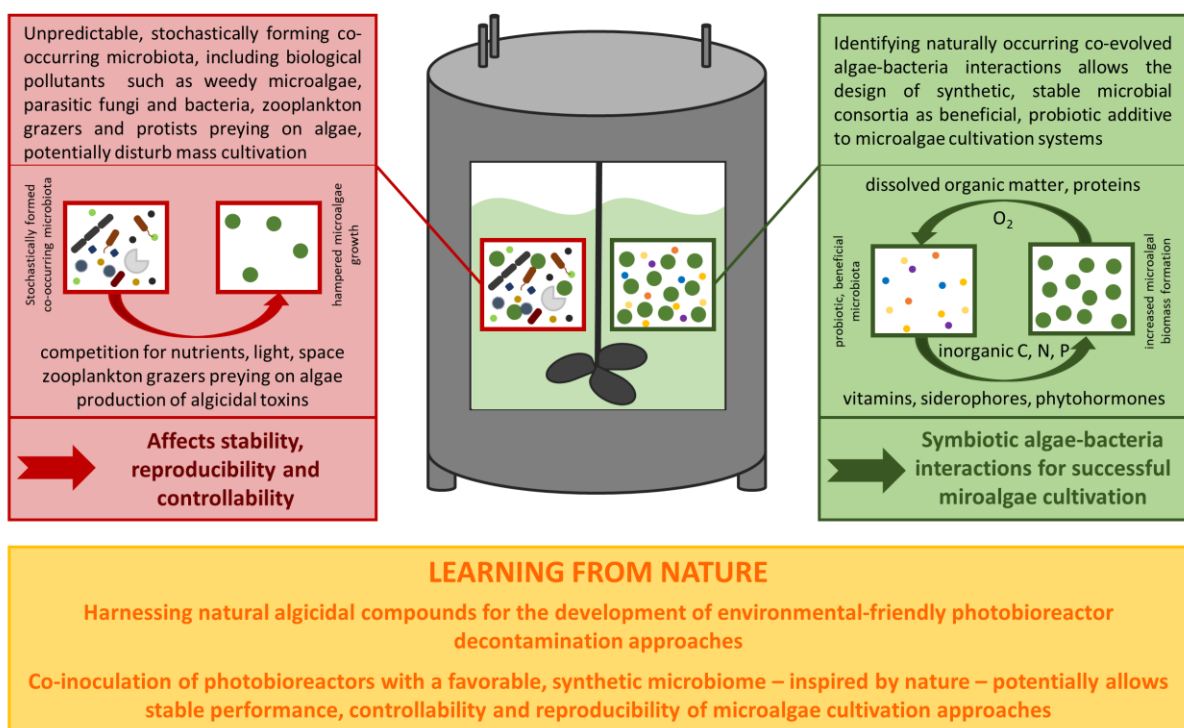


Figure 1. Overview of challenges addressed within this project and suggested approaches on how to harness co-evolved co-occurrences as well as natural microbial compounds for a sustainable success in algal biotechnology.

Profound knowledge of the interactions between algae and bacteria is mandatory to harness their biotechnological potential. Several research groups suggest the application of synthetic microbial communities – inspired by naturally occurring algae-bacteria associations – as probiotic additive to algal cultures in order to minimize the risk of contamination, provide stability and reproducibility and increase yields (Cho *et al.*, 2015; Fulbright *et al.*, 2018; Kazamia *et al.*, 2012a, 2014; Lian *et al.*, 2018). In order to identify, naturally co-evolved beneficiary constituents of the microalgae-associated microbiota the bacterial, eukaryotic and fungal community composition on seasonally occurring, differently colored snowfields in the Austrian Alps was investigated by 16S and 18S rRNA gene

amplicon sequencing. As detailed in **Chapter “1 The microbiome of alpine snow algae shows a specific inter-kingdom connectivity and algae-bacteria interactions with supportive capacities”**, distinct correlation patterns of occurring microalgae and their associated bacteria and basidiomycetous yeasts were discovered. The overall community composition on differently colored snowfields was revealed to be rather location-independent but specific in terms of microbial co-occurrences. Complementary cultivation-dependent analyses allowed the isolation and identification of nine bacterial strains promoting the growth of the industrially relevant microalga *Chlorella*. Additional physiological characterization of those promising bacterial isolates revealed that the production of siderophores, auxins and N-acylhomoserine lactone is conceivably involved in algae growth promotion.

Such symbiotic host-microbe interactions have been extensively exploited for agricultural purposes in terms of growth-promotion and pathogen-control. Bacteria can promote plant growth through the production of plant hormones like auxin, cytokinin and gibberellin, by fixing nitrogen, solubilizing phosphate and producing siderophores and thus improve nutrient uptake (Compant *et al.*, 2019). Similar beneficial effects have also been frequently described on the growth of microalgae (Amin *et al.*, 2009; Cho *et al.*, 2015; Gonzalez and Bashan, 2000; Grant *et al.*, 2014; Kazamia *et al.*, 2012b; Kim *et al.*, 2014; Le Chevanton *et al.*, 2013). **Chapter 2 “Plant growth-promoting methylobacteria harbor great potential for algal biotechnology”** highlights the potential of plant growth-promoting methylobacteria to increase the biomass formation of two industrially relevant green algae through co-cultivation. Four different methylobacteria strains belonging to two species (*M. extorquens*, *M. goesingense*) were evaluated in terms of microalgae growth-promotion and were therefore co-cultured in two different initial cell densities with three microalgal genera, including *Chlorella*, *Scenedesmus* and *Haematococcus*. Results give evidence that mutualistic inter-kingdom relationships are species-specific as well as dependent on algae-bacteria cell ratio. While the growth of *C. vulgaris* was hampered through co-cultivation with methylobacteria – possibly through shading and competition for nutrients, light and space – the biomass formation of *H. lacustris* could be increased up to 14-fold through co-cultivation compared to axenic control cultures in vitamin B₁₂ depleted medium. Confocal laser scanning microscopy of co-cultures revealed a correlation between physical proximity of algae and bacteria and a successful metabolite exchange. All three investigated microalgae were isolated from a natural biofilm, where 16S rRNA gene amplicon sequencing revealed natural co-occurrences of algae and methylobacteria. Microscopic observation of the biofilm revealed *H. lacustris* as the dominating algal taxon, supporting the assumption of evolutionary evolved, specific microalgae-bacteria co-occurrences. Complementary genome analyses of all applied methylobacteria revealed several features conceivably involved in algae growth-promotion. All tested methylobacteria harbor genes involved in the production of vitamins, including biotin, riboflavin, tetrapyrroles and folate. Additionally, all tested strains possess genes associated with iron acquisition as well as genes

attributable to the production of plant alkaloids. Profound knowledge in terms of community-ecology and algae-microbiome interactions are essential for the development of biocontrol strategies in industrial microalgae cultivation systems. These results provide a basis for the design of synthetic, beneficial bacterial probiotics with the potential to promote microalgae growth, as auspicious tool for algal biotechnology to increase stability, reproducibility and controllability.

Microbial metabolites present promising resources for several applications in algal biotechnology. Such metabolites also include volatile organic compounds (VOCs), produced by microorganisms as part of their metabolism. Their role as mediator in various interactions and communications across kingdoms has been described extensively (Effmert *et al.*, 2012; Schulz-Bohm *et al.*, 2017). Recently their involvement in the inhibition of various plant-pathogens was realized (Cernava *et al.*, 2015; Ortega *et al.*, 2016), emphasizing their potential to control diverse microbial contaminations and to replace conventional decontamination agents (Kusstascher *et al.*, 2017; Schöck *et al.*, 2018). As described in **Chapter 3 “A novel, nature-based alternative for photobioreactor decontaminations”** the algicidal effect of the naturally occurring antimicrobial volatile compound 5-isobutyl-2,3-dimethylpyrazine was assessed on three different microalgal genera including *Chlorella*, *Scenedesmus* and *Haematococcus*. Direct application of the decontaminant as well as passive treatment of algae by exposing them to vaporized pyrazines, led to a significant reduction of viable cell count for all the investigated microalgal genera. These results imply the applicability of natural volatile organic compounds as environmental-friendly alternative to conventional, hazardous detergents currently used for photobioreactor decontamination purposes.

MAIN FINDINGS OF THE PROJECT

- Evolutionary-evolved microalgae-microbiome associations comprise mutualistic inter-kingdom relationships, where cultivable constituents provide resources for designing beneficial consortia to increase yields, provide stability and reproducibility in industrial microalgae cultivation systems
- Methylobacteria harbor potential to promote microalgae growth, conceivably attributable to the production of phytohormones, vitamins and siderophores
- A novel, environmental-friendly algicidal compound was identified as promising alternative to hazardous disinfectants for photobioreactor cleaning procedures

CHAPTER 1

THE MICROBIOME OF ALPINE SNOW ALGAE SHOWS A SPECIFIC INTER-KINGDOM CONNECTIVITY AND ALGAE-BACTERIA INTERACTIONS WITH SUPPORTIVE CAPACITIES

Lisa Krug^{1,2}, Armin Erlacher², Katharina Markut², Gabriele Berg², Tomislav Cernava²

¹*Austrian Centre of Industrial Biotechnology, Graz, Austria*

²*Institute of Environmental Biotechnology, Graz University of Technology, Graz, Austria*

Abstract

Mutualistic interactions within microbial assemblages provide a viable strategy for survival under extreme conditions. Although such phenomena were often studied with bipartite systems and host-associated communities, less is known about the complexity of interaction networks of free-living microorganisms. For the first time, the interplay within algae-dominated microbial communities exposed to harsh environmental influences in the Austrian Alps was assessed to reveal the interconnectivity of eukaryotic and prokaryotic inhabitants. All analyzed snowfields showed sample-specific signatures and distinct clustering of eukaryotic and bacterial communities. Network analyses revealed that mutual exclusion prevailed among microalgae in the alpine environment, while bacteria were mainly positively embedded in the interaction networks. Especially members of *Proteobacteria*, with a high prevalence of *Oxalobacteraceae*, *Pseudomonadaceae*, and *Sphingomonadaceae* showed genus-specific co-occurrences with distinct microalgae. In addition, correlation analyses revealed distinct genus-specific clustering of microalgae and basidiomycetous yeasts. Co-cultivation experiments with isolated algae and bacteria confirmed beneficial interactions; they resulted in up to 2.6-fold more biomass. Our findings support the initial hypothesis that adverse environmental conditions in alpine systems harbor inter-kingdom supportive capacities. The understanding of mutualistic inter-kingdom interactions and the ecology of microalgae within complex microbial communities could support the development of new co-inoculation strategies for biotechnological processes.

Introduction

Microalgae and bacteria can form complex, inter-kingdom microbial communities in various natural environments and exchange different metabolites for mutualistic support (Kouzuma and Watanabe, 2015). While freshwater and marine habitats are commonly analyzed to decipher microalgae-bacteria interactions (Eigemann *et al.*, 2013; Amin *et al.*, 2012a; Cole, 1982), less is known about interactions in similar assemblages that are found on snowfields in alpine environments. Until recently, cryophilic ecosystems have been considered barren; only in the last few years a modest number of studies revealed those extreme habitats as complex evolutionary evolved ecosystems by addressing the biodiversity and functionality of glaciers, snow and ice fields (Anesio and Laybourn-Parry, 2012). Colored snow attributable to algal blooms has been known since the times of Aristotle (Werner, 2007). Snow algae have first been documented in 1818, when British sailors voyaged towards Greenland and Sir John Ross, a naval officer and Arctic explorer, observed cliffs covered in crimson red snow attributable to microalgae blooms (Ross, 1819). Later, Charles Darwin himself described the occurrence of blood red snow in the Andes Mountains (Darwin, 1915). Still, 200 years after the first documented observation of the “blood alga” many unanswered questions in terms of its evolution, lifecycle and distribution challenge scientists worldwide.

Due to the important role as primary producers and the release of dissolved organic nutrients to the environment, microalgae allow heterotrophic microorganisms to co-exist in their surroundings. Such heterotrophic microorganisms include bacteria that not only decompose organic matter but that can also support higher eukaryotes in return by nutrient exchange and complex communication systems (Berg *et al.*, 2016; Philippot *et al.*, 2013). Various metabolite exchanges including essential micro- and macronutrients were observed so far for algae-bacteria interactions in the context of coevolution and mutualistic support (Cooper and Smith, 2015; Kim *et al.*, 2014; Ramanan *et al.*, 2015). In this context, it was also found that more than 50% of otherwise autotrophic microalgal species are dependent on an external supply of vitamin B₁₂ (Croft *et al.*, 2005, 2006). In addition, Amin and colleagues could show that bacterial siderophores increase the bioavailability of chelated iron not only for bacteria but also for microalgae (Amin *et al.*, 2009). Iron is essential for microalgae during the photosynthetic process of inorganic carbon fixation (Amin *et al.*, 2009, 2012b). Moreover, the nitrogen released by bacteria as an integrative part of siderophores, provides requisite nitrogen that is essential for growth and replication in microalgae (Villa *et al.*, 2014). Furthermore, phytohormones produced by bacteria were also reported to have beneficial effects on the growth of microalgae (Amavizca *et al.*, 2017). Several plant growth-promoting bacteria harbor potential to stimulate algal growth by releasing essential minerals, vitamins, auxins and quorum sensing signaling molecules (Amavizca *et al.*, 2017; Croft *et al.*, 2006; Goecke *et al.*, 2010; Joint *et al.*, 2002).

Microalgae have attracted considerable interest worldwide in the last decades, mainly due to their applicability in the renewable energy, biopharmaceutical, and nutraceutical industry (Brennan and Owende, 2010; Spolaore *et al.*, 2006). While in early stages of the cultivation process sterile operation is still feasible, axenic cultivation in large-scale biomass production systems is neither economically nor practically feasible. Due to these limitations, increased concerns related to the potential of co-occurring microorganisms to inhibit and disturb mass-cultivation processes have resulted in a greater interest to develop preventive biocontrol strategies (Fulbright *et al.*, 2018). Here, symbiotic cultures of microalgae and bacteria provide a viable strategy for the elimination of unwanted, contaminating bacteria in aquaculture systems as already proposed by Kazamia and colleagues (Kazamia *et al.*, 2012a); this is mainly due to the principle of competitive exclusion, also known as Gause's law. The principle states that "complete competitors cannot coexist" (Hardin, 1960); ecological niches occupied by beneficial microorganisms are less accessible for microorganisms detrimental for microalgae. By tracking down the sophisticated natural algae-bacteria interactions in natural environments, the design of beneficial, synthetic microbial communities becomes a more tangible tool for biotechnological applications.

In the present study the main focus was on the decipherment of microbial community structures on differently colored snowfields sampled at two geographically distant locations representative for the Central Alps in Austria; freshwater samples served as references to confirm expected differences in population structures between terrestrial (snowfields) and limnetic (freshwater from lake) ecosystems, as the investigated environments show very differing conditions in terms of nutrient availability, temperature and light intensity. The main objective of the study was to characterize inter-kingdom interactions in seasonally occurring nutrient-poor snowfields, where microorganisms have to cope with low temperatures and high UV-radiation and are therefore considered extreme environments. We hypothesized mutualistic inter-kingdom relationships in order to allow microbes to persist in these adverse conditions. By applying co-occurrence network inferences, we focused on the identification of predominant correlations between microalgae and bacteria and putative beneficiary constituents within the microalgae-associated bacterial community. Bacterial isolates from the same sampling locations were screened for their potential to produce micro- and macronutrients attributable to increased performance of microalgae (i.e. phytohormones and siderophores). Finally, bacterial isolates obtained from differently colored snowfields and freshwater samples were co-cultivated with the microalgae *Chlorella vulgaris* BRK1 in order to investigate their direct impact on biomass formation of an industrially relevant microalgae model. The obtained results broaden our knowledge related to inter-kingdom interactions in extreme environments and provide a basis for upcoming biotechnological developments.

Material and Methods

Sampling procedure. Snow and water samples were collected 30th May and 31st May 2017 from two geographically distant locations in the Austrian Central Alps (sampling site A - Rottenmanner Tauern, N47°26'24.695'' E14°34'34.556''; sampling site B - Seetaler Alpen, N47°3'56.128'' E14°34'0.318''). Red snowfields were sampled on both sites while green and orange snow could only be found either at sampling site A or sampling site B, respectively. In addition, water samples of two separate water bodies were obtained from both sampling sites. Snow and water samples were collected in sterile 50 mL Greiner tubes (Sigma-Aldrich, Missouri, USA) and stored on ice during transportation until further processing. Upon arriving in the laboratory, microalgae occurring in differently colored snowfields were visualized microscopically using a light microscope (Leitz; Wetzlar, Germany) at 400 × magnification. The detailed sampling locations and examples of colored snowfields are shown in Figure 1.1.

Isolation of microalgae associated bacteria. In order to isolate microorganisms, all samples were plated in dilution series on nutrient agar (NA), Reasoner's 2A agar (R2A), and modified Bolds Basal Medium agar-plates (mBBM) containing 250 mg/L NaNO₃, 175 mg/L KH₂PO₄, 75 mg/L K₂HPO₄, 75 mg/L MgSO₄ × 7 H₂O, 25 mg/L CaCl₂, 25 mg/L NaCl, 2.6 mg/L H₃BO₃, 5 mg/L FeSO₄ × 7 H₂O, 8.8 mg/L ZnSO₄ × 7 H₂O, 1.4 mg/L MnCl₂ × 4 H₂O, 1.4 mg/L MoO₃, 1.6 mg/L CuSO₄ × 5 H₂O, 0.5 mg/L Co(NO₃)₃ × 6 H₂O, 0.5 mg/L EDTA, 0.3 mg/L KOH, 0.017 mg/L vitamin B₁₂, 0.013 mg/L 4-aminobenzoate, 0.003 mg/L biotin, 0.013 mg/L nicotinic acid, 0.017 mg/L hemicalcium-pentathenate, 0.05 mg/L pyridoxamine-HCl, 0.033 mg/L thiaminiumdichlorid, 0.0091 mg/L thioctic acid, 0.01 mg/L riboflavin, 0.0049 mg/L folic acid and 18 g/L agar-agar. Vitamins and heat-sensible components were added after autoclaving by sterile filtration (0.20 µm pore size). NA and R2A was incubated for 3 days at room temperature; mBBM-agar was incubated at 23 °C at a light dark cycle (L:16/D:8). The lighting was supplied by cool-white fluorescent lamps TL-D 36W/840 REFLEX Eco (Philips, Amsterdam, Netherlands) with an intensity of 3,350 lm for 3 days. A total number of 470 bacterial isolates were randomly selected and subcultured on the respective media.

Physiological characterization of cultured bacterial isolates

Screening for N-acylhomoserine lactone (AHL) production. Screening for AHL production was performed based on the studies of Morohoshi and colleagues (Morohoshi *et al.*, 2008) and McClean and colleagues (McClean *et al.*, 1997). *Chromobacterium violaceum* CV026 served as indicator strain as it is able to produce the violet pigment violacein in the presence of exogenous N-hexanoyl-homoserine lactone (C6-HSL). *S. plymuthica* 3Re4-18 (Adam *et al.*, 2016) served as positive control.

Isolates were grown over night at room temperature. Violet coloration of the indicator strain indicated AHL-production which was recorded for each strain.

Screening for indole-3-acetic acid production. Indole-3-acetic acid excretion by bacterial strains was determined by means of a modified colorimetric analysis developed by Gordon and Weber (Gordon and Weber, 1951). Glass test tubes containing 5 mL LB broth supplemented with 0.1% tryptophan were inoculated with single colonies of bacterial isolates. After cultivation at 20 °C for 5 to 7 days in the dark, the cell-free supernatant was mixed with the Salkowski reagent (50.0 mM FeCl₃, 35.0% (v/v) perchloric acid) at a ratio of 3:1 and incubated for 30 min in the dark. The auxin concentration was measured photospectrometrically using an infinite M200 spectrofluorimeter microplate reader (TECAN, Männerdorf, Switzerland) at 530 nm and quantified using a standard curve ($R^2 = 0.9894$).

Screening for siderophore production. Siderophore production was tested by sterilizing 400 mL of 1.50% agar LB-agar medium and mixing it thoroughly with 100 mL staining solution containing 98 mL dH₂O; 1 mL 0.01 M FeCl₃ 1 mL 0.1 M HCl; 0.605 g chrome azurol-S and 0.073 g cetyltrimethylammoniumbromid. After solidification in Petri dish plates, bacterial isolates were streaked out and incubated for 14 days at room temperature. Then the presence (siderophore production positive) or absence (siderophore production negative) of yellow halo zones around the isolates was noted.

***Chlorella vulgaris* quantification by fluorescence intensity analyses.**

To determine the *C. vulgaris* cell number, the algal chlorophyll A content was measured using a fluorometric approach and subsequently correlated with the respective cell number. The fluorescence emission maximum was determined by performing a fluorescence intensity scan with a pure *C. vulgaris* culture using an infinite M200 spectrofluorimeter. The microalgae culture was obtained by inoculating 20 mL mBBM with a single colony of *C. vulgaris* and subsequent incubation for 5 days at 23 °C at a light dark cycle L:16/D:8. The microalgae culture was excited at 450 nm wavelength and fluorescence emission was detected in the range between 580 and 760 nm. The fluorescence emission maximum of microalgae cultures was determined as 685 nm and subsequently the number of corresponding CFUs was determined by plating respective dilutions on mBBM. Applying a linear regression ($R^2 = 0.931$) allowed the correlation between fluorescence intensity (FI) and microalgae cell count.

Co-cultivation to evaluate the potential of bacteria to promote microalgae growth.

The growth promotion assay was performed with the unicellular microalga strain *Chlorella vulgaris* BRK1, isolated from a photobioreactor by plating respective samples on mBBM-agar and subsequent

subculturing (Krug *et al.*, 2019). For initial cultivation, 50 mL mBBM were inoculated with a single colony of *C. vulgaris* and grown for 1 day at 23 °C at a light dark cycle L:16/D:8. The axenic *C. vulgaris* culture was then transferred in 96 well plates, each well containing 200 µL algae culture. Microalgae were then inoculated with single bacterial colonies using sterile toothpicks. For the prescreening, growth-promoting experiments were performed in 8 replicates. The growth-promotion assay was repeated in 18-fold replication with bacterial isolates indicating growth-promotion during the prescreening in order to facilitate statistical analyses. The significance of the results was tested using the IBM SPSS program (version 23.0; IBM Corporation, NYC, NY, USA). All data was analyzed using Student's paired t-Test at $p < 0.01$.

Identification of bacterial isolates and phylogenetic analysis of beneficial strains.

Bacterial genomic DNA from pure cultures was extracted by mechanical disruption. Bacterial colonies from agar plates were resuspended in 300 µL sterile NaCl (0.85%) and transferred in sterile Eppendorf tubes filled with glass beads and subsequently processed in a FastPrep FP120 (MP Biomedicals, Heidelberg, Germany) instrument. After centrifugation at 3,000 rpm for 5 min the supernatant was transferred in sterile 1.5 mL tubes and served as template for the PCR. Subsequently, 16S rRNA gene fragments were amplified using primer 27F (5' - AGA GTT TGA TCM TGG CTC AG - 3') and 1492R (5' - CGG TTA CCT TGT TAC GAC TT - 3'). The PCR was performed in a total reaction volume of 30 µL containing 16.20 µL ultrapure water, 6.00 µL Taq&Go [5 ×] (MP Biomedicals, Heidelberg, Germany), 1.50 µL of each primer [10 µM], 1.80 µL MgCl₂ [25 mM] and 3 µL template (95 °C, 4 min; 30 cycles of 95 °C; 30 s; 57 °C, 30 s; 72 °C, 90 s; final extension at 72 °C, 5 min). The PCR products were purified using Wizard SV Gel and PCR-Clean-Up System (Promega Corporation, Madison, Wisconsin, USA) and DNA concentration was measured using a Nanodrop UV-Vis spectrophotometer (Thermo Fisher Scientific, Waltham, Massachusetts, USA), diluted accordingly and sent for Sanger sequencing (LGC Genomics GmbH, Berlin, Germany). Resulting 16S rRNA gene fragment sequences were then blasted against the NCBI nucleotide collection database excluding uncultured and environmental samples using the BLAST algorithm (Altschul *et al.*, 1990). A phylogenetic tree that is based on 16S rRNA gene sequence alignments was constructed with MEGA X (Kumar *et al.*, 2018). The evolutionary history was inferred by using the Neighbor-Joining method (Saitou and Nei, 1987). The percentage of replicate trees in which the associated taxa clustered together in the bootstrap test (1,000 replicates) were separately assessed (Felsenstein, 1985). Evolutionary distances were computed using the Maximum Composite Likelihood method (Tamura *et al.*, 2004) and are provided as base substitutions per site.

Microbiome analyses with bacterial and eukaryotic amplicon libraries

Total community DNA extraction and barcoding. For each sample, total community DNA from 2 mL melted snow/water was extracted using the FastDNA Kit for Soil (MP Biomedicals, Heidelberg, Germany) according to the manufacturer's instructions. The 16S rRNA gene fragment sequences were amplified in three technical replicates covering the hypervariable region 4 using the Unibac II 515f (5' - GTG YCA GCM GCC GCG GTA A - 3') and 806r (5' - GGA CTA CHV GGG TWT CTA AT - 3') primer pair (Caporaso *et al.*, 2011), which included sample-specific barcodes and Illumina sequencing adaptors. Peptide nucleic acid (PNA) was added to the PCR mix to prevent the amplification of mitochondrial (mPNA) and plastidial (pPNA) DNA from eukaryotes (Lundberg *et al.*, 2013). The PCR was performed by using a total volume of 30 µL containing 20.15 µL ultrapure water, 6 µL Taq&Go [5 ×], 1.2 µL of each primer (5 µM), 0.225 µL pPNA [100 µM], 0.225 µL mPNA [100 µM] and 1 µL DNA template. The cycling program was adjusted to an initial denaturation temperature at 96°C for 5 min, followed by 30 cycles of 96 °C for 1 min, 78 °C for 5 s, 54 °C for 1 min, and 74 °C for 1 min. The final extension was done at 74 °C for 10 min. PCR products of respective samples were quality checked by gel electrophoresis. If the quality (amount, concentration) of the PCR product was found to be insufficient during the quality check, another PCR was performed with primer pair 27F and 1492R prior to the described PCR reaction in a nested approach. The PCR products were then purified using the Wizard SV Gel and PCR-Clean-Up System according to manufacturer's protocol and served than as template for further amplifications.

From the same total community DNA extracts, 18S rRNA gene fragments of the eukaryotic community were amplified in a first PCR with the primer pair 1391f (5'- GTA CAC ACC GCC CGT C - 3') and EukBr (5'- TGA TCC TTC TGC AGG TTC ACC TAC - 3') targeting the variable region 9 (V9) of the 18S rRNA gene sequence (Amaral-Zettler *et al.*, 2009). Each forward and reverse primer contained a specific primer pad (TATGGTAATT/AGTCAGCCAG) and linker (GT/GG), as described in the protocols and standards section of the Earth Microbiome Project (www.earthmicrobiome.org) (Caporaso *et al.*, 2010). PCR reactions (20 µL) were conducted in triplicates and contained 14.6 µL ultrapure water, 4 µL Taq&Go [5 ×], 0.2 µL of forward and reverse primer each [10 µM] and 1 µL extracted DNA template. The cycling program was adjusted to the following settings: 98 °C, 5 min; 10 cycles of 98 °C, 10 s; 53 °C, 10 s; 72 °C, 30 s; 20 cycles of 98 °C, 10 s; 48 °C, 30 s; 72 °C, 30 s; final extension 72 °C, 10 min. PCR products of respective samples were quality checked by gel electrophoresis. If the quality of the PCR product was found to be insufficient, another PCR was performed prior to the described PCR reaction for nested approaches with primer pair NS1 (5' - GTA GTC ARA RGC CTT GTC TC - 3') and NS8 (5' - TCC GCA GGT TCA CCT ACG GA - 3') in a reaction mix (30 µL) containing 16.2 µL ultrapure H₂O, 6 µL Taq&Go [5 ×], 1.2 µL of each primer [10 µM], 2.4 µL MgCl₂ [25mM] and 3 µL DNA template. PCR products were then purified using the Wizard SV Gel and PCR-Clean-Up System according to manufacturer's protocol

and served as template for further amplifications. For multiplexing, sample-specific Golay barcodes were attached to the specific primer pad on forward and reverse primer respectively. Barcoded sequences were pooled and purified according to the Wizard SV Gel and PCR-Clean-Up System. Equimolar DNA concentrations of each barcoded amplicon (bacterial and eukaryotic) were then sent for paired-end Illumina HiSeq sequencing (read length: 2×300 bp) to GATC Biotech AG (Konstanz, Germany).

Initial bioinformatic analyses of 16S rRNA and 18S rRNA gene amplicons. Raw sequencing data preparation, including joining forward and reverse read pairs was done using software package QIIME 1.9.1. After removing barcodes, primer and adapter sequences reads as well as metadata were imported into QIIME 2 (2018.11 release). Further analyses of sequencing data were performed using the QIIME 2 pipeline according to tutorials provided by the QIIME developers (Caporaso *et al.*, 2010). The DADA2 algorithm (Callahan *et al.*, 2016) was used to demultiplex and denoise truncated reads. Chimeras were identified by using the VSEARCH uchime_denovo method (Rognes *et al.*, 2016) and subsequently removed. Respective reads were then summarized in a feature table. The 16S rRNA dataset was normalized to 98,216 reads per sample to account a variation in the samples reaching from 719,183 to 98,216 reads. Features were then collapsed on genus level and a reduced table containing only highly abundant taxa ($>0.1\%$ mean re. abundance) was used for generating bar charts. In analogy, the 18S rRNA dataset was normalized to 21,347 reads per sample to account for the variation in the samples reaching from 788,817 to 21,347 reads. Rarefied feature tables served as input for alpha and beta diversity analyses and statistics using QIIME 2 core diversity metrics. Principal Coordinate Analysis (PCoA) plots were constructed by calculating the unweighted UniFrac distance matrix (Lozupone and Knight, 2005). Phylogenetic metrics were constructed by aligning representative sequences using the mafft program (Katoh and Standley, 2013). After the multiple sequence alignment was masked and filtered a phylogenetic tree was generated with FastTree (Price *et al.*, 2010). The taxonomic analysis was based on a customized naïve-Bayes classifier trained on 16S and 18S rRNA gene OTUs clustered at 99% similarities with the SILVA128 database release and trimmed to a length of 400 bp (16S) and 200 bp (18S) respectively. Statistics were calculated within QIIME 2 using analysis of similarity (ANOSIM). The datasets used and/or analyzed during the current study are available in the ENA repository (<https://www.ebi.ac.uk/ena>) under the accession number PRJEB31713.

Complementary network analyses with combined datasets. Co-occurrence network analyses were calculated and rendered using Cytoscape version 3.7.0 (Shannon *et al.*, 2003) and the CoNet add-on (Faust and Raes, 2016). Highly significant inferences ($p = 0.0004$, $q = 0.0004$) were retained. Reduced feature-tables containing only features assigned to *Archaeplastida* and *Proteobacteria* with a mean relative abundance of at least 0.1% on snowfields were used for inference analyses. To ensemble

inferences Pearson and Spearman correlation measurements, Bray Curtis and Kullback-Leibler dissimilarity matrices and the mutual information option were used including Benjamini-Hochberg multiple test correction.

Correlations patterns between microalgae and their associated microbiota. Following the normalization of features assigned to the phyla *Chlorophyceae*, *Chrysophyceae* and *Basidiomycota* within the 18S rRNA dataset, they were manually blasted against the NCBI nucleotide collection database. For calculating correlations between microalgae and bacteria, the bacterial feature table was reduced by retaining only features with a mean relative abundance of at least 0.1% on snowfields. Features with the same taxonomic assignment were combined and unassigned reads were excluded from the dataset. METAGENassist (Arndt *et al.*, 2012) was employed to visualize co-occurrence patterns within the eukaryotic and bacterial communities on snowfields based on Kendall's tau rank correlation.

Results

Eukaryotic communities show habitat-specific signatures in colored snowfields and freshwater samples

The eukaryotic community structure was analyzed by 18S rRNA gene fragment amplicon sequencing of differently colored snowfields and freshwater samples from two geographically dispersed locations in the Austrian Alps (Figure 1.1).

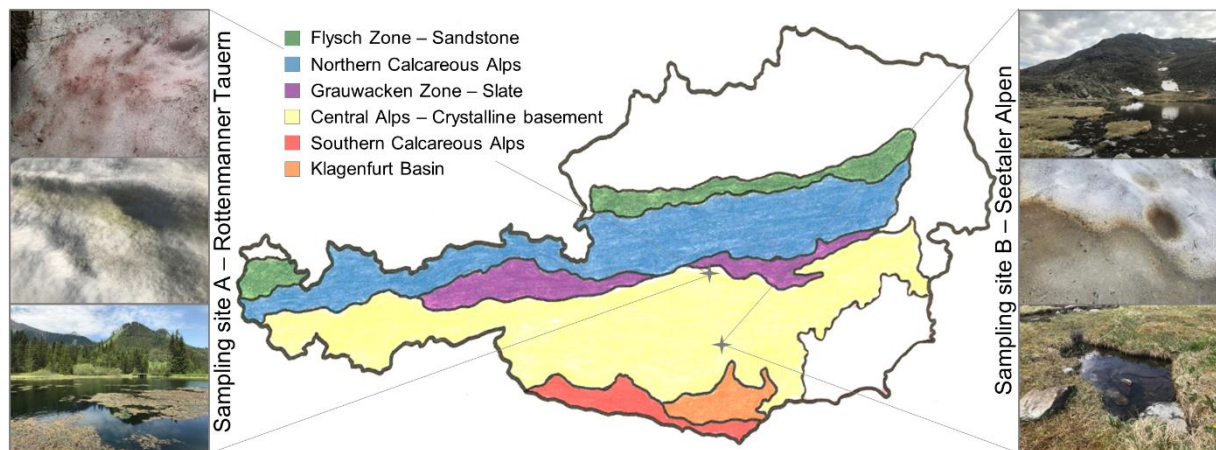


Figure 1.1. Locations of the sampling sites in the Austrian Alps. Red and green snowfields were sampled at site A (Rottenmanner Tauern) while red and orange snowfields were sampled at site B (Seetaler Alpen). In addition, two freshwater samples in close proximity of the snowfields were sampled at each sampling site.

After removing chimeric sequences, 10,374,680 reads were retained in the dataset, resulting in 3,681 features. Features were collapsed at genus level resulting in 71 eukaryotic genera with an occurrence of at least 10 reads in total. The resulting community assessment includes highly abundant eukaryotic taxa; their mean relative abundance within the sample replicates and a threshold of 0.1% over the whole dataset was used for visualizations (Figure 1.2). The green and red snowfields sampled at sampling site A were dominated by *Archaeplastida* with relative abundances of 51% and 65% respectively, followed by *Ophistokonta* with relative abundances of 49% on the green snowfield and 33% on the red snowfield. A similar pattern was observed for the freshwater samples obtained at sampling site A; *Archaeplastida* accounted for 43% and *Ophistokonta* for 33% relative of the eukaryotic community, whereas *Basidiomycota* accounted for the largest share on snowfields. The highest proportion of taxa assigned to *Ochrophyta* was found on the orange snowfield (7%) Within the phylum *Ochrophyta* not further classified *Ochromonadales* were frequently detected in one freshwater sample obtained at sampling site B with a relative abundance of 26%. *Bacillariophytina* (29%) and not further classified *Peronosporomycetes* (8%) - all members of the *Stramenopiles* clade - were the most

***Proteobacteria* and *Bacteroidetes* were predominant in bacterial communities on snowfields and in freshwater**

In a complementary approach based on the same total community DNA extracts, the bacterial community structure was analyzed by 16S rRNA gene fragment amplicon sequencing. After removing chimeric, plastid and mitochondrial sequences, 9,135,634 reads were retained in the dataset, resulting in 7,850 features. Features were collapsed on genus level and genera with an occurrence < 10 reads in the whole dataset were excluded, resulting in 539 bacterial genera. Bar charts were used to visualize the highly abundant fraction in the 16S dataset (relative abundance > 0.1%; Figure 1.3).

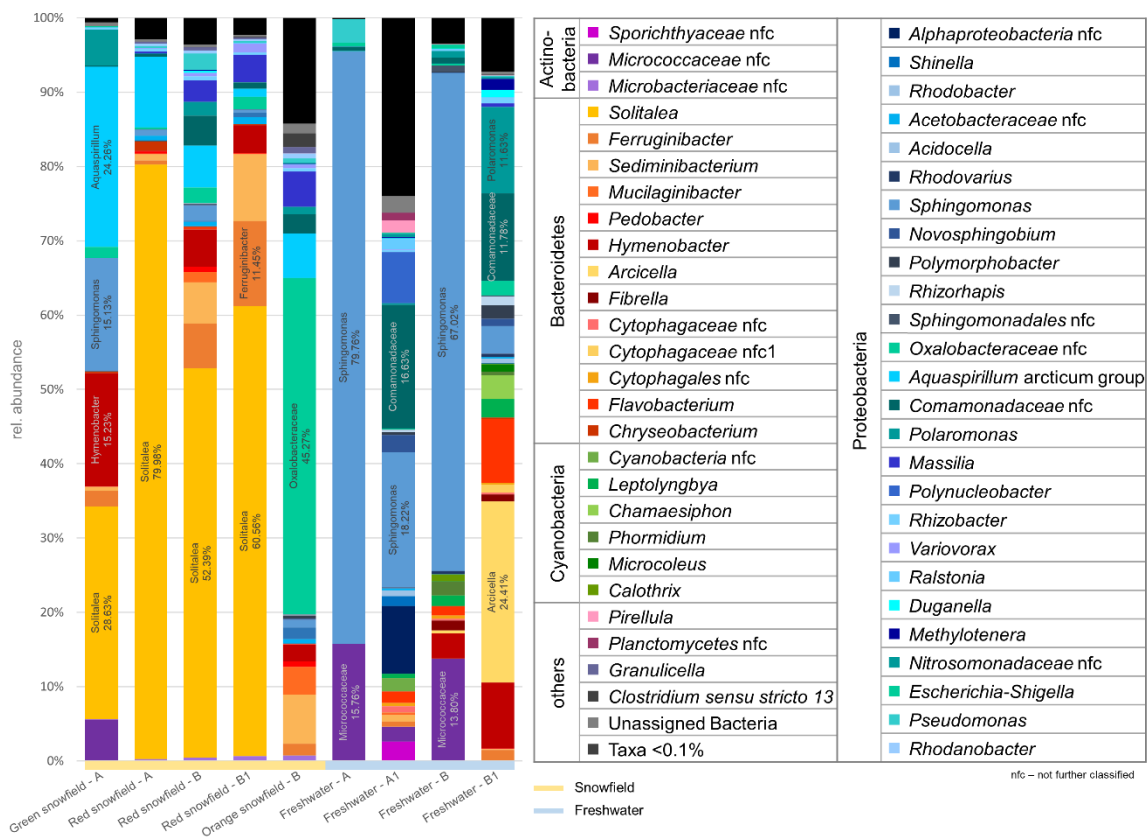


Figure 1.3. Composition of the bacterial community on differently colored snowfields and in freshwater sampled at two geographically distant locations in the Austrian Alps. Taxonomic assignments were conducted at genus level. Bar charts represent the highly abundant fraction of the bacterial community with a relative abundance $\geq 0.1\%$ in the whole dataset. Sampling site A: Rottenmanner Tauern; sampling site B: Seetaler Alpen. Labels and the relative abundances of highly abundant taxa ($>10\%$ rel. abundance) are included in the respective bar chart.

The resulting dataset comprised seven bacterial phyla that included 53 different bacterial genera. Among the red and green snowfield samples, the predominant fraction of the microbiota was assigned to *Bacteroidetes* (mean: 72%) followed by *Proteobacteria* (mean: 23%), together they accounted for $\leq 93\%$ in each sample, independent from the sampling site. On genus level, the bacterial community on red and green snowfields was dominated by *Solitalea* sp. (29% - 80%). On the green

snowfield a higher fraction of *Hymenobacter* sp. (15%) and *Aquaspirillum* sp. (24%) was observed compared to red snowfields. On the contrary, the orange snowfield sampled at sampling site B was dominated by *Proteobacteria* (66%) followed by *Bacteroidetes* (15%). The most abundant bacterial taxa on the orange snowfield were identified as members of the *Oxalobacteraceae* family (45%). Except one, freshwater samples were dominated by *Proteobacteria* (mean: 63%), in particular *Sphingomonas* (18% - 80%), followed by *Bacteroidetes* (mean 14%). In one freshwater sample (Freshwater - B1) the dominating bacterial phyla were *Bacteroidetes* (46%) and *Proteobacteria* (39%; Figure 1.3). The detailed description of relative abundances for the most abundant features is summarized in Supplementary Table S1.2; the closest taxonomic assignment according to BLAST searches against the NCBI nucleotide collection database was included.

Bacterial and eukaryotic community structures were highly habitat-specific

Bacterial community compositions substantially differed when habitats sampled in close proximity were compared. Between-sample differences of the microbiota within differently colored snowfields sampled at geographically distant locations were analyzed to study possible relationships between microalgae/eukaryotes and bacteria occurring on respective snowfields. In addition, ANOSIM tests were performed in order to identify the most influencing parameters on the composition of the bacterial community. When samples were grouped by sampling site, no clustering was observed in the PCoA plots (Figure 1.4), suggesting that the composition of the bacterial community is independent from the sampling site. On the contrary, when grouping the samples according their habitat (snowfield and freshwater), significant differences between the two investigated groups were observed ($R = 0.594$; $p = 0.001$). The same observation was found for the 18S amplicon library, the habitat had a significant influence on the structure of the eukaryotic fraction of the microbiome ($R = 0.223$; $p = 0.008$; Table 1.1).

Snowfield color reflects the bacterial and eukaryotic community structure

When the similarities of differently colored snowfields obtained from geographically distant locations were compared, ANOSIM confirmed a high correlation between the snow color and the composition of the bacterial community ($R = 0.841$; $p = 0.001$). However, when the similarities of all red colored snowfields were compared, no significant differences in the composition of the bacterial microbiota were found ($R = -0.015$, $p = 0.501$). Complementary results were obtained when the eukaryotic community composition was analyzed on differently colored snowfields. The highest and most significant impact on the eukaryotic community composition was given by the color of snowfields independent from sampling site ($R = 0.903$; $p = 0.001$). Again, when similarities of red colored snowfields were compared, no significant differences in the eukaryotic community composition were

observed ($R = 0.067$; $p = 0.229$). Similar results were obtained when similarities of freshwater samples from the two alpine locations were assessed. The sampling site had only a minor effect on the microbiome composition (18S: $R = 0.075$, $p = 0.265$; 16S: $R = 0.134$, $p = 0.116$).

Table 1.1. Statistical analyses of bacterial and eukaryotic community composition in freshwater and on snowfields sampled at two different locations, based on the unweighted UniFrac distance matrix.

| ANOSIM test 16S | | | ANOSIM test 18S | | |
|---|--------------|--------------|---|--------------|--------------|
| Groups | R | p-value | Groups | R | p-value |
| Habitat freshwater, snow | 0.594 | 0.001 | Habitat freshwater, snow | 0.223 | 0.008 |
| Snow color red, green, orange | 0.841 | 0.001 | Snow color red, green, orange | 0.903 | 0.001 |
| Red snow A - Rottenmann, B - Seetal | -0.015 | 0.501 | Red snow A - Rottenmann, B - Seetal | 0.067 | 0.229 |
| Water A - Rottenmann, B - Seetal | 0.194 | 0.116 | Water A - Rottenmann, B - Seetal | 0.075 | 0.265 |

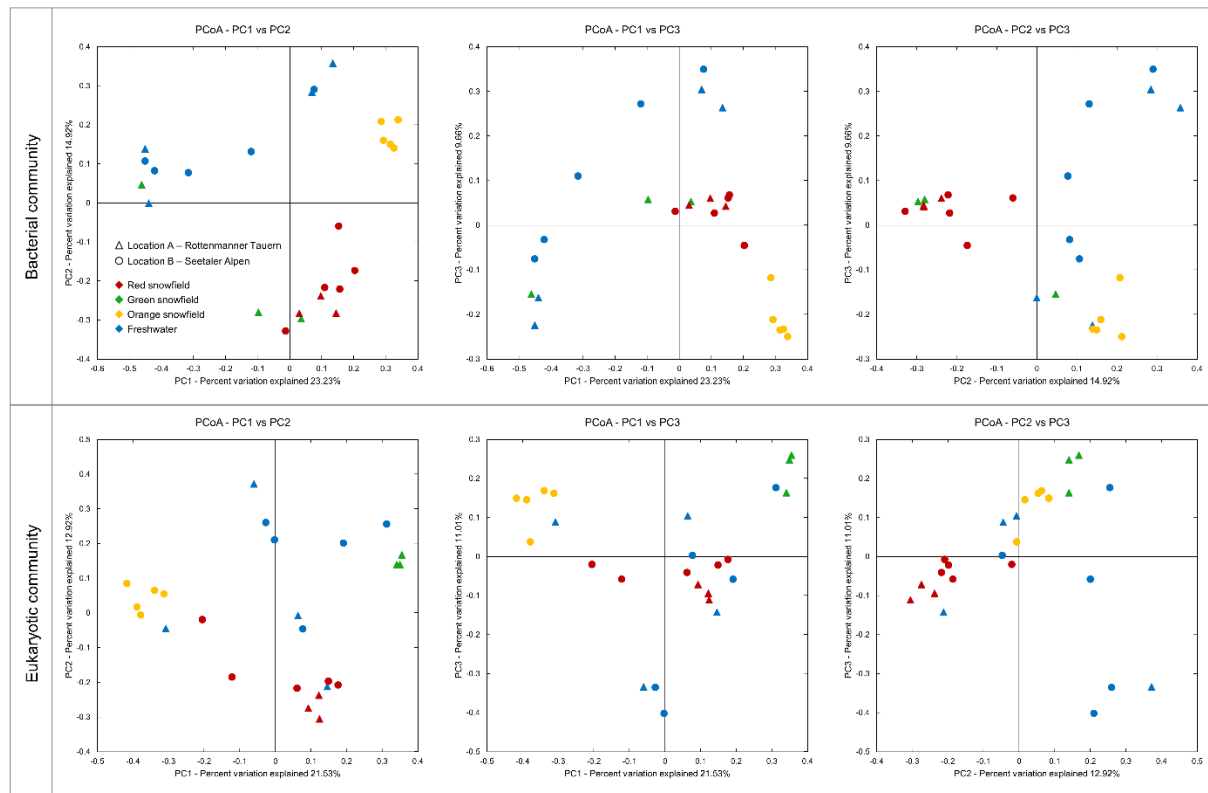


Figure 1.4. PCoA plots of bacterial and eukaryotic communities on differently colored snowfields and freshwater sampled at two geographically distant locations in the Central Alps. Community clustering is based on Bray-Curtis dissimilarities (unweighted UniFrac).

Co-occurrence network analyses revealed mutual exclusion patterns between microalgae

In order to elucidate co-occurrences between *Proteobacteria* and *Chlorophyta* on snowfields network analyses were performed (Figure 1.5.A). For network construction, the feature table was reduced by filtering for features assigned to *Proteobacteria* with a mean relative abundance of $\leq 0.05\%$ in snowfield samples and *Chlorophyta*. Within this dataset, highly significant ($p < 0.0004$; $q < 0.0004$) co-occurrences and mutual exclusion patterns between *Proteobacteria* and *Chlorophyta* on snowfields were assessed. The resulting network comprised 51 nodes with a network density of 0.655. In the co-occurrence network the algal community was represented by twelve features assigned to *Chlamydomonas*, six assigned to *Chloromonas* and one feature assigned to *Scotiella*. The *Proteobacteria* phylum comprised four features assigned to the *Acetobacteriaceae* family, one assigned to *Burkholderiaceae*, four to *Comamonadaceae*, 13 features assigned to *Oxalobacteraceae*, four *Pseudomonadaceae*, two *Rhizobiales*, three *Sphingomonadaceae* and one feature assigned to the *Xanthomonadaceae* family. Co-occurrence network inference analyses revealed that *Massilia* - a member of the *Oxalobacteraceae* family has predominantly positive interconnections (31 of a total number of 39 links). Moreover, mainly positive interactions were observed between *Massilia* and features assigned to *Chloromonas*, while exclusively negative interactions were observed between *Massilia* and features assigned to *Chlamydomonas*. Additional features assigned to taxa belonging to the *Oxalobacteraceae* family showed similar patterns (Figure 1.5.B). Analogous observations were obtained when the interconnections of *Pseudomonadaceae* and algal features were assessed; negative interconnections prevailed between *Pseudomonas* and *Chlamydomonas* while positive interconnections predominate with *Chloromonas* (Figure 1.5.C). Remarkably, one feature assigned to *Sphingomonas* was amongst the features with the most interconnections. Out of a total number of 38 interconnections, 30 indicated a co-occurrence with microalgae; seven out of eight edges indicated mutual exclusion between *Sphingomonas* and features assigned to *Chlamydomonas*, while exclusively positive correlations are found between *Sphingomonas* and features assigned to *Chloromonas*. Except one negative correlation with a feature assigned to *Aquaspirillum*, all other interconnections of *Sphingomonas* with bacterial taxa indicated co-occurrences on snowfields. Within the algal community on snowfields, features assigned to *Chloromonas* showed the most positive interconnections (in total 143 links). Negative interconnections were frequently detected between a feature assigned to *Aquaspirillum* (47 links) and several bacterial features including all members of the *Oxalobacteraceae* family; mutual-exclusion patterns were also observed between *Aquaspirillum* and five features assigned to *Chloromonas*. When holistically assessed, co-occurrence patterns prevailed within the bacterial kingdom. On the contrary, mutual exclusions prevailed within the investigated members of the *Chlorophyta* phylum and features assigned to different genera.

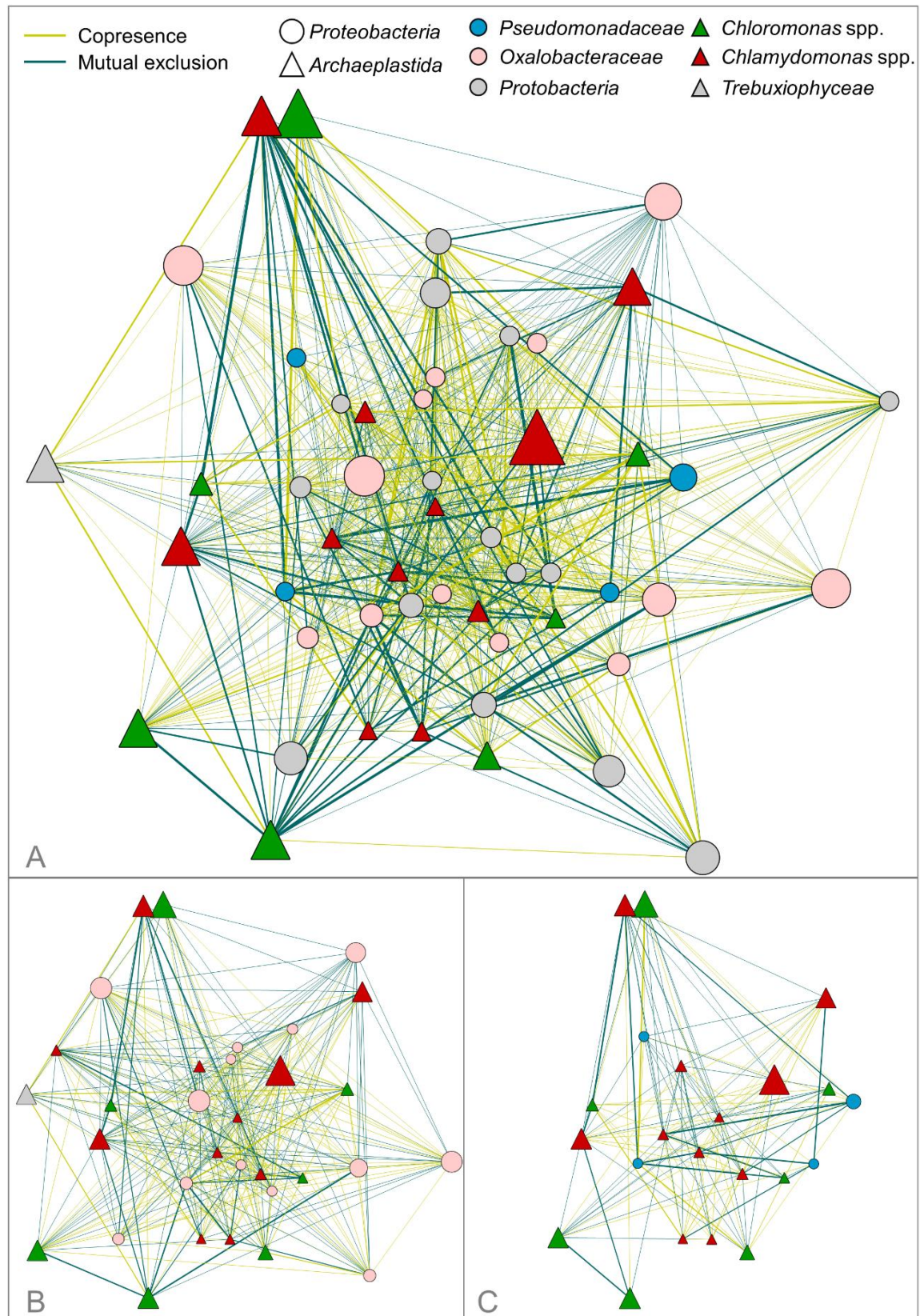


Figure 1.5. Co-occurrence network analyses of bacterial and eukaryotic taxa found on differently colored snowfields. Significant ($p < 0.0004$; $q < 0.0004$) co-occurrences (green edges) and mutual exclusion patterns (blue edges) between features assigned to *Proteobacteria* and *Archaeplastida* (A) are displayed. The node size corresponds to the relative abundance of respective taxa. The edge width indicates the significance of interactions. The co-occurrence network was reduced in order to highlight interactions between algae and *Oxalobacteraceae* (B) and *Pseudomonadaceae* (C).

Correlation analyses suggest specific mutualistic inter-kingdom associations

Complementary correlation analyses between abundances of bacterial and algal genera on snowfields showed distinct clustering (Figure 1.6.A); *Chrysophyceae* showed strong positive correlations with *Pedobacter*, *Clostridium*, *Sediminibacterium* and *Nakamurella*, while negative correlations were observed with *Aquaspirillum*, *Chryseobacterium* and *Rhizobium*. On the contrary, those taxa (*Aquaspirillum*, *Chryseobacterium* and *Rhizobium*) correlated positively with *Chlamydomonas*. For *Chloromonas* strong correlations were identified with the bacterial genera *Ferruginibacter* and *Hymenobacter*. Kendall's tau rank correlation analyses of occurrences of microalgae (*Chlorophyta*, *Chrysophyta*) and basidiomycetous yeasts found on snowfields revealed similar results in terms of genus-specificity (Figure 1.6.B). The strongest positive correlations were found between *Chrysophyceae* and several yeasts including the genera *Mrakia*, *Filobasidium*, *Hamamotoa*, *Sporobolomyces* and *Dioszegia*. *Chloromonas* showed strong positive correlations with *Leucosporidium*, while *Chlamydomonas* spp. correlated positively with *Rhodotorula*.

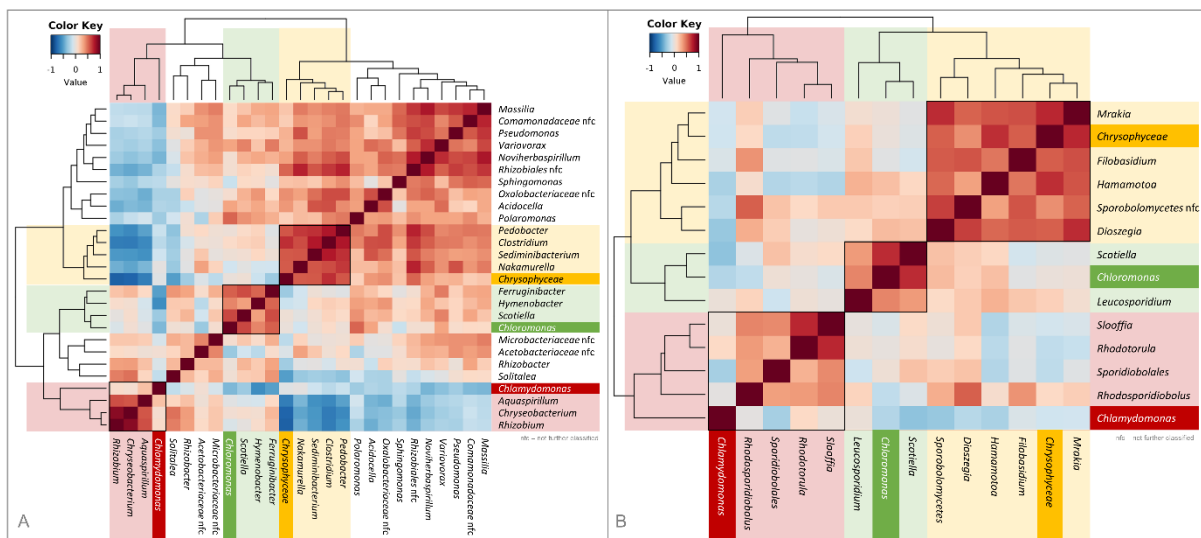


Figure 1.6. Kendall rank correlation structures between genera abundances of microalgae and their associated bacteria (A) and fungi (B) on differently colored snowfields. Distinct correlations of microalgae and their associated bacteria (A) and basidiomycetous yeasts (B) were observed for all investigated microalga genera. Correlations were calculated for microalgal (*Chlorophyceae*, *Chrysophyceae*) and bacterial features with an abundance $\geq 0.1\%$ in the snowfield samples (A). To identify correlations between algae and basidiomycetous yeasts, features assigned to *Basidiomycota* were manually blasted against the NCBI nucleotide collection. Features with the same taxonomic assignment at genus level were combined. The analyses are based on Kendall's tau rank correlation.

Physiological characterization of bacteria isolated from snowfields and freshwater

The cultivable fraction of the bacterial community isolated from snowfields and freshwater ponds were screened for their potential to produce siderophores and auxins. In total 470 bacterial isolates were tested for their physiological properties attributable to microalgae growth-promotion. A total of 52% tested isolates produced more than 3 µg/mL quantifiable auxins, whereas 12% excreted more than 15 µg/mL auxins into the cultivation media. When assessing the potential of bacterial isolates to produce siderophores, 34% of all tested isolates showed positive results. In a complementary co-cultivation approach with bacterial isolates, nine strains were identified, which significantly increased the biomass formation of *C. vulgaris* BRK1. The observed growth promotion ranged between 55% and 163% with the employed model algae (Supplementary Table S1.3). Six of the promising strains were isolated from snowfields while three derive from freshwater samples. All isolates were identified as *Proteobacteria* by Sanger sequencing of 16S gene fragments; seven were identified as *Pseudomonas* spp. (five originated from red snowfields and two from freshwater samples). The remaining two isolates were assigned to *Aeromonas salmonicida*. (*Gammaproteobacteria*, *Aeromonadaceae*) isolated from freshwater and *Janthinobacterium* sp. – a member of the family of *Oxalobacteraceae* (*Betaproteobacteria*) isolated from an orange snowfield. Further characterization of growth-promoting strains revealed that two isolates (*A. salmonicida* and *P. trivialis*, both isolated from freshwater taken at sampling site A) possess the ability to produce AHL. The evolutionary history of all growth-promoting isolates is displayed in Supplementary Figure S1.2. Supplementary Table S1.3 includes the detailed results of the physiological characterization of the most promising algae-growth promoting bacterial isolates.

Discussion

To date very few studies exist targeting microalgae-associated microbiomes in their natural environment. We have selected an extreme environment to study so far unexplored interactions between prevalent microalgae and their associated microbiota. By investigating the bacterial and eukaryotic community structure on differently colored snowfields and in freshwater samples, a habitat-specific and location-independent bacterial and eukaryotic community composition was revealed. Since for freshwater samples a nested amplification approach was necessary to meet the requirements for sequencing, a direct comparison of abundances and diversity was not possible between snowfields and freshwater samples. However, freshwater samples served as reference in order to point out the expected difference in community compositions between terrestrial (snowfields) and limnetic (lakes) ecosystems.

The inter-kingdom, co-occurrence network analyses indicated a prevalence of negative co-occurrence between microalgae on snowfields; microalgae most likely exclude each other by competing for nutrients and space following the competitive exclusion principal (Hardin, 1960). Co-occurrence analyses of *Archaeplastida* and members of the bacterial families *Pseudomonadaceae* and *Oxalobacteraceae* indicates genus-specific algae-bacteria co-occurrences; similar genotype-specific interactions have already been frequently described between higher plants and their associated microbiota. Moreover, we could demonstrate that the color of the snowfields reflects the bacterial as well as the eukaryotic microbiota, where the correlation is stronger for the eukaryotic community composition. Although the high abundant eukaryotic microbiota shows different community patterns between red snowfields sampled at different sites, statistical analyses considering the total community composition and their phylogenetic relationships, no significant differences in eukaryotic community compositions were revealed. The sampling site had a minor and not significant effect on both, the bacterial and eukaryotic community composition on snowfields as well as in freshwater. When Segawa and co-workers investigated algal communities on red colored snow in the Arctic and Antarctic by amplicon sequencing of the ITS2 fragment, they could show that bipolar taxa account for more than 37% of all reads, indicating the location-independent colonization of algae on snow (Segawa *et al.*, 2018). Our results lead to the extended hypothesis that the structure of the microbial communities on snowfields might be partially driven by the occurrence of certain microalgal species.

Deepening analyses revealed *Chlamydomonas* and *Chloromonas* as the most abundant microalgal genera in red and green snowfields respectively, both being typical colonizers of snow (Hamilton and Havig, 2017; Remias *et al.*, 2005; Seckbach, 2007). During its life cycle *Chlamydomonas nivalis* undergoes different physiological states; while vegetative cells appear as green, oval-shaped, motile, bi-flagellated cells, the microalgae form purple/red colored spores in their resting stage (Stibal *et al.*,

2007). Changes in color are explained by the accumulation of secondary carotenoids in order to provide protection against excessive light and stressful environmental conditions (Bidigare *et al.*, 1993). Green colored snowfields inhabited by *C. nivalis* are rarely found, as flagellated cells have a very short reproductive phase before they form spores to better resist excessive irradiation, desiccation, low nutrient concentrations, and freeze-thaw cycles (Lutz *et al.*, 2015). Davey and colleagues investigated the bacterial and eukaryotic community structures on red and green snow in Antarctica, where they could not find significant differences in the bacterial and eukaryotic community structure of differently colored snowfields. The authors state, this might be due to the fact that the green, vegetative algal cells are precursors for red mature cells (Davey *et al.*, 2019). In our study, the green color derives likely from *Chloromonas* spp. which are frequently detected on green snowfields; therefore, we assume that green and red snowfields are not always successive stages, but also can reflect independent phenomena. Results of cultivation-independent analyses are strongly supported by microscopic observations; distinct algal cell morphologies were observed for differently colored snow. The most abundant algal taxa found on orange colored snowfields were identified as members of the phylum *Ochrophyta*, in particular *Spumella*-like flagellates (*Chrysophyceae*). Previous studies identified members of the *Chrysophyceae* class as snow inhabitants causing yellowish coloration, that results from pigments involved in the xanthophyll cycle, which is used by chrysophytes snow algae to cope with excessive light energy (Remias *et al.*, 2013; Tanabe *et al.*, 2011).

Explorations of the bacterial community structure on differently colored snowfields revealed *Solitalea korensi* (*Sphingobacteriaceae*) as the most abundant taxon in red and green snowfields. *Polaromonas* spp., *Aquaspirillum* spp. and *Hymenobacter* spp. were amongst the most abundant genera in these snowfield. The bacterial community in orange snow was dominated by *Massilia psychrophila*, a member of the *Oxalobacteraceae* family followed by *Glaciimonas alpine*, which belongs to the same bacterial family. They are all common inhabitants of polar and alpine environments and indicators for a highly specialized community in psychrophilic environments. The two prevalent bacterial phyla *Proteobacteria* and *Bacteroidetes* share the ability to rapidly degrade organic matter which may underpin a potential direct transfer of organic carbon from algae to bacteria (Abell and Bowman, 2005). Different members of these bacterial lineages are able to degrade complex organic structures and thus feed on dead algae cells and residual cell walls. Our results are in accordance with findings from previous studies investigating the bacterial and eukaryotic community composition on snowfields in the Pacific Northwest and in Japan (Hamilton and Havig, 2017; Terashima *et al.*, 2017). Since highly similar community structures were identified at globally dispersed sampling sites, we assume highly conserved, evolutionary evolved, mutualistic relationships between certain microalgae and bacteria.

In addition to eukaryotic features assigned to *Archaeplastida*, also members of the fungal phylum *Basidiomycota* prevailed on distinct snowfields. The most prominent features included species assigned to the genera *Rhodotorula*, *Leucosporidium*, and *Mrakia*. All of these taxa were previously reported as prominent inhabitants of cryospheres (Brown *et al.*, 2015; Ruisi *et al.*, 2007; Singh *et al.*, 2014). They are specialized to persist under extreme environmental conditions due to changes in the composition of membrane lipids, production of different cryoprotectants, and additional metabolic adaptations (Buzzini *et al.*, 2012). Few literature is available elucidating fungal and algal co-occurrences and interactions on snow. Our results are in accordance with previous findings, where species of the genus *Rhodotorula* have been described as enriched co-inhabitants of algae in red colored snow in the United States (Brown *et al.*, 2015), while *Leucosporidium* and *Chloromonas* co-occurred on snow in the Canadian High Arctic (Harding *et al.*, 2011). The ability of *Rhodotorula* to assimilate various carbon sources suggests opportunistic utilization of organic matter excreted by snow algae (Singh *et al.*, 2014). Several species of the highly abundant genera *Rhodotorula*, *Leucosporidium* and *Rhodosporidium* are able to produce rhodotorulic acid, a highly efficient iron chelating agent (Atkin *et al.*, 1970; Miller, 1989). Furthermore, species of those genera have traits attributable to plant growth-promotion (Ignatova *et al.*, 2015; Wang *et al.*, 2016a; Xin *et al.*, 2009) and thus may support algal communities in a mutualistic relationship. Basidiomycetous yeasts have also been identified as part of the lichen holobiont where close associations between basidiomycete lineages and specific lichen species are prevalent (Spribille *et al.*, 2016). Correlation analyses between abundances of microalgae (*Chlorophyta* and *Chrysophyta*) and yeasts on differently colored snowfields indicated that the presence of certain microalgae structures the co-occurring fungal community on snow.

In the present study, significant differences between bacterial and eukaryotic community compositions in alpine freshwater and snowfield samples were observed. This further reinforced the finding that community structures in alpine systems are primarily habitat-specific and less affected by the geographic location of the sampling site, which had a minor and not significant effect. The eukaryotic community in freshwater was dominated by *Chlamydomonas angulosa* followed by members of *Chromista*. According to a study conducted by Gómez-Pereira and colleagues, members of *Sphingobacteria*, which were highly abundant bacterial taxa in freshwater samples, can attach to algae cells as they contain several surface adhesion proteins and peptidases for degradation of algae exudates (Gómez-Pereira *et al.*, 2012). This suggests a well-adapted co-existence of these microorganisms in aquatic systems. By attaching to the algae's surface, bacteria can feed more efficiently on carbon released by algae in their phycosphere and in return provide essential nutrients and vitamins to the algae (Gómez-Pereira *et al.*, 2012).

Complementary growth promotion experiments with the industrially relevant microalga *C. vulgais* that were included in the present study, facilitated to identification of nine promising isolates that positively contributed to the model algae's growth; seven of those isolates were identified as *Pseudomonas* spp. In a related study, Fu and colleagues (Fu *et al.*, 2018) investigated the interactions between *Pseudomonas* sp. strain SI-3 and the microalgae *Ulva prolifera* and found several bacterial genomic traits contributing to their symbiotic relationship. In contrast, members of the bacterial family *Pseudomonadaceae* have also been reported to be able to produce algicidal compounds, indicating the specificity of growth-promoting and detrimental effects on different algae (Kim *et al.*, 2018; Noh *et al.*, 2017). These findings are also reflected by our co-occurrence network analyses where positive interaction between *Pseudomonadaceae* and *Chloromonas* spp. prevailed, while negative inferences were calculated between *Pseudomonadaceae* and *Chlamydomonadaceae*. *Pseudomonas* spp. are prominent siderophore producers (Cornelis and Matthijs, 2002; Essén *et al.*, 2007), which allows them to provide chelated iron to microalgae. As all organisms require iron as cofactor for metabolic enzymes and mediator for redox reactions and electron transfer, it is an essential micronutrient to maintain life (Cassat and Skaar, 2013; Miethke and Marahiel, 2007). While microalgae themselves are not able to produce siderophores, because they lack genes involved in siderophore synthesis, they often rely on iron from bacterial chelates in seawater (Hopkinson and Morel, 2009). Amin and colleagues demonstrated a "carbon for iron mutualism" as dinoflagellate algae were involved in assimilation of iron complexed in siderophores and in return released dissolved organic matter (DOM) in their surrounding and thereby support bacterial growth (Amin *et al.*, 2009, 2012b, 2015). Except one growth-promoting isolate (*P. veronii*) all identified *Pseudomonas* spp. produced siderophores, indicating their possible contribution to the fitness of microalgae communities. Auxins – an important class of phytohormones – are known to promote growth of plants by stimulating cell division, growth, leaf formation, root development, and fruit setting (Finet and Jaillais, 2012). Several studies focused on the effects of phytohormones on the performance and fitness of microalgae whereby improved biomass formation and lipid production were observed (Bajguz and Piotrowska-Niczyporuk, 2014; de-Bashan *et al.*, 2008; Liu *et al.*, 2016; Ozioko *et al.*, 2015; Yu *et al.*, 2017). All but one growth-promoting bacteria isolated in the course of the present study produced auxin (> 5 µg/ml). Only one of the promising *Pseudomonas* strains also showed the ability to produce N-acylhomoserine lactones. AHL is one of the most common signal molecules involved in cell-to-cell communication systems like quorum sensing (Waters and Bassler, 2005). In the context of microalgae, Rivas and colleagues analyzed the interactions of *Botryococcus braunii* and its associated bacteria in a mass cultivation system and found two AHL producing bacterial species embedded in biofilms of the algal cell surface (Rivas *et al.*, 2010). One of these strains significantly increased microalgal growth, suggesting involvement in inter-kingdom-signaling processes. In addition, it was hypothesized that biofilm forming bacteria adhering

to the algae's surface might enhance bioavailability of certain beneficial or essential compounds due to close proximities of consumer and producer. Although cultivation dependent analyses were conducted under industrially relevant conditions, compared to adverse *in situ* conditions, our complementary results provide evidence for evolutionary evolved relationships with inter-kingdom supportive capacities in alpine systems. However, profound identification of algae-bacteria/algae-fungi interactions requires further experiments and was out of scope of the present study.

In natural habitats, algae-bacteria interactions are complex and essential for both partners. By investigating evolutionary evolved microbiome-microalgae associations in an extreme environment, we aimed to deepen the knowledge of specific algae-bacteria interactions. The goal was to provide a basis for the design of synthetic bacterial consortia with beneficial effects on microalgae as a promising tool for biotechnological productions. We found, that mutualistic associations involving members of three different kingdoms are i) highly prevalent in the investigated alpine system, ii) directed in terms of the specificity of the interacting partners, and iii) that positive algae-bacteria interactions are highly efficient in increasing microalgal biomass without additional nutrient supply. Furthermore, we have identified different members of *Proteobacteria*, especially *Pseudomonas* spp. as cultivable constituents of the microbiome that can be employed to increase algal growth in artificial systems. These findings can be further exploited to increase yields and to provide stability together with reproducibility in industrial microalgae cultivation systems by targeted co-inoculations with compatible bacterial strains.

Supplementary Material

Table S1.1. Taxonomic assignment of highly abundant features within the 19S rRNA gene amplicon dataset. The mean relative abundance [%] for the respective group of samples is shown, including closest taxonomic assignment when blasting sequences against the NCBI nucleotide collection database. Darker colors indicate higher abundances of respective feature.

| Feature ID | Green snowfield | Red snowfield | Orange snowfield | Freshwater | Species | Family | Order | Class | Phylum |
|-----------------------------------|-----------------|---------------|------------------|------------|-------------------------------------|---------------------|---------------------|---------------------|---------------------|
| c0ff0505b4615b7e5ade5e1bca8e04b2 | 10.39 | 16.42 | <0.00 | 5.85 | <i>Chlamydomonas nivalis</i> | Chlamydomonadaceae | Chlamydomonadales | Chlorophyceae | Chlorophyta |
| 448c7b32f300024bc31e4b505d26605d | 3.39 | 18.31 | 5.94 | 1.75 | <i>Rhodotorula glutinis</i> | Sporidiobolaceae | Sporidiobolales | Microbotryomycetes | Basidiomycota |
| dd38b973c46378b067c9e51a51feb7be | 2.54 | 11.59 | 2.05 | 3.96 | <i>Slooffia cresolica</i> | Sporidiobolaceae | Sporidiobolales | Microbotryomycetes | Basidiomycota |
| 818f5dd22a66b73b51b811eabd35b63 | 0.01 | 0.01 | 0.00 | 9.12 | <i>Chlamydomonas angulosa</i> | Chlamydomonadaceae | Chlamydomonadales | Chlorophyceae | Chlorophyta |
| 44f43de574acf89e75ee02d1329e226c | 2.87 | 10.56 | <0.00 | 0.14 | <i>Leucosporidium antarcticum</i> | Leucosporidiaceae | Leucosporidiales | Microbotryomycetes | Basidiomycota |
| 920e8ad1272bf3b4e234533b72bed8f7 | 16.02 | 1.33 | 5.13 | 0.30 | <i>Leucosporidium antarcticum</i> | Leucosporidiaceae | Leucosporidiales | Microbotryomycetes | Basidiomycota |
| b06392de347d1cd0f4b357b012644e93 | <0.00 | 0.12 | 20.38 | 0.72 | <i>Mrakia frigida</i> | Mrakiaceae | Cystoflobasiales | Tremellomycetes | Basidiomycota |
| 15ff9eb7803479bb1c6bec335aefa7e | 0.00 | 0.00 | 0.00 | 5.87 | <i>Synedra berolinensis</i> | Fragilariaceae | Fragilariales | Bacillariophyceae | Bacillariophyta |
| 3002a1b9d3a1f003165347ea9c6f08a0 | 0.00 | <0.00 | 0.07 | 5.74 | <i>Spumella</i> sp. | Chromulinaceae | Chromulinales | Chrysophyceae | Stramenopiles |
| f66edbf1c5a94e9041ab838892e3b790 | 0.51 | 6.65 | 0.21 | 0.11 | <i>Chloromonas</i> sp. | Chlamydomonadaceae | Chlamydomonadales | Chlorophyceae | Chlorophyta |
| 1a9d461418f16b421c86dffcbcc9888aa | 5.14 | 3.88 | 2.19 | 0.43 | <i>Rhodotorula glutinis</i> | Sporidiobolaceae | Sporidiobolales | Microbotryomycetes | Basidiomycota |
| 029a9185e535a94f2300b07860205bd5 | 15.52 | 0.13 | 0.05 | 0.08 | <i>Chloromonas actinochloris</i> | Chlamydomonadaceae | Chlamydomonadales | Chlorophyceae | Chlorophyta |
| 08610d18bc3ca811a714e6b408f20b | 14.40 | 0.01 | 0.15 | 0.17 | <i>Chloromonas nivalis</i> | Chlamydomonadaceae | Chlamydomonadales | Chlorophyceae | Chlorophyta |
| 6ed5b6524bb2fa2aedbd829c72fa9eb9 | 3.33 | 2.33 | 0.00 | 1.11 | <i>Chlamydomonas nivalis</i> | Chlamydomonadaceae | Chlamydomonadales | Chlorophyceae | Chlorophyta |
| 2aa10d1c98c0729a9e862653855f8697 | 0.00 | 0.00 | 0.00 | 3.61 | <i>Malassezia globosa</i> | Malasseziaceae | Malasseziales | Exobasidiomycetes | Basidiomycota |
| eab9f2270b7b787b648c39c3f12966a | 6.50 | 0.05 | 0.05 | 1.88 | <i>Leucosporidium antarcticum</i> | Leucosporidiaceae | Leucosporidiales | Microbotryomycetes | Basidiomycota |
| b0e596639c7d1fc7131b11423593126c | 0.42 | 2.48 | 1.99 | 0.29 | <i>Rhodospiridiobolus fluvialis</i> | Sporidiobolaceae | Sporidiobolales | Microbotryomycetes | Basidiomycota |
| 90115a7ba5901e5cc3ab8d485e0df0d7 | 0.00 | 0.00 | 0.00 | 2.75 | <i>Peronospora belbahrii</i> | Peronosporaceae | Peronosporales | Oomycetes | Oomycota |
| 9b6eea2c450e59d3ac8d45a43cc300b1 | 0.21 | 2.09 | 0.40 | 0.72 | <i>Rhodotorula glutinis</i> | Sporidiobolaceae | Sporidiobolales | Microbotryomycetes | Basidiomycota |
| af55015aaf3ad1630fac766d8e43e13e | 0.00 | 0.02 | 7.40 | 0.28 | Fungal sp. | unclassified fungus | unclassified fungus | unclassified fungus | unclassified fungus |

Table S1.2. Taxonomic assignment of highly abundant features within the 16S rRNA gene amplicon dataset. The mean relative abundance [%] for the respective group of samples is shown, including closest taxonomic assignment when blasting sequences against the NCBI nucleotide collection database. Darker colors indicate higher abundances of respective feature.

| Feature ID | Green snowfield | Red snowfield | Orange snowfield | Freshwater | Species | Family | Order | Class | Phylum |
|-----------------------------------|-----------------|---------------|------------------|------------|--------------------------------------|---------------------|--------------------|---------------------|----------------|
| 564adb46dc431643b5234c74c867503c | 19.21 | 30.52 | 0.01 | <0.00 | <i>Solitalea koreensis</i> | Sphingobacteriaceae | Sphingobacteriales | Sphingobacteria | Bacteroidetes |
| 60082725460ec2576c151294f7526b68 | 6.12 | 12.41 | 0.00 | <0.00 | <i>Solitalea koreensis</i> | Sphingobacteriaceae | Sphingobacteriales | Sphingobacteria | Bacteroidetes |
| d6cbeeffd6a3ac4426b3e-ddbf834f6a7 | 0.59 | 13.84 | <0.00 | 0.00 | <i>Solitalea koreensis</i> | Sphingobacteriaceae | Sphingobacteriales | Sphingobacteria | Bacteroidetes |
| 2d233d8565b9e009f0b9a8168c1af830 | 15.45 | 4.11 | 5.65 | 0.02 | <i>Aquaspirillum arcticum</i> | Neisseriaceae | Neisseriales | Betaproteobacteria | Proteobacteria |
| bb329a9d1474d8a2344dbb881.14fc03 | 1.38 | 0.44 | 23.49 | 0.33 | <i>Massilia psychrophila</i> | Oxalobacteraceae | Burkholderiales | Betaproteobacteria | Proteobacteria |
| 861e0a55a13a33bb77e42809320cdd04 | 11.19 | 2.76 | 0.01 | <0.00 | <i>Hymenobacter lapidarius</i> | Flavobacteriaceae | Flavobacteriales | Flavobacteria | Bacteroidetes |
| 347cca0dd59c45fffa1320818250ce64 | 0.22 | 4.77 | 0.00 | 0.00 | <i>Solitalea koreensis</i> | Sphingobacteriaceae | Sphingobacteriales | Sphingobacteria | Bacteroidetes |
| 83f680f6221facbcdaddc6788b83a1b | 11.48 | 0.12 | 0.18 | 27.93 | <i>Sphingomonas echinoides</i> | Sphingomonadaceae | Sphingomonadales | Alphaproteobacteria | Proteobacteria |
| 740f59085004b6d15b55d1dc7e61c7dea | 8.68 | 1.05 | 0.00 | 0.00 | <i>Aquaspirillum arcticum</i> | Neisseriaceae | Neisseriales | Betaproteobacteria | Proteobacteria |
| a924253e03a8e32c319f7ace4c3e4acc | 1.28 | 3.22 | 0.22 | <0.00 | <i>Ferruginibacter paludis</i> | Chitinophagaceae | Sphingobacteriales | Sphingobacteria | Bacteroidetes |
| b7690f942b90ae2547fedeeaa9f94ff9 | 0.06 | 0.35 | 7.66 | 0.02 | <i>Glacilimonas alpina</i> | Oxalobacteraceae | Burkholderiales | Betaproteobacteria | Proteobacteria |
| 9df43f8481c60436961214944679522e | 0.01 | 2.03 | 1.85 | 0.11 | <i>Massilia eurypsychrophila</i> | Oxalobacteraceae | Burkholderiales | Betaproteobacteria | Proteobacteria |
| fd797ac1c36a415f9daa21fa5ff79f | 0.00 | 0.13 | 7.24 | 0.10 | <i>Massilia psychrophila</i> | Oxalobacteraceae | Burkholderiales | Betaproteobacteria | Proteobacteria |
| 9daf1aa1f8c64060a6213a2d9eccb54d | 0.01 | 1.87 | 1.70 | 0.00 | <i>Parasediminibacterium paludis</i> | Chitinophagaceae | Sphingobacteriales | Sphingobacteria | Bacteroidetes |
| abbaa41465a3250f40e64f76fe2b6606 | <0.00 | 2.39 | 0.00 | 0.00 | <i>Solitalea canadensis</i> | Sphingobacteriaceae | Sphingobacteriales | Sphingobacteria | Bacteroidetes |
| 7b877ef3195b709308275f4a69d3fc41 | 0.20 | 1.85 | 0.96 | 0.00 | <i>Ferruginibacter paludis</i> | Chitinophagaceae | Sphingobacteriales | Sphingobacteria | Bacteroidetes |
| aed49d1bac57b960398e066fbc4b3c43 | 4.83 | 0.21 | 0.79 | 0.06 | <i>Polaromonas jejuensis</i> | Comamonadaceae | Burkholderiales | Betaproteobacteria | Proteobacteria |
| 2167a4bd43cfc77b8a5ee0dc0a6c1c4 | 0.52 | 1.76 | 0.13 | <0.00 | <i>Helimonas saccharivorans</i> | Chitinophagaceae | Sphingobacteriales | Sphingobacteria | Bacteroidetes |
| d7fc725cfc10426d401ea2a9e3729671 | 5.53 | <0.00 | 0.00 | 7.75 | <i>Psychromicrobium silvestre</i> | Micrococcaceae | Micrococcales | Actinobacteria | Actinobacteria |
| 10530664a462938c5f77b52cc03e801 | 4.03 | <0.00 | 0.00 | 0.00 | <i>Hymenobacter lapidarius</i> | Flavobacteriaceae | Flavobacteriales | Flavobacteria | Bacteroidetes |

Table S1.3. Detailed results of growth promotion experiments with *C. vulgaris* and bacterial strains isolated from snowfields and freshwaters. Experiments were performed in 18-fold replication; results which reached level of significance ($p < 0.05$) are shown. Increased algal biomass formation is given in percentage compared to axenic microalgae culture. ● Sampling site A (Rottenmanner Tauern); ■ Sampling site B (Seetaler Alpen). Color represents habitat of bacterial isolates (red – red snowfield, orange – orange snowfield, blue – freshwater). The mean rel. abundance for representative features in the 16S amplicon dataset is also included for the respective isolates.

| Origin | Isolate | Representative Feature ID | Increased algal biomass formation [%] | Siderophore production | Auxin production [$>5 \mu\text{g/mL}$] | AHL production | Mean rel. abundance [%] | | | |
|--------|------------------------------------|----------------------------------|---------------------------------------|------------------------|--|----------------|-------------------------|------------|-------------|-------------|
| | | | | | | | Red snow | Green snow | Orange snow | Fresh-water |
| ● | <i>Pseudomonas</i> sp. 1Ab3 | 51bdbc262c549bf4dd1bd63ead56862f | 81 ± 16 | + | + | - | 0.57 | 0 | 0.18 | 0.01 |
| ● | <i>Aeromonas salmonicida</i> 2Bb9 | e8a3eccd511ebdc315b734b16a3d4333 | 95 ± 25 | - | + | + | 0 | <0.00 | 0 | <0.00 |
| ● | <i>Pseudomonas trivialis</i> 2Ca3 | 51bdbc262c549bf4dd1bd63ead56862f | 63 ± 26 | + | + | + | 0.57 | 0 | 0.18 | 0.01 |
| ■ | <i>Pseudomonas antarctica</i> 3Ab1 | 51bdbc262c549bf4dd1bd63ead56862f | 55 ± 19 | + | + | - | 0.57 | 0 | 0.18 | 0.01 |
| ■ | <i>Pseudomonas</i> sp. 3Ac8 | 460abde6df34176fefbcf523245c58c9 | 108 ± 13 | + | + | - | 0.03 | 0 | 0 | 0 |
| ■ | <i>Pseudomonas</i> sp. 3Ea4 | 6428107321f281acb5d1dd6ddebcd54 | 136 ± 28 | + | - | - | 0.01 | 0 | 0.02 | 0 |
| ■ | <i>Pseudomonas</i> sp. 3Eb1 | 51bdbc262c549bf4dd1bd63ead56862f | 75 ± 27 | + | + | - | 0.57 | 0 | 0.18 | 0.01 |
| ■ | <i>Pseudomonas veronii</i> 3Ba6 | 66fe7b08aedb8be2f70da2d3bc1cf65d | 63 ± 25 | - | + | - | 0 | <0.00 | 0 | <0.00 |
| ■ | <i>Janthinobacterium</i> sp. 3Dc5 | 1ca898bc470ce685731f68ac29e95269 | 163 ± 24 | + | + | - | 0.06 | 0 | 0.75 | 0.02 |

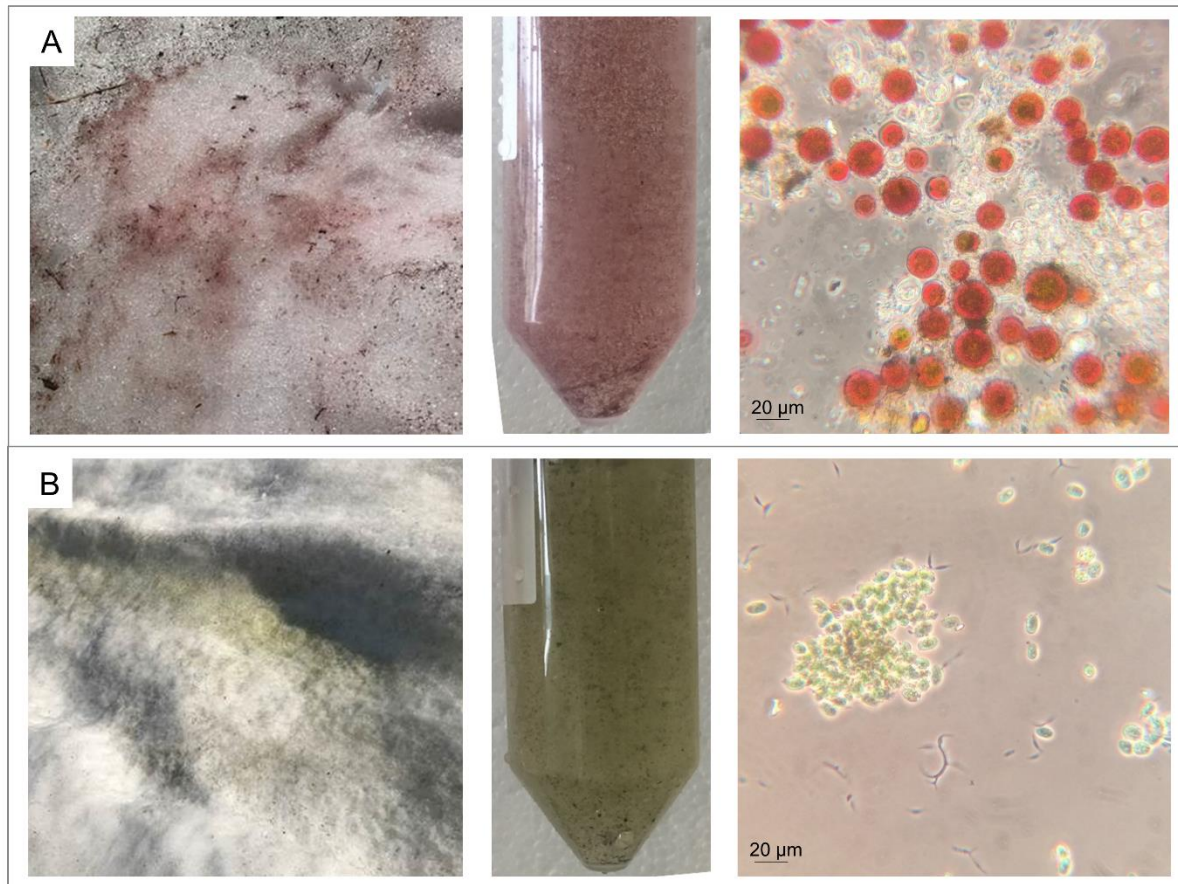


Figure S1.1. Red (A) and green (B) snowfield sampled at site A (Rottenmanner Tauern). Microscopic observation of melted snow gave first evidence of the presence of different microalgal species on differently colored snowfields.

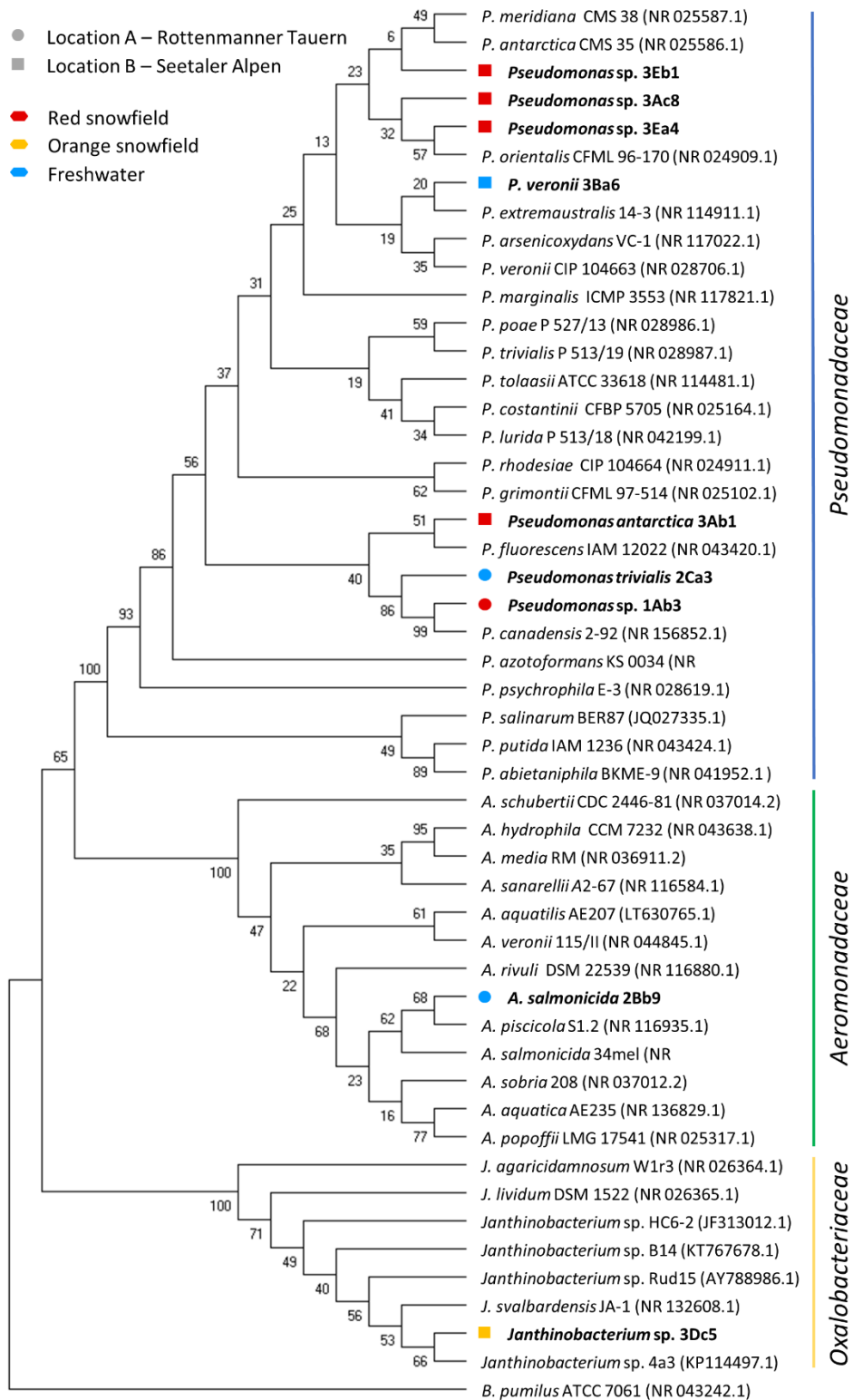


Figure S1.2. Phylogenetic tree based on 16S rRNA gene fragment alignments, showing the positions of the isolates with microalgae growth-promoting properties among other isolates of *Pseudomonas*, *Aeromonas* and *Janthinobacterium*. The percentage of replicate trees in which the associated taxa clustered together in the bootstrap test (1000 replicates) are shown next to the branches. The analysis involved 50 nucleotide sequences. All ambiguous positions were removed for each sequence pair (pairwise deletion option). *B. pumilus* was used as outgroup. GenBank accession numbers are shown in parentheses.

CHAPTER 2

PLANT GROWTH-PROMOTING METHYLOBACTERIA INCREASE THE BIOMASS OF BIOTECHNOLOGICALLY RELEVANT MICROALGAE

Lisa Krug^{1,2}, Christina Morauf³, Christina Donat³, Henry Müller², Tomislav Cernava^{2*}, Gabriele Berg²

¹Austrian Centre of Industrial Biotechnology, Graz, Austria

²Institute of Environmental Biotechnology, Graz University of Technology, Graz, Austria

³bio-ferm GmbH, Erber Campus 1, 3131 Getzersdorf, Austria

Abstract

Microalgae, a diverse group of single-celled organisms exhibiting versatile traits, find broad applications in industry e.g. as feedstock for biofuel production, as animal feed and pharmaceuticals, or as sustainable alternative to synthetic fertilizers. However, high production costs require further efforts to optimize fermentation and to enhance biomass yields. In naturally occurring microalgae biofilms, which were studied by complementary 16S rRNA gene fragment amplicon sequencing, algae showed a mutual co-occurrence network with methylobacteria. Therefore, four strains of the genus *Methylobacterium*, well-known for their plant growth-promoting traits, were studied in co-cultivation experiments to assess the effect on growth of three industrially relevant microalgae (*Chlorella vulgaris*, *Scenedesmus vacuolatus* and *Haematococcus lacustris*). After seven days of co-incubation, for *S. vacuolatus* and *H. lacustris*, a significant increase in algal biomass formation of 1.3-fold to up to 14-fold could be observed. Visualization of mixed cultures using confocal laser scanning microscopy revealed a high abundance of methylobacteria in the phycosphere of *H. lacustris* and *S. vacuolatus*, visually attached to algae's surface forming a biofilm-like "protection shield". Genome analyses revealed that features attributable to enhanced algal growth include genes involved in the synthesis of vitamins, siderophores and plant hormones. Our results support the hypothesis of symbiotic relationships of algae and bacteria with inter-kingdom supportive capacities, underlining the potential of microbial consortia as promising tool for sustainable biotechnology and agriculture.

Introduction

In the recent past, the potential of microalgae for industrial purposes increasingly gained importance at global scale. Due to their versatile characteristics including high lipid content and their ability to accumulate high-valuable compounds, they are used as feedstock for biofuel production, as animal feed and pharmaceuticals, or as sustainable alternative to synthetic fertilizers (Brennan and Owende, 2010; Renuka *et al.*, 2018; Spolaore *et al.*, 2006). In order to meet industrial demands, microalgae are cultivated either in open pond systems for bulk material production or in closed photobioreactors for the production of high-value compounds. However, under both cultivation conditions unwanted, co-occurring microorganisms such as bacteria, fungi, zooplankton or other weedy microalgae potentially disturb mass cultivations and can lead to a complete collapse of the cultures and thus rise production costs (Benemann and Oswald, 1996; Wang *et al.*, 2013). Especially for the production of biofuels, efforts need to be made in order to reduce costs and enhance biomass yields by optimizing cultivation conditions for an efficient microalgae cultivation that can compete with non-sustainable alternatives. One means of increasing microalgae populations and thus enhancing yields might be the co-inoculation with beneficial microorganisms as already successfully applied in agriculture for increasing yields of vascular land plants (Berg, 2009; Lugtenberg and Kamilova, 2009; Berg *et al.*, 2013). Algae benefit from micro- and macronutrients provided by the bacteria, and in return, release dissolved organic carbon into their surroundings. Efforts have been made in identifying bacteria which positively contribute to the algal fitness, especially nitrogen-fixing bacteria of the genera *Azospirillum*, *Rhizobium* and *Bacillus* known for their beneficial effect on plants score well (Gonzalez and Bashan, 2000; de-Bashan *et al.*, 2008; Hernandez *et al.*, 2009; de-Bashan and Bashan, 2010; Kim *et al.*, 2014; Amavizca *et al.*, 2017). However, less is known about the algae-associated microbiota as well as algae-microbe interaction of the members of the plant microbiome.

The species-specific plant microbiota forms complex networks and contributes multiple aspects to the functioning of the plant holobiont, such as (i) seed germination and growth, (ii) nutrient supply, (iii) resistance against biotic and abiotic stress factors, and (iv) production of bioactive metabolites (Berg *et al.*, 2017). To understand the complexity of microbial interaction patterns bioinformatic network- and co-occurrence analyses can be exploited (Barberán *et al.*, 2012), which allows to identify hub species, and explore the potential for diverse types of species interactions within the microbiome. The existence of specific types of microbial interactions and their consequences for population dynamics or functions, however, require testing in relevant model systems. Those mutualistic interkingdom networks are not only limited to land plants, but also extend to green algae (Hom *et al.*, 2015; Xie *et al.*, 2013). Following the same principles of plant growth-promoting rhizobacteria, algae-associated bacteria harbor potential to stimulate growth and morphogenesis of algae by releasing

essential minerals, vitamins, auxins and quorum sensing signaling molecules (Joint *et al.*, 2002; Croft *et al.*, 2006; Goecke *et al.*, 2010; Amavizca *et al.*, 2017). The equivalent to the rhizosphere – the immediate surrounding of roots with increased biological and chemical activity in soil – is the phycosphere, which is the area surrounding a phytoplankton cell, rich in dissolved organic matter and metabolites exuded by the cell in the surrounding water, stimulating the growth of heterotrophic bacteria (Seymour *et al.*, 2017). Less is known about the structure and function of the phycosphere microbiome, although studies show negative (Hom *et al.*, 2015) and positive impacts of bacteria on algal growth (Amin *et al.*, 2009; Cooper and Smith, 2015; Croft *et al.*, 2005; Hernandez *et al.*, 2009; Kim *et al.*, 2014).

In order to understand and exploit the phycosphere microbiota, we analyzed the naturally occurring microbiome of algae in a first step, and studied the algae-microbe interaction for selected bacteria in a second step. For the latter we used model organisms for industrial relevant microalgae *Chlorella vulgaris*, *Scenedesmus vacuolatus* and *Haematococcus lacustris* used as feedstock for biofuel production due to their high amount of carbohydrates and as source material for the production of astaxanthin, a strong antioxidant used as pharmaceutical (Sharma and Sharma, 2017; Khan *et al.*, 2018). The phycosphere microbiota study by 16S rRNA gene fragment amplicon sequencing provided evidence for natural co-occurrences of algae and methylobacteria. Therefore, plant-associated methylobacteria, which are already known for their plant-beneficial traits, were selected from our strain collection SCAM (Strain collection of antagonistic microorganisms, UBT at TU Graz). They belong to three different species, *Methylobacterium extorquens*, *M. mesophilicum* and *M. goesingense*, and were originally isolated from different plant species (Verginer *et al.*, 2010). Through co-cultivation experiments, the potential of methylobacteria to induce and promote the growth of microalgae was evaluated. In order to provide deeper insights into the mechanisms and bacterial features behind growth-promoting effects of beneficial bacteria, whole genomes of *M. extorquens* Rab1 and *M. mesophilicum* Sab1 were sequenced and analyzed. The obtained results provide the background for novel co-cultivation approaches that make use of inter-kingdom supporting capacities of beneficial, plant-associated bacteria.

Materials and Methods

Sampling procedure. Samples were collected on November 1st 2016 by removing a natural biofilm on the surface of outdoor furniture in Graz (Austria; 47° 4" N, 15° 26" O) at an altitude of 353 meter above sea level, in three replicates, where macroscopic observations and coloration of biofilm indicated the occurrence of microalgae (Supplementary Figure S2.1.A). Upon arrival in the laboratory, samples were resuspended in 3 mL sterile NaCl (0.85%) and visualized microscopically using a light microscope (Leitz, Wetzlar, Germany) at 200 × magnification (Supplementary Figure S2.1.B).

Isolation and identification of microalgae. In order to isolate microalgae, the resuspended samples were plated in dilution series on Bolds Basal Medium agar plates (BBM) containing 250 mg/L NaNO₃, 175 mg/L KH₂PO₄, 75 mg/L K₂HPO₄, 75 mg/L MgSO₄ × 7 H₂O, 25 mg/L CaCl₂, 25 mg/L NaCl, 2.6 mg/L H₃BO₃, 5 mg/L FeSO₄ × 7 H₂O, 8.8 mg/L ZnSO₄ × 7 H₂O, 1.4 mg/L MnCl₂ × 4 H₂O, 1.4 mg/L MoO₃, 1.6 mg/L CuSO₄ × 5 H₂O, 0.5 mg/L Co(NO₃)₃ × 6 H₂O, 0.5 mg/L EDTA, 0.3 mg/L KOH, 0.017 mg/L vitamin B₁₂, 0.013 mg/L 4-amino-benzoate, 0.003 mg/L biotin, 0.013 mg/L nicotinic acid, 0.017 mg/L hemicalcium-pentathenate, 0.05 mg/L pyridoxamine-HCl, 0.033 mg/L thiaminiumdichlorid, 0.0091 mg/L thioctic-acid, 0.01 mg/L riboflavin, 0.0049 mg/L folic acid and 18 g/L agar-agar. Vitamins and heat sensitive components were added after autoclaving by sterile filtration (0.20 µm pore size). In order to obtain pure cultures single algae colonies were repeatedly subcultured on BBM-agar and incubated at 23 °C at a light dark cycle (L:16/D:8). The lighting was supplied by cool-white fluorescent lamps TL-D 36W/840 REFLEX Eco (Philips, Amsterdam, Netherlands) with an intensity of 3,350 lm.

In order to identify isolated microalgae species, cells were resuspended in 300 µL 0.85% NaCl and transferred in sterile Eppendorf tubes filled with glass beads. After mechanical disruption using a FastPrep FP120 instrument (MP Biomedicals, Germany) suspensions were centrifuged at 3,000 rpm for 5 min. Supernatant served as template for the following PCR reaction. Partial 18S rRNA gene fragment was amplified using primer pair NS1 (5' - GTA GTC ARA RGC CTT GTC TC - 3') and NS8 (5' - TCC GCA GGT TCA CCT ACG GA - 3') in a reaction mix (30 µL) containing 16.2 µL ultrapure H₂O, 6 µL Taq&Go [5 ×], 1.2 µL of each primer [10 µM], 2.4 µL MgCl₂ [25mM] and 3 µL DNA template. The cycling program was adjusted to the following settings: 95°C, 10 min; 40 PCR products were then purified using the Wizard SV Gel and PCR-Clean-Up System (Promega Corporation, Madison, Wisconsin, USA) according to manufacturer's protocol. 18S rRNA gene fragments were sequenced by LGC genomics (Berlin, Germany) and subsequently aligned against the NCBI nucleotide collection database.

Algae-associated microbiome analyses using 16S rRNA gene fragment amplicon libraries

Total community DNA extraction and barcoding. Total community DNA of three biological replicates was extracted using the FastDNA Kit for Soil (MP Biomedicals, Heidelberg, Germany) according to the manufacturer's protocol. The 16S rRNA gene fragments were amplified in three technical replicates covering the hypervariable region 4 using the Unibac II 515f (5' - GTG YCA GCM GCC GCG GTA A - 3') and 806r (5' - GGA CTA CHV GGG TWT CTA AT - 3') primer pair (Caporaso *et al.*, 2011), which included sample-specific barcodes and Illumina sequencing adaptors. Peptide nucleic acid (PNA) was added to the PCR mix to prevent the amplification of mitochondrial (mPNA) and plastidial (pPNA) DNA from eukaryotes (Lundberg *et al.*, 2013). The PCR was performed by using a total volume of 30 µL containing 20.15 µL ultrapure water, 6 µL Taq&Go [5 ×], 1.2 µL of each primer (5 µM), 0.225 µL pPNA [100 µM], 0.225 µL mPNA [100 µM] and 1 µL DNA template. The cycling program was adjusted to an initial denaturation temperature at 96°C for 5 min, followed by 30 cycles of 96 °C for 1 min, 78 °C for 5 s, 54 °C for 1 min, and 74 °C for 1 min. The final extension was done at 74 °C for 10 min. The PCR products of all samples were quality checked by gel electrophoresis. Subsequently, the PCR products were purified using the Wizard SV Gel and PCR-Clean-Up System according to manufacturer's protocol. Equimolar DNA concentrations of each barcoded amplicon were sent for paired end Illumina HiSeq sequencing (read length: 2 × 300 bp) to GATC Biotech AG (Konstanz, Germany).

Bioinformatic analyses of 16S rRNA gene fragments amplicons. Initial data processing, including joining of forward and reverse read pairs was done using software package QIIME 1.9.1 (Caporaso *et al.*, 2010). After removing barcodes, primer and adapter sequences reads as well as metadata were imported into QIIME 2 (2018.11 release). Further analyses of sequencing data were performed using the QIIME 2 pipeline according to tutorials provided by the QIIME developers (Caporaso *et al.*, 2010). The DADA2 algorithm (Callahan *et al.*, 2016) was used to demultiplex and denoise truncated reads and remove chimeras. Taxonomic analyses are based on a Naïve-Bayes classifier trained on the SILVA 128 release database (Quast *et al.*, 2013) clustering at 99% similarity. After removing mitochondrial, chimeric and plastid sequences, the 16S rRNA dataset was normalized to 264,542 reads. A normalized feature table served as input for the OTU table (`make_out_network.py`) using QIIME 1.9.1. OTU-network was generated and rendered using Cytoscape version 3.7.0 (Shannon *et al.*, 2003). Features assigned to *Methylobacterium* were manually aligned against the NCBI nucleotide collection using the BLAST algorithm (Altschul *et al.*, 1990).

Evaluation of microalgae growth-promoting effects of *Methylobacterium* spp. through co-cultivation experiments

Bacterial strains and initial culture conditions. For growth assays *M. extorquens* Rab1 (deposited at DSMZ; DSM 21961), *M. mesophilicum* Sab1 (deposited at DSMZ; DSM 21962), *M. goesingense* Vab1 and *M. goesingense* Vab2 were selected from our strain collection SCAM (Strain collection of antagonistic microorganisms, UBT at TU Graz). They were originally isolated from different plant species (Verginer et al., 2010). Bacteria were cultured on MIS (methanol, inorganic salt) agar plates containing 1.8 g/L $(\text{NH}_4)_2\text{SO}_4$, 0.2 g/L $\text{MgSO}_4 \times 7 \text{H}_2\text{O}$, 1.4 g/L $\text{NaH}_2\text{PO}_4 \times 2 \text{H}_2\text{O}$, 1.9 g/L K_2HPO_4 and 18 g/L agar-agar. After autoclaving 5 mL/L methanol and 1 mL/L sterile filtered (0.20 μm pore size) trace element solution containing 500.0 mg/L EDTA, 200.0 mg/L $\text{FeSO}_4 \times 7 \text{H}_2\text{O}$, 10.0 mg/L $\text{ZnSO}_4 \times 7 \text{H}_2\text{O}$, 3.0 mg/L $\text{MnCl}_2 \times 4 \text{H}_2\text{O}$, 30.0 mg/L H_3BO_3 , 20.0 mg/L $\text{CoCl}_2 \times 6\text{H}_2\text{O}$, 1.0 mg/L $\text{CuCl}_2 \times 6 \text{H}_2\text{O}$, 2.0 mg/L $\text{NiCl}_2 \times 6 \text{H}_2\text{O}$ and 3.0 mg/L $\text{Na}_2\text{MoO}_4 \times 2 \text{H}_2\text{O}$ were added.

Co-cultivation to evaluate the potential of bacteria to promote microalgae growth. The effect of four different methylobacteria strains on the growth of three different microalgal genera, including *Chlorella*, *Scenedesmus* and *Haematococcus* was evaluated through co-cultivation experiments. In order to explore the effect of the bacterial load on the performance of the microalgae, bacteria were added in two different cell concentrations (OD_{600} 0.2 and OD_{600} 0.5) at the beginning of the experiments. Fluorescence intensity (FI) of algal cultures was determined after 7 days of incubation for all investigated microalgae and additionally after 14 days for *C. vulgaris* G1-G and *S. vacuolatus* G1-G. For the preparation of bacterial pre-cultures, 100 μL of the respective bacterial suspension were plated on 15 to 20 MIS agar plates. After 7 days of incubation at 30 °C bacterial lawn was harvested using sterile object slide, resuspended in NaCl (0.85%) and further used to achieve a final absorbance OD_{600} of 0.5 and 0.2 in the final volume. For *C. vulgaris* G1-G, co-culture experiments were performed in 12 replicates in 12-well plates containing a final volume of 3 mL vitamin depleted BBM medium (dBBM) containing 250 mg/L NaNO_3 , 175 mg/L KH_2PO_4 , 75 mg/L K_2HPO_4 , 75 mg/L $\text{MgSO}_4 \times 7 \text{H}_2\text{O}$, 25 mg/L CaCl_2 , 25 mg/L NaCl, 2.6 mg/L H_3BO_3 , 5 mg/L $\text{FeSO}_4 \times 7 \text{H}_2\text{O}$, 8.8 mg/L $\text{ZnSO}_4 \times 7 \text{H}_2\text{O}$, 1.4 mg/L $\text{MnCl}_2 \times 4 \text{H}_2\text{O}$, 1.4 mg/L MoO_3 , 1.6 mg/L $\text{CuSO}_4 \times 5 \text{H}_2\text{O}$, 0.5 mg/L $\text{Co}(\text{NO}_3)_3 \times 6 \text{H}_2\text{O}$, 0.5 mg/L EDTA, 0.3 mg/L KOH. Algal pre-cultures were obtained by inoculating 50 mL BBM with a single colony of the respective microalgae. When sufficient cell density was reached, culture served as inoculum for co-cultivation experiments to reach a final FI of 154 ± 29 , which corresponds to $5.08 \pm 0.94 \times 10^4$ CFU/mL. For *S. vacuolatus* G1-O growth experiments were performed as described for *C. vulgaris*. FI of algal cultures at the beginning of the experiments was adjusted to 152 ± 21 ,

corresponding to $3.51 \pm 0.47 \times 10^4$ CFU/mL. For *H. lacustris* G1-R, co-culture experiments were performed in 12 replicates in sterile 100 mL flasks sealed with aluminum foil containing a total volume of 10 mL dBBM. Algal pre-cultures were obtained by rinsing two BBM agar plates containing *H. lacustris* cultures with dBBM. The FI was adjusted to 33 ± 8 at the beginning of the experiments, corresponding to $7.04 \pm 1.65 \times 10^3$ algal CFU/mL.

All co-cultures were incubated at 23 °C at a light dark cycle (L:16/D:8). The lighting was supplied by cool-white fluorescent lamps TL-D 36W/840 REFLEX Eco (Philips, Amsterdam, Netherlands) with an intensity of 3,350 lm. Biomass formation was determined by measuring the fluorescence intensity at 685 nm when excited at 450 nm using an infinite M200 spectrofluorimeter (TECAN; Switzerland) after 7 days for all included algae and additionally after 14 days for *C. vulgaris* and *S. vacuolatus*. In order to conclude on algal cell count, the FI was determined and simultaneously algal CFUs were determined by plating respective dilutions on BBM agar. Applying a linear regression allowed the correlation between FI and microalgae cell count (*C. vulgaris* G1-G: $R^2 = 0.95$, Supplementary Figure 2.2.A; *S. vacuolatus* G1-O: $R^2 = 0.98$, Supplementary Figure 2.2.B; *H. lacustris* G1-R: $R^2 = 0.87$; Supplementary Figure 2.2.C).

Visualization of co-cultures. All microscopic visualizations were done using a Leica TCS SPE confocal laser scanning microscope (Leica Microsystems GmbH, Mannheim, Germany) and the oil immersion objectives Leica ACS APO 40.0 \times 1.15 (183.33 $\mu\text{m} \times$ 183.33 μm) and ACS APO 63 \times 1.30 (116.40 $\mu\text{m} \times$ 116.40 μm). Solid-state lasers were used with 405 nm, 488 nm, 532 nm, 635 nm excitation. The micrograph included in the OTU network was obtained with the natural community within the sampled biofilm following staining with the LIVE/DEAD bacterial viability kit (ThermoFisher Scientific, MA, USA) in combination with calcofluor white (0.15%; Sigma-Aldrich, Missouri, USA). Micrographs of co-cultures were obtained with *M. goeisingense* Vab1 and *C. vulgaris*, *S. vacuolatus* and *H. lacustris*, respectively, with an initial bacterial optical density of 0.5 after 7 days of incubation. For visualization of mixed cultures, 1 mL of the respective cultures were transferred into 1.5 mL reaction tubes and let stand for 2 to 3 hours to allow sedimentation of the microorganisms. The supernatant was discarded and the remaining cultures were stained using the LIVE/DEAD bacterial viability kit in combination with calcofluor white at a concentration of 0.15%.

Genome Analyses

Genomic DNA extraction. *M. extorquens* Rab1 and *M. mesophilicum* Sab1 were grown on solid MIS medium and incubated for 7 days at 30 °C. Cells were then collected from the plates using a sterile pipet tip and resuspended in 500 μL sterile NaCl (0.85%). Genomic DNA was extracted using the MasterPure DNA purification kit (Epicentre, WI, USA). DNA quality and quantity were checked by

agarose gel electrophoresis, fluorometry (Qubit 4, Thermo Fisher Scientific, MA, USA) and spectrophotometry using a UV-Vis spectrophotometer (NanoDrop 2000c, Thermo Fisher Scientific, MA, USA). Subsequently, genomic DNA of *M. extorquens* Rab1 (5.05 µg; 0.19 µg/mL) and *M. mesophilicum* Sab1 (8.02 µg; 0.30 µg/mL) was sent for Illumina NextSeq 500/550 V2 (150 bp paired-end sequencing; LGC Genomics GmbH, Berlin, Germany).

Genome assembly and annotation. The genomes of *M. extorquens* Rab1 and *M. mesophilicum* Sab1 were assembled using SPAdes (Bankevich *et al.*, 2012) and arranged into scaffolds. The scaffolds were then reassembled by using reference genomes (*M. extorquens* Rab1: NZ_CP021054.1; *M. mesophilicum* Sab1: NC_010505.1) and AlignGraph (Bao *et al.*, 2014) in order to extend and join scaffolds. The annotation was done by using the Rapid Annotation using Subsystem Technology (RAST; Aziz *et al.*, 2008).

Results

Microalgae and methylobacteria naturally co-occur in mixed-community biofilms

The bacterial fraction occurring in the microalgae-dominated biofilm was further investigated by 16S rRNA gene fragment amplicon sequencing. After removal of chimeric, mitochondrial and chloroplast sequences, 264,542 reads remained in the dataset, resulting in 92 features. The bacterial microbiome consisted of seven phyla with *Proteobacteria* (61%) being the most dominant followed by *Bacteroidetes* (32%) and *Cyanobacteria* (7%; Figure 2.1).

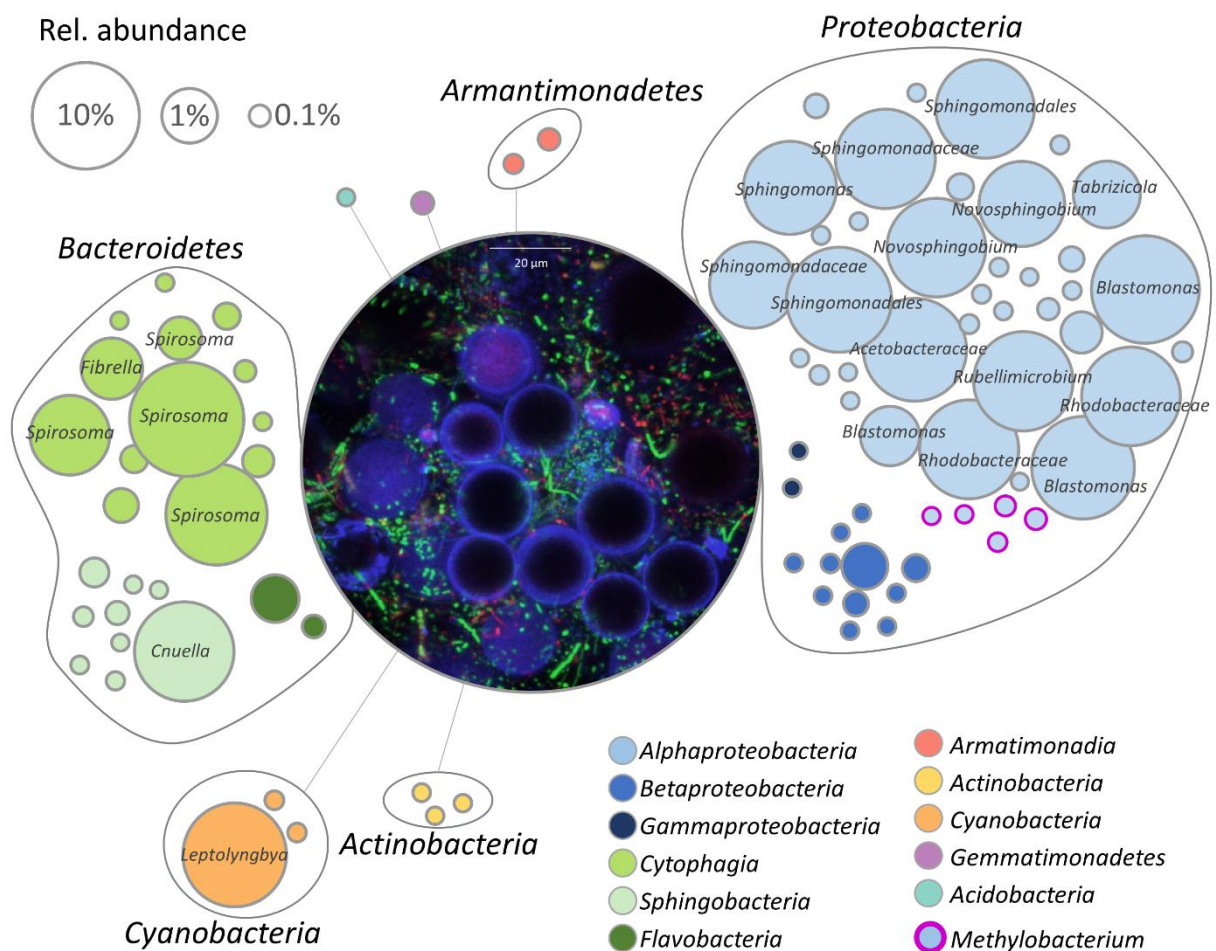


Figure 2.1. Network showing the bacterial community within the biofilm. Each node represents a feature (99% cut-off level), whereas the node size corresponds to their relative abundance. Taxonomy of highly abundant features (>1%) is included. The central micrograph shows the natural microbial community within the biofilm after staining using the LIVE/DEAD bacterial viability kit in combination with calcofluor white (0.15%). Blue: algal cell wall (cellulose, chitin), green: viable bacterial cells, red: dead bacteria.

Acidobacteria, *Actinobacteria*, *Armatimonadetes* and *Gemmatimonadetes* occurred in relative abundance less than 1%. On class level, *Alphaproteobacteria* (58%) were the dominating group followed by *Cytophagia* (27%) and *Cyanobacteria* (7%); *Sphingobacteriia* (4%), *Betaproteobacteria* (2%), *Flavobacteria* (1%), *Acidobacteria* (<1%), *Actinobacteria* (<1%), *Armatimonadia* (<1%) and

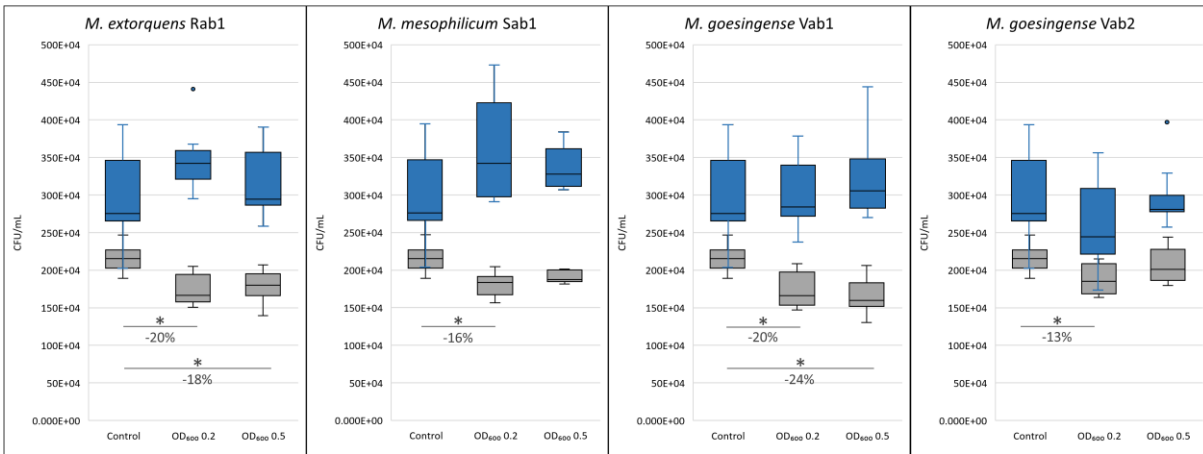
Gammaproteobacteria (<1%) occurred in a substantially lower relative abundance. Members of the order *Sphingomonadales* (41%) were most frequently detected, followed by *Cytophagales* (27%), *Rhodobacterales* (9%) and *Rhodospirillales* (8%). In total, 49 bacterial genera were identified with *Spirosoma* (24%) being the dominating fraction, followed by *Porphyrobacter* (11%) and not further classified *Sphingomonadales* (11%). Despite *Methylobacterium* spp. accounted for a low proportion of the total bacterial community only, the network indicate that they are embedded in a mutualistic interaction with algae (Figure 2.1). Five distinct features in the analyzed sample represented the genus and were also manually aligned against the NCBI nt collection; Supplementary Table S1 lists respective feature ID and closest hit after BLAST search. Visualization of the natural biofilm using a confocal laser scanning microscope revealed *H. lacustris* as the dominating algal taxon (Figure 2.1, Supplementary Figure S2.1).

Co-cultivation of microalgae and methylobacteria leads to significantly increased biomass formation

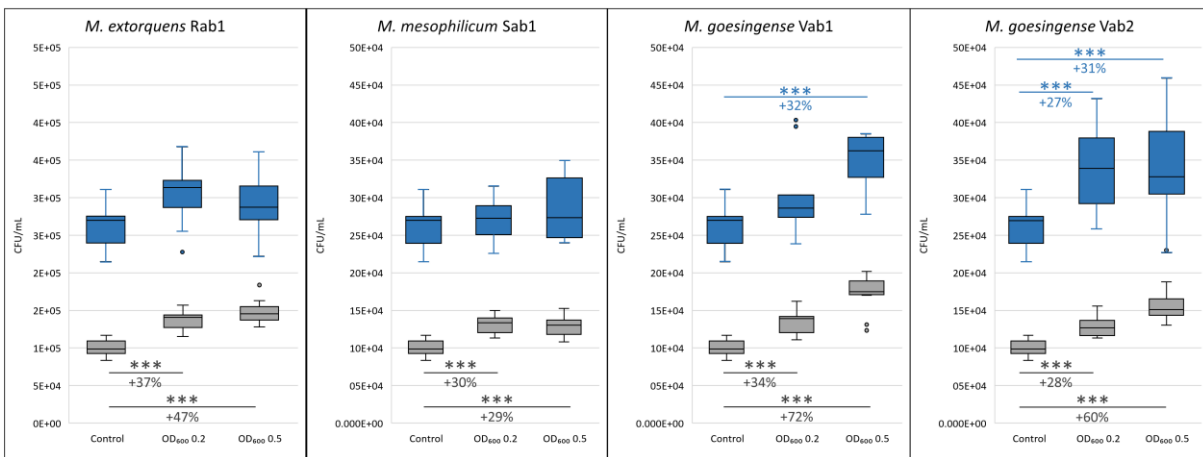
Co-cultivation experiments revealed varying effects of methylobacteria on the growth of different microalgal genera. While co-cultivation with methylobacteria led to a significant decrease in algal cell count for *C. vulgaris* G1-G, contrary effects were revealed for *S. vacuolatus* G1-O and *H. lacustris* G1-R. Both, growth-promoting as well as growth-inhibiting effects of methylobacteria were stronger after seven days of co-cultivation but decreased after 14 days of incubation. Over all, the growth-promotion of methylobacteria was more explicit, when the bacterial population density was higher at the beginning of the experiments.

In detail, a significant decrease in microalgal biomass was observed for *C. vulgaris* G1-G when co-cultured with all tested methylobacteria with an initial optical density of 0.2 after seven days of incubation compared to the axenic control. For *M. extorquens* Rab1 and *M. goesingense* Vab1 a significant decrease in microalgal biomass formation was also observed when the initial bacterial cell density was adjusted to an OD₆₀₀ of 0.5. After 14 days of incubation, no significant differences in *C. vulgaris* G1-G cell count were measured between the control samples and co-cultures (Figure 2.2.A). Co-cultivation of *S. vacuolatus* G1-O and all tested methylobacteria led to a significant increase in algal cell count after seven days of incubation, independent from initial bacterial cell load; however, a higher initial cell density of both *M. goesingense* strains resulted in even better performance of the microalga after seven days of co-culturing. After 14 days of incubation, the effect of algal-growth promotion diminished; significant increase in algal cell count was only observable for co-cultures with *M. goesingense* Vab1 with an initial bacterial OD₆₀₀ of 0.5 and for co-cultures with *M. goesingense* Vab2 (Figure 2.2.B).

A: *C. vulgaris* G1-G



B: *S. vacuolatus* G1-O



C: *H. lacustris* G1-R

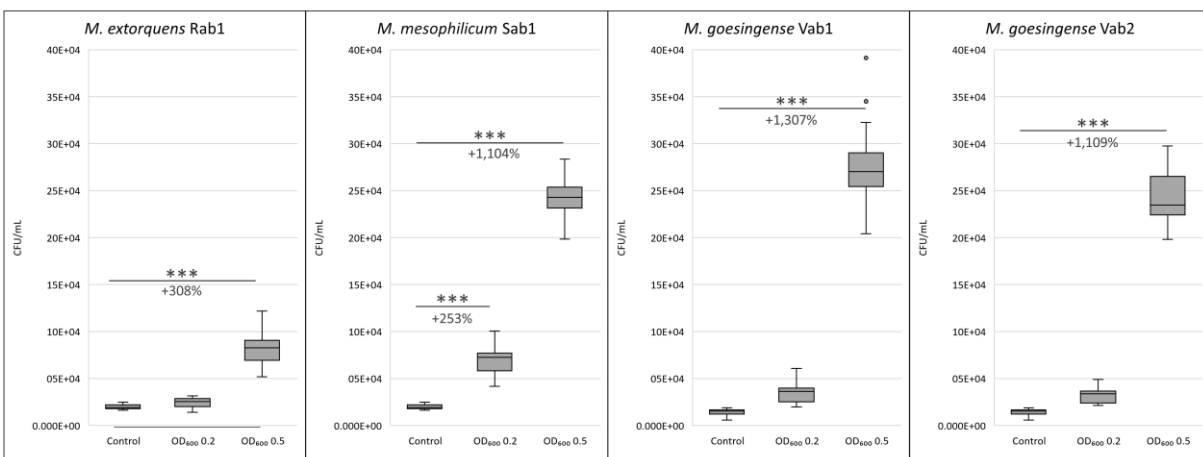


Figure 2.2. Microalgal cell counts after seven (grey) and 14 (blue) days of incubation. *C. vulgaris* G1-G (A), *S. vacuolatus* G1-O (B) and *H. lacustris* G1-R were co-inoculated with four different *Methylobacterium* strains in two differing cell concentrations (initial cell densities: OD₆₀₀ 0.2 and 0.5). Algal CFU was determined by measuring the fluorescence intensity (FI). For each box, the central line indicates the median, while the bottom and top edges of the box indicate the 25th and 75th percentiles, respectively. The whiskers extend to the most extreme data points not considered outliers. Asterisks indicate significant differences in algal cell count compared to the control (* *p*-value ≤ 0.05; ** *p*-value ≤ 0.01; *** *p*-value ≤ 0.001). The percentage of increased/reduced microalgal cell count compared to the control is included.

The effect of microalgae growth-promotion was greatest for *H. lacustris*; co-culturing with an initial bacterial optical density of 0.5 led to a 4-fold, 12-fold, 14-fold and 12-fold amount of biomass for *M. extorquens* Rab1, *M. mesophilicum* Sab1, *M. goesingense* Vab1 and *M. goesingense* Vab2 respectively, compared to the control group. Co-inoculation with a lower load of bacterial cells (OD₆₀₀ 0.2) led only in the case of *M. mesophilicum* Sab1 to a significant increase in *H. lacustris* biomass (3.5-fold) after seven days of incubation (Figure 2.2.C). A detailed breakdown of algal CFUs is provided in Supplementary Table S2.2, S2.3 and S2.4.

Visualization of mixed cultures using confocal laser scanning microscopy

Visualization of mixed cultures revealed very loose associations between methylobacteria and *C. vulgaris* G1-G. Here, methylobacteria and algae were randomly and evenly distributed in the media and no distinct clustering was observed (Figure 2.3.A). Methylobacteria seem to embed *S. vacuolatus* cells and form cell aggregates (Figure 2.3.B) and were found closely attached to the surface of viable *H. lacustris* cells (Figure 2.3.C and 2.3.D). Methylobacteria were also found in close proximity to disrupted, leaking algal cells, seemingly feeding on microalgal cell debris (Figure 2.3.D).

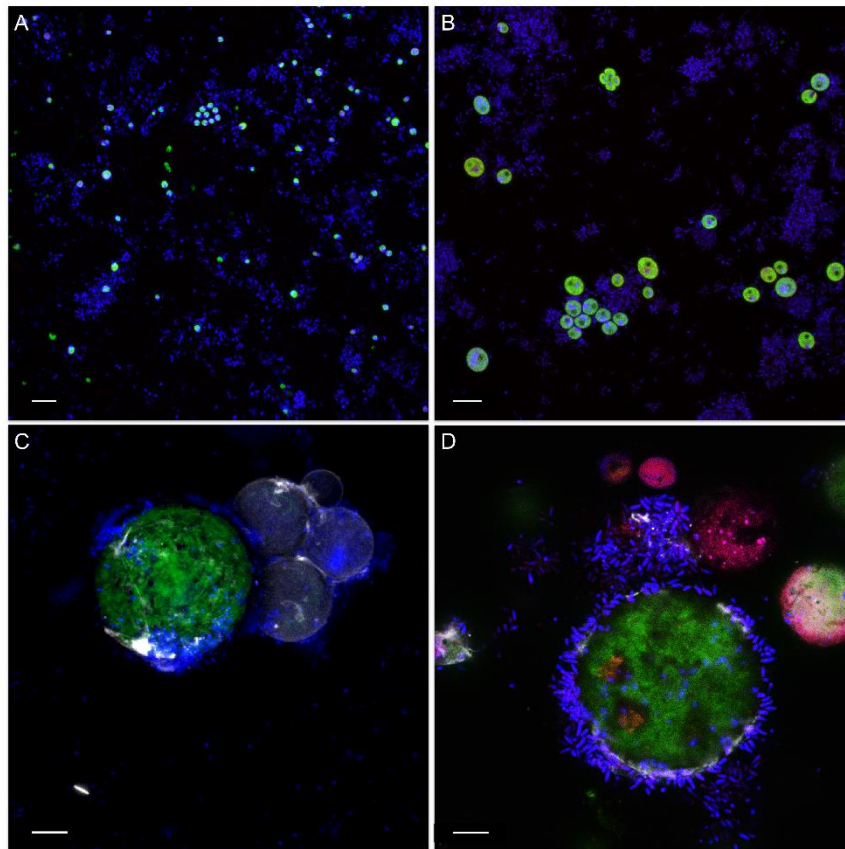


Figure 2.3. Confocal laser scanning micrographs showing mixed cultures containing different algae (A: *C. vulgaris* G1-G, B: *S. vacuolatus* G1-O, C & D: *H. lacustris* G1-R) inoculated with *M. goesingense* Vab1 with an initial optical density of 0.5 after seven days of incubation. Green: autofluorescence of algae; blue: methylobacteria; red: dead cells. Micrographs show microbes after staining using the LIVE/DEAD bacterial viability kit (ThermoFisher Scientific, MA, USA) in combination with calcofluor white (0.15%). Scale bar: 10 µm

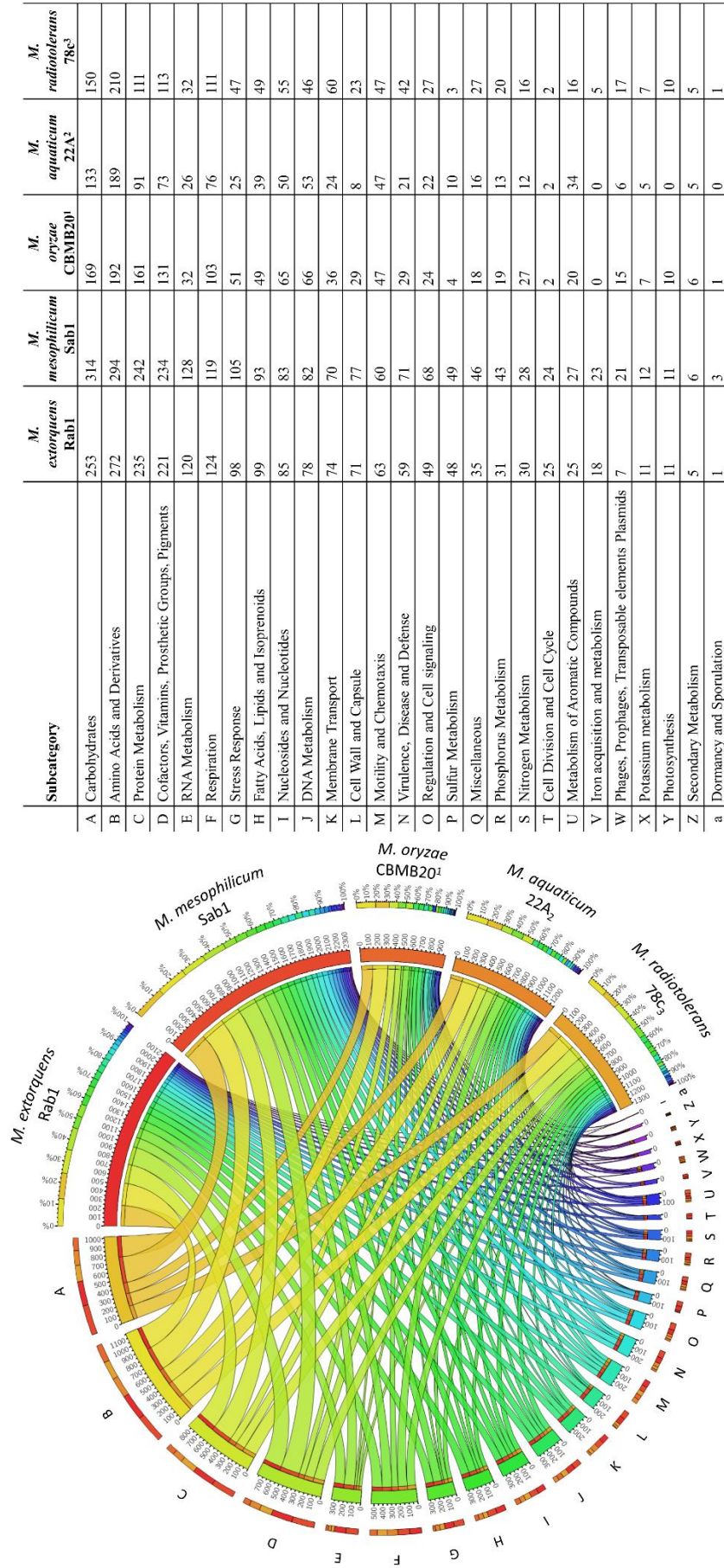
Whole genome sequencing of methylobacteria provides indication for various beneficial traits

The total genome size was determined to be 5,747,629 bp, featuring a GC content of 68.2% (*M. extorquens* Rab1) and 6,367,318 bp, with a GC content of 68.6% (*M. mesophilicum* Sab1). The genome analyses revealed 5,952 and 7,795 coding sequences for *M. extorquens* Rab1 and *M. mesophilicum* Sab1, respectively. Detailed statistics are provided in Table 2.1 including reference genomes of plant-associated methylobacteria. Identified features were assigned to subcategories with the SEED database (Overbeek *et al.*, 2005). The analyzed genomes harbored between 221 (*M. extorquens* Rab1) and 234 (*M. mesophilicum* Sab1) genes associated with the synthesis of cofactors, vitamin, prosthetic groups and pigments, including genes responsible for the synthesis of biotin, riboflavin, tetrapyrroles and folate. Between 18 and 23 genes were identified responsible for iron acquisition and metabolism, whereas *M. extorquens* Rab1 harbored eleven and *M. mesophilicum* Sab1 16 genes associated with the production of siderophores. Both investigated methylobacteria harbored four genes associated with the synthesis of auxins. Details related to the distribution of features within both analyzed genomes as well as reference genomes of plant-associated methylobacteria are displayed in Figure 2.4, including detailed feature counts per organism per subcategory.

Table 2.1. Detailed genome statistics for the analyzed *Methylobacterium* isolates. The genomes were sequenced using Illumina NextSeq paired-end sequencing. Information about reference genomes of plant-associated methylobacteria is included. ¹Kwak *et al.*, 2014, ²Tani *et al.*, 2015, ³Evers *et al.*, 2015.

| | <i>M. extorquens Rab1</i> | <i>M. mesophilicum Sab1</i> | <i>M. oryzae CBMB20¹</i> | <i>M. aquaticum 22A²</i> | <i>M. radiotolerans 78c³</i> |
|-------------------------------|-----------------------------------|-------------------------------------|---|---|---|
| Total genome size [bp] | 5,747,629 | 6,367,318 | 6,286,629 | 5,348,274 | 6,788,652 |
| GC content [%] | 68.2 | 68.6 | 69.8 | 71.1 | 71.2 |
| N50 | 252,941 | 132,863 | - | - | 57,566 |
| L50 | 8 | 13 | 1 | 1 | 38 |
| Number of scaffolds | 343 | 1660 | 1 | 1 | 271 |
| Number of features | 6,004 | 7,852 | 6,308 | 5,315 | 7,790 |
| Number of coding seqs | 5,952 | 7,795 | 6,243 | 5,212 | 7,740 |
| Number of RNAs | 52 | 57 | 65 | 103 | 50 |

Figure 2.4. Feature distribution within the analyzed *Methylobacterium* genomes and reference genomes of plant-associated methylobacteria. A detailed feature count per organism per subcategory was included according to the SEED database after annotation using RAST. (Aziz et al., 2008). ¹Kwak et al., 2014, ²Tani et al., 2015, ³Eevers et al., 2015.



Discussion

Our study provides further evidence for the potential of methylobacteria to significantly increase biomass formation of two industrially relevant green algae through co-cultivation. Genome analyses of all applied *Methylobacterium* spp. revealed a number of features attributable to the observed algae growth-promotion, including genes involved in the production of vitamins, siderophores and auxins. All tested microalgae were isolated from a natural biofilm, where analyses of the bacterial community composition gave evidence for natural co-occurrences of methylobacteria and microalgae. This hypothesis is supported by previous studies, where methylobacteria were identified in the phycosphere of *Chlorella*, *Scenedesmus*, *Micrasterias* and *Chlamydomonas* (Calatrava *et al.*, 2018; Krohn-Molt *et al.*, 2017; Levy *et al.*, 2009). The identified features occurred in rather low abundances when compared to other bacterial constituents, which is mainly due to their K-strategic lifestyle based on the utilization of methanol.

Analyzing the genomes of different methylobacteria revealed that all investigated strains harbor several features which have already been described to positively contribute to algae growth. All four tested genomes harbored genes involved in the production of a variety of vitamins, including cobalamin, biotin, thiamin and riboflavin, indicating the potential of methylobacteria to support algae growth. Croft and colleagues demonstrated that more than 50% of otherwise heterotrophic algae are dependent on an external supply of those vitamins (Croft *et al.*, 2006). In natural ecosystems those vitamins are provided by the surrounding bacteria which in return are provided with dissolved organic matter by the algae (Croft *et al.*, 2005). Besides genes involved in the synthesis of vitamins, all investigated strains harbored genes attributable to the production of plant hormones. Several studies have demonstrated that phytohormones can stimulate the growth and lipid production of microalgae (Amin *et al.*, 2015; de-Bashan *et al.*, 2008; Liu *et al.*, 2016; Yu *et al.*, 2017). Additionally, all four genomes contained genes involved in iron acquisition and metabolism. It was previously shown that microalgae benefit from bacterial siderophores as the bioavailability of chelated iron is increased resulting in a “carbon for iron mutualism” where algae assimilate iron complexed in bacterial siderophores and in return provided the for the bacteria essential dissolved organic matter (Amin *et al.*, 2009, 2012a, 2015).

The conducted co-cultivation experiments give evidence, that methylobacteria harbor great potential to stimulate the growth of certain microalgae through a species-specific relationship. After seven days of incubation, a significant decrease in biomass formation was observed for *C. vulgaris* irrespective of the applied methylobacteria. We assume that *C. vulgaris* and methylobacteria might compete for nutrients during the initial growth phase, which has negative effects on the microalgae.

Another possible explanation for the lower algal biomass when co-cultured with methylobacteria might be due to increased shading which attenuates light penetration (Kazamia *et al.*, 2012a). Carotenoids are known to have not only photoprotective capacities, but are also involved in the light-harvesting process during photosynthesis by expanding the light absorption spectrum. Detailed analyses of the methylobacteria genomes revealed that all strains harbored genes related to the synthesis of bacterial light-harvesting proteins, as well as the photosynthetic reaction center of the photosystem type-II. Therefore, the beta-carotenoid-containing methylobacteria might also hamper photosynthetic activity of *Chlorella* through the competition for light (Van Dien *et al.*, 2004). Although methylobacteria are able to produce vitamin B₁₂ – an essential compound for many algae – Croft and colleagues could show that many microalgal species belonging to the genus *Chlorella* do not necessarily require cobalamin for proliferation (Croft *et al.*, 2006). The obtained visualizations of co-cultures revealed very loose associations between algae and methylobacteria in the case of *C. vulgaris*. The fact, that methylobacteria are not accumulated in the phycosphere of *C. vulgaris*, and thus impede a direct metabolite exchange, might also hamper a successful symbiotic relationship. Taken all these considerations into account, we suppose that the negative effect due to competition for nutrients, light and space outweighs the possible beneficial impact of the bacteria through the production of vitamins, auxins and siderophores for this bacteria-microalgae combination.

More distinctive effects were observed for *S. vacuolatus*; a significant increase in biomass formation was observed when co-cultured with methylobacteria after seven days of incubation. The best results were achieved with both *M. goesingense* strains when they were added with an initial bacterial optical density of 0.5. While after 14 days the growth promoting effect of *M. extorquens* and *M. mesophilicum* was lost, significantly more algal biomass formation was still monitored in co-cultures with *M. goesingense*, underlining the specificity of bacteria-microalgae symbioses. *M. goesingense* might metabolize the available nutrients more efficiently or harbors features which allows it to reduce the dissolved organic carbon produced by *S. vacuolatus* and thus the growth promoting effect was observed for prolonged time periods. Confocal laser scanning microscopy revealed algae cells that appeared to be embedded and attached to bacterial aggregates. Similar colonization patterns were previously observed with methylobacteria and *Chlamydomonas*, where bacteria enable the growth of algae in a nitrogen depleted medium by mineralizing certain amino acids and peptides and thereby produce ammonium which consequently can be assimilated by the algae (Calatrava *et al.*, 2018).

The algae growth-promoting effect of all investigated methylobacteria was strongest for *H. lacustris*, where up to 14-fold more algal biomass was formed after seven days of incubation compared to the control. As reported by Croft and colleagues, many *Haematococcus* species are dependent on an external supply of vitamins (Croft *et al.*, 2006). In our vitamin-depleted medium, those essential

micro-nutrients are provided by methylobacteria, allowing the microalgae to thrive. Visualization of *H. lacustris* co-cultures revealed that symbiotic bacteria appeared in close proximity of the microalgae, seemingly attached to the algal surface allowing direct metabolite exchange. Similar colonization patterns of methylobacteria were observed on higher land plants, where bacteria are found attached to surface areas on leaves, attracted by the emitted methanol towards the stomata. The methanol produced by plants is a result of pectin-methylesterases de-esterifying the pectin within the cell wall during growth (Fall and Benson, 1996; Kutschera, 2007). During its life cycle, *H. lacustris* undergoes different cell stages; vegetative, motile cells become spherical, nonmotile cyst cells under unfavorable conditions (Wayama *et al.*, 2013); after seven days of incubation, only a few flagellated cells were observable, while mostly green coccoid cells (palmelloid) and transitioning cells were found. In these stages, the microalgae change their extracellular matrix during the formation of a primary cell wall. Vesicles transport granules from the cytoplasm to the inner layer of the extracellular matrix resulting in the development of a two-layered cell wall. The outer layer and parts of the intermediate tripartite crystalline layer peels off. As soon as this stage is reached calcofluor-white staining results positive, indicating the presence of β -1,4-glycosidic linkages (Hagen *et al.*, 2002). Since the cell wall composition of *Haematococcus* is known to share similarities to those of plants, as they form primary and secondary cell walls consisting of cellulose and pectin along with other polysaccharides, a similar mechanism might be responsible for the attraction of methylobacteria in their surroundings (Wang *et al.*, 2004). We found highest growth-promoting effects for *H. lacustris* indicating that physical proximity is essential for successful metabolite exchange and thus growth enhancement, as already suggested in previous studies (Gonzalez and Bashan, 2000; Hernandez *et al.*, 2009). Moreover, microscopic observation of the sampled biofilm revealed *H. lacustris* as the dominating algal species. Natural co-occurrences of *H. lacustris* and methylobacteria, as revealed through 16S rRNA gene fragment amplicon sequencing, support the hypothesis of specific, evolutionary evolved co-occurrences of certain microalgae and bacteria.

Our results provide new insights into the potential of algae growth-promotion of two different methylobacteria species on three different microalgal genera. Moreover, the observations lead us to the conclusion that symbiotic relationships are conceivably species-specific. In addition, our results provide evidence that a balanced ratio between symbiotic bacteria and microalgae is essential for a successful algae growth-promotion, which facilitates a mutualistic relationship without interferences through the competition for nutrients, light and space. Profound knowledge of the interactions between algae and bacteria is crucial to harness their biotechnological potential. The exploration of natural algae-bacteria relationships facilitates the design of synthetic microbial communities, which are a promising tool for biotechnology and might lead to improved production procedures in the future.

Supplementary Material

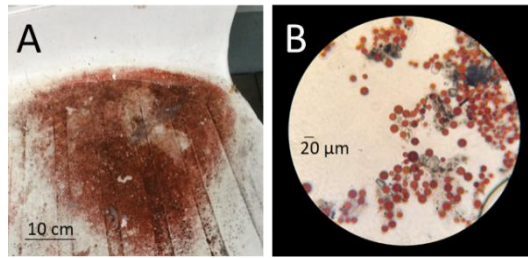
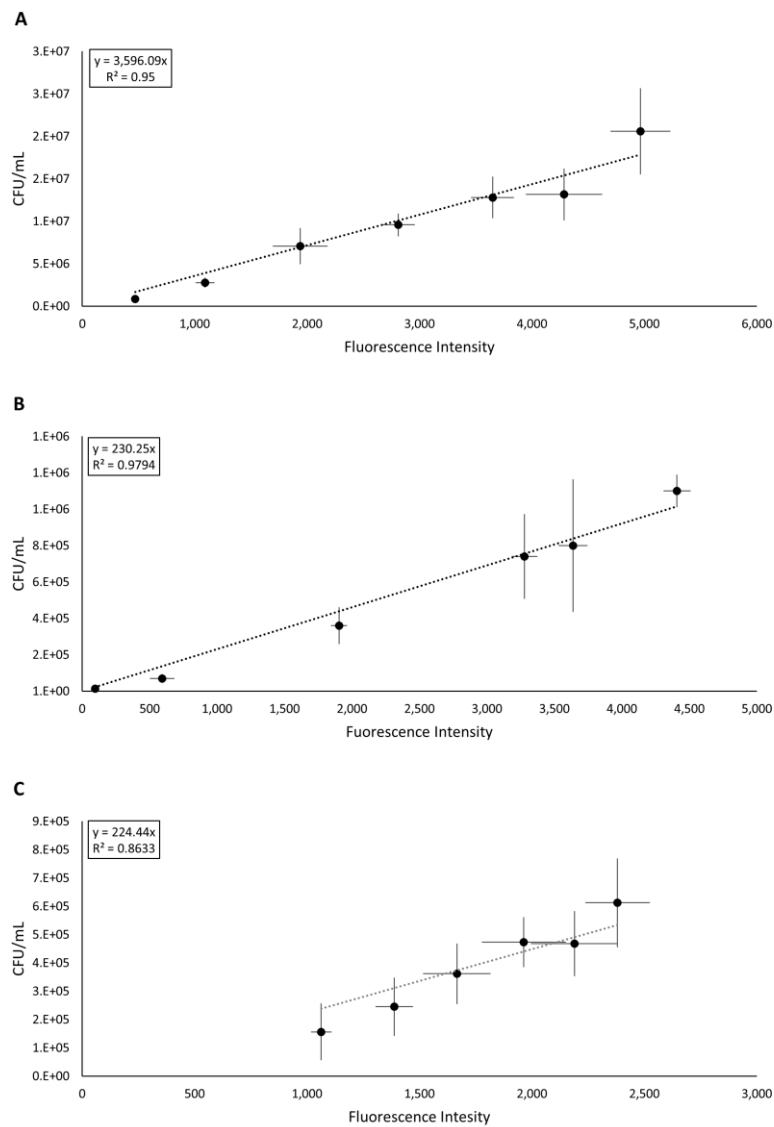


Figure S2.1. Macroscopic and microscopic visualization of the sampled biofilm with a typical coloration for microalgae-dominated communities. Samples obtained from outdoor furniture showed indications for the presence of *Haematococcus* sp. due to the specific red color (A). A microscopic observation confirmed a high abundance of microalgae in the obtained samples (B).



Supplementary Figure S2.2. Correlation between fluorescence intensity and algal cell count for *C. vulgaris* G1-G (A), *S. vacuolatus* G1-O (B) and *H. lacustris* G1-R (C).

Supplementary Table S2.1. Closest alignment hits of features representing the genus *Methylobacterium*.
Sequences were aligned against the NCBI nucleotide collection using the BLAST algorithm.

| Feature ID | Closest NCBI hit | Accession NO. |
|----------------------------------|---|---------------|
| 3372941629954ad743c804e88345969d | <i>Methylobacterium indicum</i> strain DP28.3 | MK968432.1 |
| 6e98ad9b6beaa6c0546f6cc9b274d0fa | Uncultured <i>Methylobacterium</i> sp. | LC466937.1 |
| ac829040ac43f4d961a191fd8e5a915d | <i>Methylobacterium</i> sp. strain I-S-R3-1 | MK398052.1 |
| d8456fac09d0bb7dfd62de648ca0a933 | <i>Methylobacterium</i> sp. 14-324 | EF558714.1 |
| f58bba003c01c620836eafcae31a7198 | <i>Methylobacterium</i> sp. CSCXZN6.6 | LC484783.1 |

Supplementary Table S2.2. *C. vulgaris* G1-G cell count after seven days and 14 days of incubation. Algal cell count of mixed cultures with differing initial bacterial cell densities (OD₆₀₀ = 0.2 and 0.5) were compared with control cultures where no additional bacteria were added. Significances were calculated using ANOVA for normally distributed values and the Kruskal-Wallis test for non-parametric analyses including Bonferroni multiple test correction. Asterisk indicates significant differences (p -value ≤ 0.05) in algal cell count compared to control samples after the respective time of incubation.

***C. vulgaris* G1-G**

***M. extorquens* Rab1**

| | T7 [$\times 10^6$ CFU/mL] | difference in CFU count after 7 days | T14 [$\times 10^6$ CFU/mL] | difference in CFU count after 14 days |
|-----------------------|-------------------------------|---|--------------------------------|---|
| control | 2.16 \pm 0.12 | | 2.96 \pm 0.54 | |
| OD ₆₀₀ 0.2 | 1.74 \pm 0.18* | -20% | 3.43 \pm 0.37 | +16% |
| OD ₆₀₀ 0.5 | 1.78 \pm 0.18* | -18% | 3.13 \pm 0.42 | +6% |

***M. mesophilicum* Sab1**

| | T7 [$\times 10^6$ CFU/mL] | difference in CFU count after 7 days | T14 [$\times 10^6$ CFU/mL] | difference in CFU count after 14 days |
|-----------------------|-------------------------------|---|--------------------------------|---|
| control | 2.16 \pm 0.12 | | 2.96 \pm 0.54 | |
| OD ₆₀₀ 0.2 | 1.81 \pm 0.15* | -16% | 3.63 \pm 0.66 | +23% |
| OD ₆₀₀ 0.5 | 1.90 \pm 0.07 | -12% | 3.36 \pm 0.30 | +14% |

***M. goeingense* Vab1**

| | T7 [$\times 10^6$ CFU/mL] | difference in CFU count after 7 days | T14 [$\times 10^6$ CFU/mL] | difference in CFU count after 14 days |
|-----------------------|-------------------------------|---|--------------------------------|---|
| control | 2.16 \pm 0.12 | | 2.96 \pm 0.54 | |
| OD ₆₀₀ 0.2 | 1.73 \pm 0.22* | -20% | 2.98 \pm 0.43 | +1% |
| OD ₆₀₀ 0.5 | 1.64 \pm 0.21* | -24% | 3.23 \pm 0.51 | +9% |

***M. goeingense* Vab2**

| | T7 [$\times 10^6$ CFU/mL] | difference in CFU count after 7 days | T14 [$\times 10^6$ CFU/mL] | difference in CFU count after 14 days |
|-----------------------|-------------------------------|---|--------------------------------|---|
| control | 2.16 \pm 0.12 | | 2.96 \pm 0.54 | |
| OD ₆₀₀ 0.2 | 1.88 \pm 0.19* | -13% | 2.59 \pm 0.56* | -12% |
| OD ₆₀₀ 0.5 | 2.08 \pm 0.21 | -4% | 3.05 \pm 0.43 | +3% |

Supplementary Table S2.3. *S. vacuolatus* G1-O cell count after seven days and 14 days of incubation. Algal cell count of mixed cultures with differing initial bacterial cell densities ($OD_{600} = 0.2$ and 0.5) were compared with control cultures where no additional bacteria were added. Significances were calculated using ANOVA for normally distributed values and the Kruskal-Wallis test for non-parametric analyses including Bonferroni multiple test correction. Asterisk indicates significant differences (p -value ≤ 0.05) in algal cell count compared to control samples after the respective time of incubation.

S. vacuolatus* G1-O**M. extorquens* Rab1**

| | T7 [$\times 10^5$ CFU/mL] | difference in CFU count after 7 days | T14 [$\times 10^5$ CFU/mL] | difference in CFU count after 14 days |
|-----------------------|-------------------------------|---|--------------------------------|---|
| control | 1.01 \pm 0.01 | | 2.56 \pm 0.27 | |
| OD ₆₀₀ 0.2 | 1.38 \pm 0.12* | +36% | 3.04 \pm 0.38 | +15% |
| OD ₆₀₀ 0.5 | 1.48 \pm 0.14* | +47% | 2.93 \pm 0.36 | +10% |

***M. mesophilicum* Sab1**

| | T7 [$\times 10^5$ CFU/mL] | difference in CFU count after 7 days | T14 [$\times 10^5$ CFU/mL] | difference in CFU count after 14 days |
|-----------------------|-------------------------------|---|--------------------------------|---|
| control | 1.01 \pm 0.01 | | 2.56 \pm 0.27 | |
| OD ₆₀₀ 0.2 | 1.31 \pm 0.11* | +30% | 2.71 \pm 0.27 | +2% |
| OD ₆₀₀ 0.5 | 1.30 \pm 0.12* | +28% | 2.85 \pm 0.39 | +8% |

***M. goeisingense* Vab1**

| | T7 [$\times 10^5$ CFU/mL] | difference in CFU count after 7 days | T14 [$\times 10^5$ CFU/mL] | difference in CFU count after 14 days |
|-----------------------|-------------------------------|---|--------------------------------|---|
| control | 1.01 \pm 0.01 | | 2.56 \pm 0.27 | |
| OD ₆₀₀ 0.2 | 1.35 \pm 0.14* | +34% | 3.02 \pm 0.56 | +14% |
| OD ₆₀₀ 0.5 | 1.73 \pm 0.23* | +72% | 3.49 \pm 0.36* | +32% |

***M. goeisingense* Vab2**

| | T7 [$\times 10^5$ CFU/mL] | difference in CFU count after 7 days | T14 [$\times 10^5$ CFU/mL] | difference in CFU count after 14 days |
|-----------------------|-------------------------------|---|--------------------------------|---|
| control | 1.01 \pm 0.01 | | 2.56 \pm 0.27 | |
| OD ₆₀₀ 0.2 | 1.29 \pm 0.13* | +28% | 3.36 \pm 0.53* | +27% |
| OD ₆₀₀ 0.5 | 1.62 \pm 0.25* | +60% | 3.48 \pm 0.68* | +32% |

Supplementary Table S2.4. *H. lacustris* G1-R cell count after seven days and 14 days of incubation. Algal cell count of mixed cultures with differing initial bacterial cell densities ($OD_{600} = 0.2$ and 0.5) were compared with control cultures where no additional bacteria were added. Significances were calculated using ANOVA for normally distributed values and the Kruskal-Wallis test for non-parametric analyses including Bonferroni multiple test correction. Asterisk indicates significant differences (p -value ≤ 0.05) in algal cell count compared to control samples after the respective time of incubation.

***H. lacustris* G1-R**

***M. extorquens* Rab1**

| | T7 [$\times 10^4$ CFU/mL] | difference in CFU count after 7 days |
|-----------------------|-------------------------------|---|
| control | 2.00 \pm 0.29 | |
| OD ₆₀₀ 0.2 | 2.44 \pm 0.54 | +22% |
| OD ₆₀₀ 0.5 | 8.15 \pm 1.77* | +308% |

***M. mesophilicum* Sab1**

| | T7 [$\times 10^4$ CFU/mL] | difference in CFU count after 7 days |
|-----------------------|-------------------------------|---|
| control | 2.00 \pm 0.29 | |
| OD ₆₀₀ 0.2 | 7.06 \pm 1.63* | +254% |
| OD ₆₀₀ 0.5 | 24.03 \pm 0.24* | +1,104% |

***M. goesingense* Vab1**

| | T7 [$\times 10^4$ CFU/mL] | difference in CFU count after 7 days |
|-----------------------|-------------------------------|---|
| control | 2.00 \pm 0.29 | |
| OD ₆₀₀ 0.2 | 3.68 \pm 1.27 | +84% |
| OD ₆₀₀ 0.5 | 28.08 \pm 0.81* | +1,307% |

***M. goesingense* Vab2**

| | T7 [$\times 10^4$ CFU/mL] | difference in CFU count after 7 days |
|-----------------------|-------------------------------|---|
| control | 2.00 \pm 0.29 | |
| OD ₆₀₀ 0.2 | 3.22 \pm 0.86 | +61% |
| OD ₆₀₀ 0.5 | 24.14 \pm 2.81* | +1,109% |

CHAPTER 3

A NOVEL, NATURE-BASED ALTERNATIVE FOR PHOTOBIOREACTOR DECONTAMINATIONS

Lisa Krug^{1,2}, Armin Erlacher², Gabriele Berg² and Tomislav Cernava²

¹*Austrian Centre of Industrial Biotechnology, Graz, Austria*

²*Institute of Environmental Biotechnology, Graz University of Technology, Graz, Austria*

Abstract

Large-scale microalgae cultivations are increasingly used for the production of animal feed, nutritional supplements and various high-value bioproducts. Due to the process size and other limitations, contaminations of microalgae fermentations with other photoautotrophic microorganism are frequently observed. In the present study, we explored the applicability of 5-isobutyl-2,3-dimethylpyrazine for the removal of contaminating microalgae from industrial photobioreactors. In order to select a representative microbial population for susceptibility experiments, reactor samples were obtained from a multi-stage cultivation process. Assignments of 18S rRNA gene fragment amplicons indicated that *Haematococcus*, *Chlorella*, and *Scenedesmus* were the three most frequently occurring microalgae genera in the selected reactors. Following the isolation of representative algae cultures, susceptibility tests were conducted with the antimicrobial pyrazine. It was demonstrated that all isolated contaminants are highly susceptible to the bioactive compound. The highest tolerance towards the alkylpyrazine was observed with *Scenedesmus vacuolatus*; solutions with 1.66% (v/v) of the active compound were required for its deactivation. Further tests with the vaporized pyrazine showed consistent reductions in the viability of treated microalgae. This pilot study provides evidence for the applicability of a novel, nature-based alternative for bioreactor decontaminations.

Introduction

The industrial relevance of microalgae as production systems for valuable bioproducts and as promising feedstocks for biofuel production is constantly increasing (Chisti, 2007; Plaza *et al.*, 2009; Shurtz *et al.*, 2017). Modern cultivation processes are optimized for high-yield production and utilize various eukaryotic whole cell systems for a broad spectrum of bioproducts. *Chlorella*, *Dunaliella*, and *Scenedesmus* are the most commonly employed genera in production-scale photobioreactors with production capacities of up to 3,000 tons per year; various other photoautotrophs are used for more specific fermentations (Pulz and Gross, 2004). Microalgae cultivation is considered as sustainable, because it only requires solar energy under photoautotrophic conditions to produce a range of highly valuable products, including pharmaceuticals, fertilizers and food supplements (Borowitzka, 2013). Industrial-scale cultivations under conditions required for bulk material production are mostly based on open pond systems. In contrast, the production of high-valuable compounds from microalgae is mainly done on the basis of closed photobioreactors in order to reproduce production conditions, increase the control of cultivation variables and reduce the risk of contaminations (Jerney and Spilling, 2018; Pulz, 2001). Under both process conditions, one of the main constraints for an efficient cultivation of microalgae is the potential contamination with biological pollutants, such as bacteria, fungi, zooplankton or other undesirable microalgae (Bínová *et al.*, 1998; Borowitzka, 2013; Letcher *et al.*, 2013; Wang *et al.*, 2016). Some contaminants like *Poteroiochromonas* spp. (*Chrysophyta*) not only compete for nutrients with the cultivated algae, but also impair their growth by toxin production (Reich and Spiegelstein, 1964). This can even result in a collapses of the cultivation batch as shown by Ma and colleagues (Ma *et al.*, 2017). In order to reduce or prevent the negative impact of contaminations, a range of viable strategies have been implemented so far. Common strategies include early harvesting of the product to avoid serious biomass losses, or the use of a number of chemical, biological and physical treatments (Carney and Lane, 2014). As a safety precaution in-between cultivation processes, photobioreactors are often emptied and decontaminated with different treatments (Singh and Sharma, 2012; Wang *et al.*, 2012, 2013). Common decontamination procedures include rinsing of the reactors with sodium hypochlorite or the application of hydrogen peroxide (Johnston *et al.*, 2005; Klapes and Vesley, 1990). Here, the low stability and the high reactivity of the disinfectant are often disadvantageous for the process environment. Due to various safety reasons and the instability and reactivity of the currently employed decontaminants, efficient alternatives could improve industrial-scale microalgae cultivations.

One so far untapped environmentally friendly alternative for bioreactor decontamination could be the application of naturally occurring antimicrobials that are emitted by highly competitive microorganisms. Studies with *Paenibacillus polymyxa* isolates from plant roots and endophytes from

inner plant tissues showed that they produce various highly antimicrobial volatile organic compounds (VOCs; Rybakova *et al.*, 2017). Among other bioactive compounds in their volatiles, alkylpyrazines were identified as carriers of antimicrobial effects of the beneficial bacteria. These isolates not only showed high inhibition efficiency against plant pathogenic fungi, but also the potential to inhibit potential human pathogens (Cernava *et al.*, 2015). These results imply that mimicking the bioactive volatiles of *P. polymyxa* is a promising strategy to control diverse microbial contaminations. This strategy was already applied for the decontamination of biological surfaces and to reduce contamination in processed meat products (Kusstascher *et al.*, 2017; Schöck *et al.*, 2018) and is patented for specific applications (Aichner *et al.*, 2013). In the present study, 5-isobutyl-2,3-dimethylpyrazine was employed, because of its similar effect to the pyrazine mixture emitted by *P. polymyxa* GndWu39, which is a highly competitive biocontrol agent (Fürnkranz *et al.*, 2012). We wanted to find out if this alkylpyrazine derivative is effective against representative microalgae contaminations at concentrations that were previously shown to be sufficient to treat bacterial contaminants (Schöck *et al.*, 2018). In order to evaluate its applicability, the model pyrazine was evaluated by implementing two different application strategies that could also find application in full-size bioreactors.

Materials and Methods

Characterization of microalgae populations in photobioreactors. In order to obtain a complete picture of the eukaryotic community in the photobioreactors of a local producer, we collected samples from reactors that are connected in a multi-stage process. In total eight liquid samples from five different reactors were obtained. The samples were placed on ice and transported in 50 mL plastic tubes to a nearby laboratory. Total community DNA from the reactor samples was extracted using the FastDNA[®] Kit for Soil (MP Biomedicals, USA), amplified and barcoded with the primer pair 1391f (5'-GTA CAC ACC GCC CGT C-3') and EukBr (5'-TGA TCC TTC TGC AGG TTC ACC TAC-3') targeting the variable region 9 (V9) of the 18S rRNA gene (Amaral-Zettler *et al.*, 2009). Each forward and reverse primer contained a specific primer pad (TATGGTAATT/AGTCAGCCAG) and linker (GT/GG), as described in the protocols and standards section of the Earth Microbiome Project (earthmicrobiome.org/; Thompson *et al.*, 2017). PCR reactions (20 μ L) were executed in triplicates and contained 14.6 μ L ultrapure water (Roth, Karlsruhe, Germany), 4 μ L Taq&Go (5 \times ; MP Biomedicals, France), 0.2 μ L of forward and reverse primer each (10 μ M) and 1 μ L DNA template (98 $^{\circ}$ C, 5 min; 10 cycles of 98 $^{\circ}$ C, 10 s; 53 $^{\circ}$ C, 10 s; 72 $^{\circ}$ C, 30 s; 20 cycles of 98 $^{\circ}$ C, 10 s; 48 $^{\circ}$ C, 30 s; 72 $^{\circ}$ C, 30 s; final extension 72 $^{\circ}$ C, 10 min). PCR products of respective samples had a length of 200bp and were quality checked by gel electrophoresis. PCR products were purified using Wizard[®] SV Gel and PCR clean-up system (Promega, Fitchburg, USA) according to manufacturer's protocol. Purified, barcoded samples were pooled equimolarly and sent for paired-end MiSeq Illumina sequencing (GATC Biotech, Germany). Sequencing data was analyzed using the QIIME 1.9.0 pipeline (Caporaso *et al.*, 2010). Barcodes, primer and adapter sequences were removed and the sequences were quality filtered (maximum unacceptable phred quality score: 19; phred offset: 33). Chimeras were removed from the 18S rRNA gene sequences by using usearch61 to perform both *de novo* (abundance based) and reference based chimera detection. OTU tables were created by an open reference method with UCLUST at a 97 % cut-off level for the 18S rRNA gene sequences (Edgar, 2010). OTUs were identified by performing a standard nucleotide BLAST with the NCBI nucleotide collection database excluding uncultured and environmental sample sequences (Altschul *et al.*, 1990). The final OTU network was constructed by filtering all sequences assigned to *Chlorella*, *Scenedesmus* and *Haematococcus*. Detailed description of QIIME scripts used in bioinformatics analyses are listed in Supplementary Table S4.

Isolation and identification of microalgae. In order to perform susceptibility tests, the unicellular microalgae *C. vulgaris*, *S. vacuolatus* and *H. lacustris* were isolated from industrial microalgae reactors. Dilution series of respective samples were plated on solid modified Bold's Basal Medium (Bold, 1949) (mBBM) containing 250 mg/L NaNO₃, 175 mg/L KH₂PO₄, 75 mg/L K₂HPO₄, 75 mg/L MgSO₄ \times 7 H₂O, 25 mg/L CaCl₂, 25 mg/L NaCl, 2.6 mg/L H₃BO₃, 5 mg/L FeSO₄ \times 7 H₂O, 8.8 mg/L ZnSO₄ \times 7 H₂O, 1.4 mg/L

MnCl₂ × 4 H₂O, 1.4 mg/L MoO₃, 1.6 mg/L CuSO₄ × 5 H₂O, 0.5 mg/L Co(NO₃)₃ × 6 H₂O, 0.5 mg/L EDTA, 0.3 mg/L KOH, 0.017 mg/L vitamin B₁₂, 0.013 mg/L 4-aminobenzoate, 0.003 mg/L biotin, 0.013 mg/L nicotinic acid, 0.017 mg/L hemicalcium-pentathenate, 0.05 mg/L pyridoxamine-HCl, 0.033 mg/L thiaminiumdichlorid, 0.0091 mg/L thioctic-acid, 0.01 mg/L riboflavin, 0.0049 mg/L olic acid and 18 g/L agar-agar. Vitamins and heat-sensitive components were added after autoclaving by sterile filtration (0.20 µm pore size). In order to obtain pure microalgae cultures single colonies were picked using a heat sterilized inoculation loop and transferred onto fresh mBBM agar plates. Plates were incubated at room temperature at a light/dark cycle (L:16 h/D:8 h).

In order to identify isolated microalgae species, cells were resuspended in 300 µL 0.85 % NaCl and transferred in sterile Eppendorf tubes filled with glass beads. After mechanical disruption using a FastPrep FP120 instrument (MP Biomedicals, Germany) suspensions were centrifuged at 3,000 rpm for 5 min. Supernatant served as template for the following PCR reactions. Partial 18S rRNA gene sequence was amplified by using primer pair TAREuk454FWD1 (5'- CCA GCA SCY GCG GTA ATT CC-3') and TAREukREV3P (5'-ACT TTC GTT CTT GAT YRA-3') covering the variable region 4 (V4; 200bp; Stoeck *et al.*, 2010). The PCR was performed in a total volume of 30 µL containing 16.2 µL ultrapure water, 6 µL Taq&Go (5 ×), 2.4 µL MgCl₂ [25mM], 1.2 µL of each primer [10 µM] and 3 µL template DNA (98 °C, 30 s; 10 cycles of 98 °C, 10 s; 53 °C, 10 s; 72 °C, 30 s, followed by 20 cycles of 98 °C., 10 s; 48 °C, 30 s; 72 °C, 30 s; final extension at 72 °C, 10 min). In addition, 18S rRNA gene sequences were amplified using primer pair NS1 (5' - GTA GTC ARA RGC CTT GTC TC - 3') and NS8 (5' - TCC GCA GGT TCA CCT ACG GA - 3')(White *et al.*, 1990). The PCR was performed in a reaction mix (20 µL) containing 16 µL ultrapure H₂O, 6 µL Taq&Go (5 ×), 1.2 µL of each primer [10 µM], 2.4 µL MgCl₂ [25mM] and 3 µL DNA template. PCR products were purified using Wizard SV Gel and PCR clean-up system according to manufacturer's protocol. 18S rRNA gene fragments were sequenced by LGC genomics (Berlin, Germany) and subsequently aligned against the NCBI nucleotide collection database excluding uncultured and environmental sample sequences using the BLAST algorithm (Altschul *et al.*, 1990).

Decontamination experiments in fluid suspensions. To obtain pre-cultures for the following experimental procedure, flasks containing 20 mL mBBM were inoculated with a single colony of *Haematococcus* sp., *Scenedesmus* sp. and *Chlorella* sp. respectively and incubated at room temperature at a light/dark cycle (L:16 h/D:8 h) for 5 to 7 days. Following successful cultivation, 1 mL of the pre-culture served as inoculum for 9 mL mBBM. After incubation for 3 days under the above-mentioned conditions, algae suspensions were treated with different concentrations (0.33 %, 1.0 %, 1.66 %) of 5-Isobutyl-2,3-dimethylpyrazine. Experiments were performed in triplicates; for the negative controls equal volumes of 0.85 % NaCl were added instead of the pyrazine. Efficiency of

treatment was determined by counting CFU on solid mBBM plates that were incubated at room temperature at a light/dark cycle (L:16 h/D:8 h)

Decontaminations with vaporized alkylpyrazines. Pre-cultures for each tested algae species were obtained by inoculating 30 mL mBBM with single colonies of *H. lacustris*, *S. vacuolatus* and *C. vulgaris* respectively. For *H. lacustris* 5 mL of the pre-culture were further transferred to a 1 L ground flask for 7 days under permanent illumination and aeration. After successful cultivation, the number of living cells in the pre-culture was determined by applying the drop plate technique. For all tested microalgae, 5 mL of the pre-culture suspension were then transferred in sterile 100 mL flasks and dried under sterile conditions. After evaporation of the fluid medium, the flasks were connected to 100 mL flasks filled 500 μ L pyrazine or H₂O (control); connectors and openings were sealed with paraffin oil. Each of the experiments was performed in triplicates. After 5 h of incubation and vaporization of the alkylpyrazine in the lower flask at 50 °C, the dried algae were rinsed with 2 mL mBBM. The living cell count was determined by using the drop plate technique. After incubation at room temperature at a light/dark cycle (L:16 h/D:8 h) the CFU number was determined for the controls and the pyrazine-treated samples.

Microscopic visualizations of treated algae. For visualization model microalgae were cultivated in 300 mL flask containing 10 mL sterile mBBM and incubated at room temperature at a light/dark cycle (L:16 h/D:8 h). When high cell density was reached, cultures were incubated with 10 μ L/mL pyrazine. Micrographs of *C. vulgaris*, *S. vacuolatus* and *H. lacustris* cultures before and after treatment were obtained with a light microscope (Leitz; Wetzlar, Germany) at 400 \times magnification and in combination with a phase contrast objective.

Statistical analyses. Results presented in the diagrams are the average of three replicates. Statistical analyses were performed using the IBM SPSS program (version 23.0; IBM Corporation, NY, USA). All data was analyzed using Student's paired t-Test at $p < 0.01$.

Results

Diversity of the eukaryotic community in photobioreactors

The overall dataset that was obtained by sequencing of 18S rRNA gene fragments in eight reactor samples contained a total of 4,992,008 reads. After removal of bacterial and archaeal sequences 4,886,808 reads remained, and were clustered in 554 operational taxonomic units (OTUs). The overall structure of the eukaryotic community is shown in Table 3.1. In the filtered dataset, a major proportion consisting of 4,512,85 reads (92.3%) was clustered in 245 OTUs (44.3%) and assigned to *Haematococcus* (genus level); 1,871 reads (0.04%) were clustered in five OTUs (0.9%) and assigned to *Scenedesmus* and 37,986 reads (0.78%) in 25 OTUs (4.5%) to *Chlorella* (Figure 3.1). In total 286 OTUs (51.6%) were assigned to *Plantae* and included seven genera in addition to the mentioned microalgae. 113 OTUs (20.4%) were assigned to *Chromista* sharing 140,545 reads and further classified as three different genera including *Ochromonas* (106 OTUs, 140,519 reads), *Poterioochromonas* (6 OTUs, 18 reads) and *Spumella* (1 OTU, 8 reads). Moreover, 21 fungal species were identified (35 OTUs, 6.3%; 531 reads). *Protista* were represented by 73 OTUs (13.2%) and further identified as 23 different genera, whereby the most abundant genus was *Ripella* with a total amount of 28 OTUs and 160,259 reads; a total of 190,531 reads was assigned to *Protista*. Six OTUs (1.1%) were assigned to *Animalia* (1,289 reads, assigned to four different species). In addition, 41 OTUs (7.4%) remained unassigned (579 reads). Overall, the unambiguously identified fraction of contaminating microorganisms in the photobioreactors was 7.7% based on read numbers.

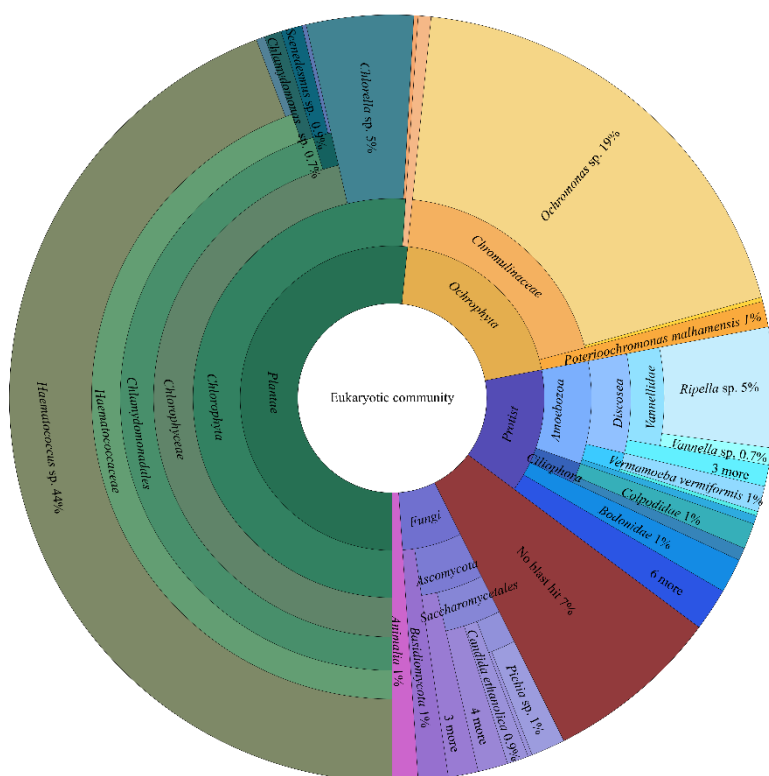


Figure 3.1. Composition of the eukaryotic reactor community in an industrial *Haematococcus* sp. cultivation process. Taxonomic information is based on 18S rRNA gene sequence analyses and assignments within the NCBI database. Each circle represents a different taxonomic rank (innermost circle: kingdom; outermost circle: genus). The percentage represents the relative number of OTUs for each taxonomic group over the whole cultivation process.

Selection of representative microalgae isolates for decontamination experiments

Based on the microbiome analysis of the multi-stage cultivation process, three microalgae isolates were selected that represent the reactor's algae population. The genera *Haematococcus*, *Scenedesmus*, and *Chlorella* together accounted for 93.1% of the reads and 49.7% of the OTUs in the analyzed reactors (Figure 3.2). Manual BLAST searches assigned the representative OTU sequences of abundant (>100 reads) *Haematococcus* hits to two *H. lacustris* entries in the NCBI database (Supplementary Table S3.1).

Table 3.1. Biodiversity in photobioreactors assessed with 18S rRNA gene fragment amplicon sequencing. The community structure of eukaryotic taxa within an industrial scale photobioreactor was assessed with the QIIME 1.9.0 pipeline and BLAST searches within the NCBI nucleotide database.

| | | OTU count | | Read count | |
|---|-------------------------|-----------|----------|------------|----------|
| | | absolute | rel. [%] | absolute | rel. [%] |
| Animalia | <i>Rotifera</i> | 4 | 0.72 | 1,282 | 0.03 |
| | <i>Anthropoda</i> | 1 | 0.18 | 1 | < 0.01 |
| | <i>Chordata</i> | 1 | 0.18 | 1 | < 0.01 |
| 6 OTUs (1.08%) 1,284 reads (0.03%) | | | | | |
| Chromista | <i>Ochrophyta</i> | 113 | 20.40 | 140,545 | 2.88 |
| Fungi | <i>Ascomycota</i> | 28 | 5.05 | 461 | 0.01 |
| | <i>Basidiomycota</i> | 7 | 1.26 | 70 | < 0.01 |
| 148 OTUs (26.71%) 141,076 reads (2.89%) | | | | | |
| Plantae | <i>Chlorophyta</i> | 283 | 51.08 | 4,553,107 | 93.17 |
| | <i>Angiosperm</i> | 2 | 0.36 | 216 | < 0.01 |
| | <i>Streptophyta</i> | 1 | 0.18 | 10 | < 0.01 |
| 268 OTUs (51.62%) 4,553,333 reads (93.18%) | | | | | |
| Protista | <i>Amoebozoa</i> | 46 | 8.30 | 178,377 | 3.65 |
| | <i>Apicomplexa</i> | 1 | 0.18 | 27 | < 0.01 |
| | <i>Ciliophora</i> | 9 | 1.62 | 696 | 0.01 |
| | <i>Euglenophyta</i> | 4 | 0.72 | 1167 | 0.02 |
| | <i>Euglenozoa</i> | 8 | 1.44 | 9,867 | 0.20 |
| | <i>Excavata</i> | 1 | 0.18 | 39 | < 0.01 |
| | <i>Heterokontophyta</i> | 1 | 0.18 | 270 | 0.01 |
| | <i>Perclozoa</i> | 1 | 0.18 | 8 | < 0.01 |
| <i>Rhizaria</i> | 2 | 0.36 | 8 | < 0.01 | |
| 73 OTUs (7.40%) 190,531 reads (3.90%) | | | | | |
| No blast hit | | 41 | 7.40 | 579 | 0.01 |

Representative *Chlorella* sequences for OTUs with the same read threshold were assigned to *C. vulgaris* and two additional *Chlorella* sp. entries. Only one *Scenedesmus* OTU met the read threshold and the representative sequence was assigned to *S. vacuolatus*. Accordingly, reactor isolates assigned to *H. lacustris*, *C. vulgaris*, and *S. vacuolatus* were selected for the decontamination efficiency experiments. The identity of respective isolates was confirmed by Sanger sequencing of 18S rRNA gene fragment.

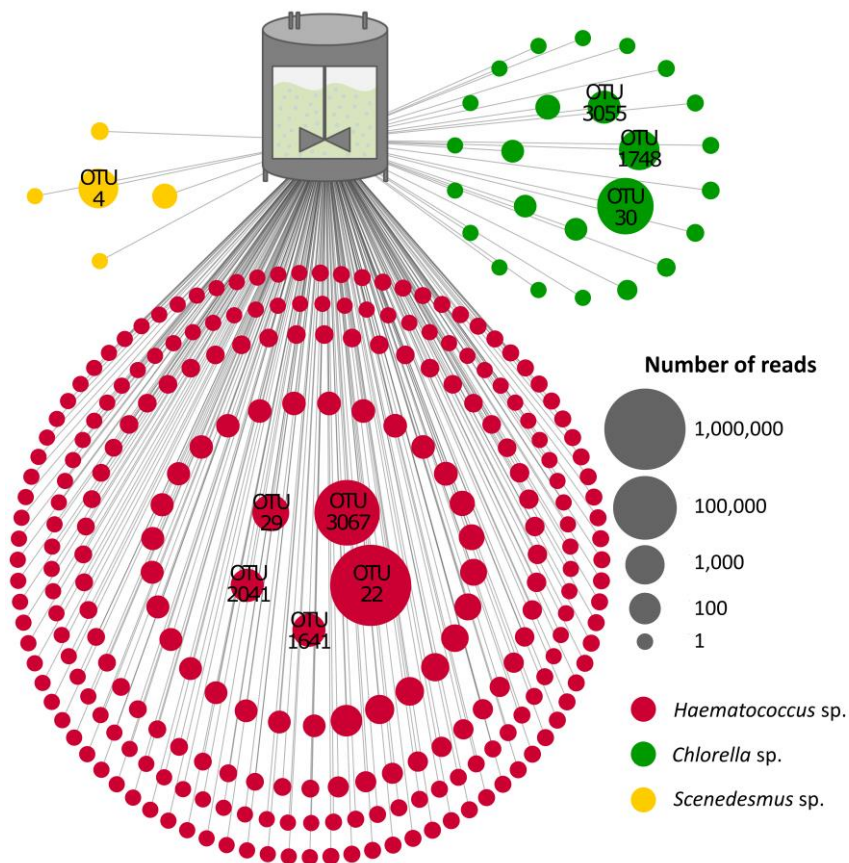


Figure 3.2. Schematic visualization of a dominant microalgae subpopulation in an industrial cultivation process. The pictured OTUs were assigned to *Chlorella* (green), *Haematococcus* (red) and *Scenedesmus* (yellow). Node sizes correspond to the number of reads that was assigned to each OTU. All OTUs with more than 100 reads were labeled and subjected to manual BLAST searches against NCBInt. Taxonomic assignments at species level are included in Table S1.1.

Microalgae treatments with liquid alkylpyrazines

The application of liquid 5-isobutyl-2,3-dimethylpyrazine in microalgae cultures was highly efficient and led to significant reductions of cell viability for all three treated algae species. In case of *S. vacuolatus*, treatments showed mean reduction rates of 98.2% after two hours, 99.0% after four hours, 99.8% after six hours, and 100% after 30 hours of incubation (Figure 3.3a). This was observed

with the lowest tested alkylpyrazine concentration (v/v) of 3.3 $\mu\text{L}/\text{mL}$. Higher pyrazine concentrations of 10.0 $\mu\text{L}/\text{mL}$ and 16.6 $\mu\text{L}/\text{mL}$ led to a reduction rate of 100% after two hours of incubation. For *C. vulgaris* and *H. lacustris* a reduction rate of 100% was already observed after two hours of incubation with each of the tested concentration (3.3 $\mu\text{L}/\text{mL}$, 10.0 $\mu\text{L}/\text{mL}$ and 16.6 $\mu\text{L}/\text{mL}$; Figure 3.3b and 3.3c; Supplementary Table S3.2).

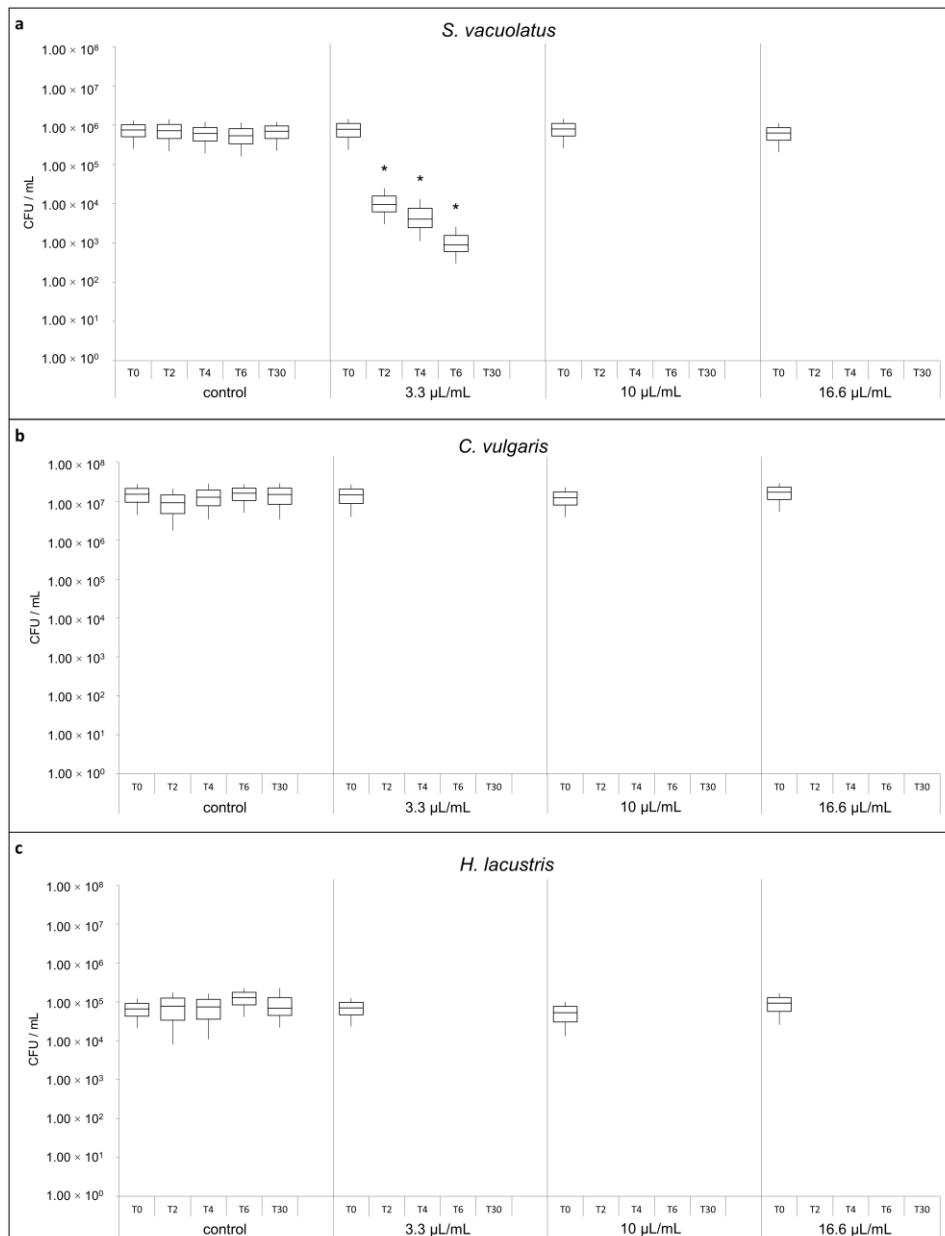


Figure 3.3. Cultivation-based quantification of viable *S. vacuolatus* (a), *C. vulgaris* (b) and *H. lacustris* (c) cells after treatment with liquid pyrazine. Bars represent the number of viable microalgae cells. Samples were treated with different pyrazine concentrations as indicated in the graph and analyzed at different time points; T0: before treatment; T2: after two hours of incubation; T4: after four hours of incubation; T6: after six hours of incubation; T30: after 30 hours of incubation. Asterisks represent significant differences in cell viability as evaluated with Student's paired t-test at $p < 0.01$.

Exposure of microalgae to vaporized alkyipyrazines

The number of viable cells was significantly reduced for all tested microalgae after the desiccation procedure. The average reductions for *C. vulgaris* (20.0%), *H. lacustris* (90.3%) and *S. vacuolatus* (99.8%) were highly dissimilar (Supplementary Table S3.3). Treatment of microalgae with vaporized 5-isobutyl-2,3-dimethylpyrazine resulted in similar reductions as already observed with fluid applications. For *C. vulgaris* which had the highest recovery rate after the dehydration step, a decrease of 100% in CFU was observed. The same reduction rates were achieved when *S. vacuolatus* and *H. lacustris* were treated; after five hours of incubation a reduction rate of 100% in cell viability was observed for all microalgae isolates (Figure 3.4).

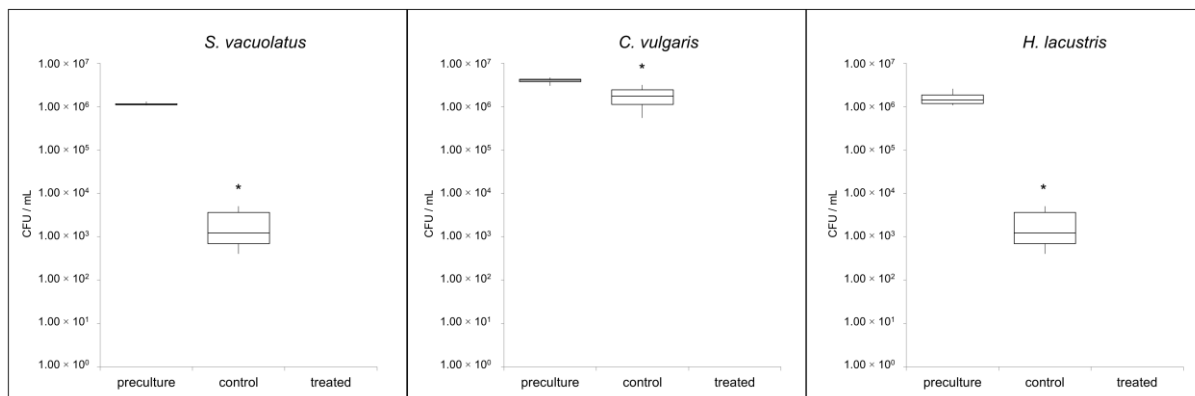


Figure 3.4. Quantification of viable *S. vacuolatus* (a), *C. vulgaris* (b) and *H. lacustris* (c) cells after treatment with vaporized 5-isobutyl-2,3-dimethylpyrazine. Bars represent CFU counts following 5 h of exposure to the alkyipyrazine in sealed flasks. Asterisks represent significant differences in cell viability as evaluated with Student's paired t-test ($p < 0.01$).

Microscopic visualization of the effects

In order to visualize the effects of alkyipyrazine treatments on the representative microalgae isolates, fluid cultures were treated with $1.0 \mu\text{L/mL}$ 5-isobutyl-2,3-dimethylpyrazine for six hours. Microscopic visualization of microalgae cells after treatment showed ruptured cell walls and cell debris in close proximity to algal cytoplasm for all three species (Figure 3.5). Moreover, cells with a seemingly intact cytoplasmic membrane and missing cell wall were frequently observed. Most of the cells were visibly impaired by the application of the biocidal compound as indicated by morphological changes when compared to controls that remained untreated. Other effects beside those on the microalgae's cell walls and cytoplasmic membrane were not observed. The resolution of the obtained micrographs was not sufficient to provide information on changes of intracellular compartments.

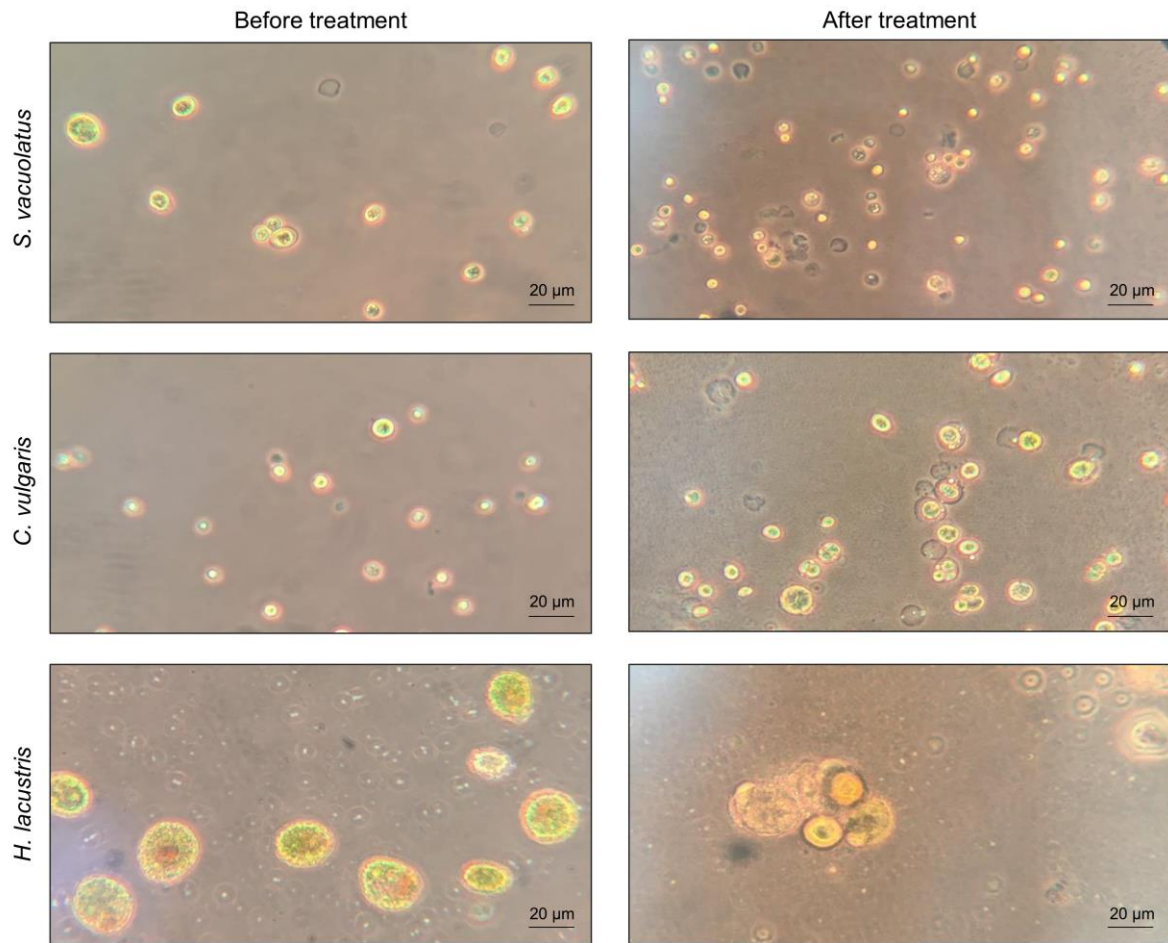


Figure 3.5. Micrographs of microalgae cells before and after treatment in fluid pyrazine solution. The three microalgae isolates were treated for six hours and transferred to microscope slides without any further preparations. For all treatments, the bioactive compound was added in a concentration of 1% (v/v).

Discussion

This is the first study to demonstrate the biocidal effect of alkylpyrazines on different microalgae species. The efficacy assessment was guided by an analysis of the eukaryotic community and included three representative microalgae isolates for a first evaluation of the compound's efficacy towards eukaryotic contaminants. Irrespective of the application form, the viability of the implemented test organisms was drastically reduced. Moreover, we observed a complete removal of the model contaminates when an isolate-specific concentration of the active compound was applied.

In microalgae cultivations both eukaryotic as well as prokaryotic contaminants can substantially affected the fermentation process. In particular, open pond microalgae cultivation systems are highly susceptible to various kinds of contaminations, which can influence the performance of the desired inoculant (Carney and Lane, 2014). Huo and colleagues identified and isolated the wild strain *Scenedesmus* sp. FS as a contaminant from an outdoor *Chlorella zofingiensis* culture. By showing high alkali resistances and possessing the ability to adapt to stresses of environmental changes, the wild strain was able to quickly replace *C. zofingiensis* and occupy an ecological niche in the photobioreactor (Huo *et al.*, 2017). Recent studies also showed that the occurrence of the microalgae *Coelastella* sp. or the co-fermentation of *P. malhamensis* – a member of the phylum *Ochrophyta* – in a microalgae cultivation system can lead to significant biomass yield losses or even the collapse of the main culture (Dawidziuk *et al.*, 2017; Ma *et al.*, 2017). These findings reinforce the need for more efficient decontamination of photobioreactors and microalgae cultivation vessels.

In the present study we assessed the efficacy of a volatile antimicrobial alkylpyrazine derivative on three microalgae species - all members of the phylum *Chlorophyta* - which can affect the productivity of the cultivated species due to specific interactions within the community and/or niche occupation (Huo *et al.*, 2017). One of the isolates (*Haematococcus* sp.) was the cultivated microalgae in the analyzed process, but was still included in the study as model contaminant, because we found a high number of different OTUs for the same genus. This finding indicated genetic variance of the main inoculum, thus differences in the productivity of the inoculated strain are likely.

While algae accounted for more than 93% of the total eukaryotic population, the second most abundant eukaryotic lineage was assigned to *Protista*, in particular *Amoebozoa*. This group of protists is ubiquitously found in the environment, particularly in freshwater bodies and soil, mainly within biofilms. Some members of this group are known to endure desiccation and harsh environmental conditions for up to 20 years (Balczun and Scheid, 2018; Sriram *et al.*, 2008). Insufficient cleaning procedures after cultivations may result in an enrichment and manifestation of these organisms due to their enhanced persistence.

Only microalgae were included in this pilot study; however, foregoing studies suggest a broad applicability of certain alkylpyrazines for decontamination purposes. It was shown that the same compound can be employed to reduce highly complex bacterial communities on hatching eggs (Kusstascher *et al.*, 2017). The applicability of alkylpyrazines for inactivation of eukaryotic contaminants is supported by the findings of the present study. Here, all tested microalgae were highly susceptible to the bioactive compound irrespective of the treatment approach. An incubation of 30 h was required to completely eliminate all tested isolates when the lowest 5-isobutyl-2,3-dimethylpyrazine concentration was applied. This was mainly due to the resistance of the *S. vacuolatus* isolate at lower concentrations of the antimicrobial compound. In a similar context, *Scenedesmus* sp. LXI has been reported to resist Methylisothiazolinone (MIT), a widely used synthetic biocide in water-containing solutions (Wang *et al.*, 2018). Here, the photosynthetic apparatus was damaged by the biocide, but the cell respiration and ATP synthesis remained unaffected. After removal of the biocide, the algae cultures were shown to completely recover. The production of antioxidant enzymes such as superoxide dismutase (SOD) and catalase (CAT) was shown to be crucial for the resistance against MIT-induced damages (Wang *et al.*, 2018). By increasing the synthesis of several antioxidant enzymes and non-enzymatic components like β -carotenes or flavonoids, many algae are able to resist reactive oxygen species (ROS) whose formation is induced by various environmental stresses such as extremes of temperature, high salt concentrations, herbicides or UV-radiation (Mallick and Mohn, 2000). In the present study, increased concentrations and the application of the vaporized pyrazine led to complete elimination of viable cells for all tested microalgae. Notably, the preparation required for vaporization experiments led to decreased CFU counts in the control treatments that likely resulted from the desiccation-stress that the microalgae were exposed to. Gray and colleagues showed that aquatic microalgae belonging to the family *Chlorophyceae* (e.g. *Scenedesmus* sp.) and *Trebuxiophyceae* (e.g. *Chlorella* sp.) can recover from desiccation after one to five days when rehydrated and re-illuminated (Gray *et al.*, 2007). However, the resilience to desiccation differs among different microalgae species (Wieners *et al.*, 2018).

Microscopic observation of microalgae cells frequently showed impaired cell walls and ruptured cells. This is a first indication that pyrazines target the algal cell wall or decrease its stability by direct or indirect interactions. The cell wall composition differs within the employed model species. *Scenedesmus* spp. are known to have pectic layers within their cell wall, which contributes to the stability of the cell wall (Bisalputra and Weier, 1963). The other two species lack this skeletal unit as their cell wall comprises mainly mannose and glucose (Bisalputra and Weier, 1963; Hagen *et al.*, 2002; Loos and Meindl, 1982). The observed tolerance of the *Scenedesmus* isolates against the employed alkylpyrazine is potentially linked to structural characteristics of its cell wall. However, the detailed

mode of action of bioactive alkylpyrazines against microalgae remains to be elucidated in upcoming studies.

Microalgae are often produced for human consumption and subjected to specific regulations related to food safety (Enzing *et al.*, 2014). Non-hazardous decontaminations during the production process could improve the quality of the final products by minimizing the occurrence of toxic compounds. In 2002 the Flavor and Extract Manufacturers Association (FEMA) determined pyrazine derivatives to be generally recognized as safe (GRAS) and are considered safe for human consumption at certain intake levels (Adams *et al.*, 2002). Their evidence is supported by the fact that various foods harbor pyrazine derivatives itself. Especially in vegetables various pyrazines are widely distributed. They occur in trace amounts in numerous plants where they are responsible for the aroma and the characteristic odor of several vegetables (Murray and Whitfield, 1975). Pyrazine derivatives can further be frequently found in bacteria and in insects where they are assumed to be involved in chemical communication between microorganisms (Beck *et al.*, 2003; Bramwell *et al.*, 1969; Buttery *et al.*, 1969; Rybakova *et al.*, 2016; Vander Meer *et al.*, 2010). Currently used disinfectants such as hydrogen peroxide or sodium hypochlorite have not only negative effects on humans, but also on the environment. Thus, microalgae producers would benefit from new, environmental friendly, natural disinfectants in the cultivation process. In order to make the presented method applicable for industrial decontaminations, extended evaluations with more test organisms and larger sample sizes to validate the promising effects will be required. Further developments of the presented decontamination method could provide a highly efficient alternative for conventional treatments of bioreactors.

Supplementary Material

Table S3.1. Closest hits of OTUs represented by more than 100 reads. Reference sequences were aligned with NCBI's standard nucleotide BLAST against the NCBI nucleotide collection database excluding uncultured and environmental sample sequences.

| OTU ID | Closest NCBI hit | Accession number | Identity | Read count |
|----------|---|------------------|----------|------------|
| OTU 22 | <i>Haematococcus lacustris</i> 18S ribosomal RNA gene | KY364700.1 | 99% | 4,367,178 |
| OTU 2041 | <i>Haematococcus lacustris</i> strain KMMCC 1552 18S ribosomal RNA gene | JQ315538.1 | 100% | 143,109 |
| OTU 29 | <i>Haematococcus lacustris</i> 18S ribosomal RNA gene | KY364700.1 | 97% | 713 |
| OTU 3067 | <i>Haematococcus lacustris</i> 18S ribosomal RNA gene | KY364700.1 | 92% | 201 |
| OTU 1641 | <i>Haematococcus lacustris</i> 18S ribosomal RNA gene | KY364700.1 | 99% | 196 |
| OTU 30 | <i>Chlorella vulgaris</i> isolate 18S rRNA small subunit ribosomal RNA gene | MF686452.1 | 100% | 35,252 |
| OTU 1748 | <i>Chlorella</i> sp. ZJU0201 18S ribosomal RNA gene | JX097053.1 | 100% | 2,451 |
| OTU 3055 | <i>Chlorella</i> sp. SAG 222-2a 18S rRNA gene (partial) | FM205857.1 | 100% | 171 |
| OTU 4 | <i>Scenedesmus vacuolatus</i> 18S small subunit rRNA | X56104.1 | 99% | 1,831 |

Table S3.2. CFU/mL counts following treatments in liquid alkylpyrazine solutions. Different incubation times were tested in combination with three distinct pyrazine concentrations. A control without supplementation of the bioactive compound was included for comparisons.

| | time [h] | control [$\times 10^5$ CFU/mL] | 0.33 μ L/mL [$\times 10^5$ CFU/mL] | 1.00 μ L/mL [$\times 10^5$ CFU/mL] | 1.66 μ L/mL [$\times 10^5$ CFU/mL] |
|----------------------|----------|---------------------------------|---|---|---|
| <i>S. vacuolatus</i> | 0 | 2.64 \pm 0.17 | 2.83 \pm 0.37 | 2.93 \pm 0.34 | 2.23 \pm 0.19 |
| | 2 | 2.84 \pm 0.65 | 0.05 \pm 0.03 | 0.00 \pm 0.00 | 0.00 \pm 0.00 |
| | 4 | 2.41 \pm 0.52 | 0.03 \pm 0.02 | 0.00 \pm 0.00 | 0.00 \pm 0.00 |
| | 6 | 2.41 \pm 0.89 | 0.01 \pm 0.00 | 0.00 \pm 0.00 | 0.00 \pm 0.00 |
| | 30 | 2.44 \pm 0.22 | 0.00 \pm 0.00 | 0.00 \pm 0.00 | 0.00 \pm 0.00 |
| <i>C. vulgaris</i> | 0 | 55.3 \pm 8.02 | 53.3 \pm 9.78 | 46.2 \pm 6.67 | 58.3 \pm 2.50 |
| | 2 | 42.3 \pm 19.3 | 0.00 \pm 0.00 | 0.00 \pm 0.00 | 0.00 \pm 0.00 |
| | 4 | 58.1 \pm 22.8 | 0.00 \pm 0.00 | 0.00 \pm 0.00 | 0.00 \pm 0.00 |
| | 6 | 54.8 \pm 2.40 | 0.00 \pm 0.00 | 0.00 \pm 0.00 | 0.00 \pm 0.00 |
| | 30 | 57.9 \pm 16.8 | 0.00 \pm 0.00 | 0.00 \pm 0.00 | 0.00 \pm 0.00 |
| <i>H. lacustris</i> | 0 | 0.24 \pm 0.03 | 0.25 \pm 0.02 | 0.20 \pm 0.05 | 0.33 \pm 0.05 |
| | 2 | 0.34 \pm 0.18 | 0.00 \pm 0.00 | 0.00 \pm 0.00 | 0.00 \pm 0.00 |
| | 4 | 0.32 \pm 0.15 | 0.00 \pm 0.00 | 0.00 \pm 0.00 | 0.00 \pm 0.00 |
| | 6 | 0.45 \pm 0.04 | 0.00 \pm 0.00 | 0.00 \pm 0.00 | 0.00 \pm 0.00 |
| | 30 | 0.48 \pm 0.35 | 0.00 \pm 0.00 | 0.00 \pm 0.00 | 0.00 \pm 0.00 |

Table S3.3. Total CFU/mL counts following the treatment with vaporized 5-isobutyl-2,3-dimethylpyrazine and an incubation time of five hours.

| Organism | Preculture [$\times 10^5$ CFU/mL] | Control [$\times 10^5$ CFU/mL] | Treatment [$\times 10^5$ CFU/mL] |
|----------------------|------------------------------------|---------------------------------|-----------------------------------|
| <i>S. vacuolatus</i> | 57.4 \pm 4.49 | 0.11 \pm 0.09 | 0.00 \pm 0.00 |
| <i>C. vulgaris</i> | 39.6 \pm 7.09 | 31.7 \pm 3.60 | 0.00 \pm 0.00 |
| <i>H. lacustris</i> | 20.5 \pm 5.84 | 4.10 \pm 2.10 | 0.00 \pm 0.00 |

Table S3.4: QIIME scripts used for bioinformatics analyses of the amplicon dataset. For network rendering and diversity analyses, the OTUs were manually identified with nucleotide BLAST searches within the NCBI nucleotide collection database.

| Process step | Script | Pipeline, plugins and parameters |
|--|-----------------------------|---|
| Join reads | join_paired_ends.py | QIIME 1.9.0 (SeqPrep) |
| Remove barcodes from sequences | extract_barcodes.py | QIIME 1.9.0 |
| Assign sequences to samples / Check quality | split_libraries_fastq.py | QIIME 1.9.0 (quality score: 19; phred offset: 33) |
| Identify chimeric sequences | identify_chimeric_seqs.py | QIIME 1.9.0 / usearch61 |
| Remove chimeric sequences | filter_fasta.py | QIIME 1.9.0 |
| Identify OTUs | pick_open_reference_otus.py | QIIME 1.9.0 / UCLUST (97% cutoff level) / DB: SILVA release 119 |
| Compute node and edge table for OTU network | make_otu_network.py | QIIME 1.9.0 |

ADDITIONAL PUBLICATION 1

THE TEA LEAF MICROBIOME SHOWS SPECIFIC RESPONSES TO CHEMICAL PESTICIDES AND BIOCONTROL APPLICATIONS

Tomislav Cernava^{1,2,3}, Xiaoyulong Chen^{1,3*}, Lisa Krug², Haoxi Li^{1,3}, Maofa Yang^{1,3}, Gabriele Berg²

¹College of Tobacco Science, Guizhou University, 550025, Guiyang, China

²Institute of Environmental Biotechnology, Graz University of Technology, Petersgasse 12, A -8010 Graz

³Guizhou Provincial Key Laboratory for Agricultural Pest Management of the Mountainous Region, 550025, Guiyang, China

Abstract

The plant microbiome is known to be influenced by certain biotic as well as abiotic factors. Nevertheless, the drivers for specific changes in microbial community composition and structure are largely unknown. In the present study, the effects of chemical and biological treatments for plant protection on the indigenous microbiome of *Camellia sinensis* (L.) Kuntze were contrasted. Assessment of bacteria-specific ribosomal RNA gene fragment amplicons from a representative set of samples showed an increased microbial diversity in treated plants when compared to untreated samples. Moreover, distinct microbial fingerprints were found for plants subjected to a conventional pesticide treatment with lime sulphur as well as for plants that were biologically treated with a *Piriformospora indica* spore solution. The bacterial community of pesticide-treated plants was augmented by 11 taxa assigned to *Proteobacteria* and *Actinobacteria*. In contrast, plants from biological control treatments were augmented by 10 taxa representing a more diversified community enrichment and included members of *Actinobacteria*, *Proteobacteria*, *Bacteroidetes*, *Planctomycetes*, and *Verrucomicrobia*. Complementary, molecular quantification of fungi in the samples showed a significantly lower number of internal transcribed spacer copies in plants subjected to biological control treatments, indicating the highest efficiency against fungal pathogens. The overall results show that leaves that are used for tea production show distinct microbiome shifts that are elicited by common pest and pathogen management practices. These shifts in the microbial population indicate non-target effects of the applied treatments.

Published in "Science of the Total Environment"

ADDITIONAL PUBLICATION 2

NICOTIANA TABACUM SEED ENDOPHYTES SHARE A COMMON CORE STRUCTURE AND GENOTYPE-SPECIFIC SIGNATURES IN DIVERGING CULTIVARS FROM ASIA AND THE AMERICAS

Xiaoyulong Chen^{1,2}, Lisa Krug³, Hong Yang^{1,2}, Haoxi Li^{1,2}, Baoyu He¹, Maofa Yang^{1,2}, Gabriele Berg³, and Tomislav Cernava^{1,2,3}

¹College of Tobacco Science, Guizhou University, 550025, Guiyang, China

²Guizhou Provincial Key Laboratory for Agricultural Pest Management of the Mountainous Region, 550025, Guiyang, China

³Institute of Environmental Biotechnology, Graz University of Technology, Petersgasse 12, A -8010 Graz

Abstract

Seed endophytes of crop plants have recently received increased attention due to their implications in plant health and the potential to be included in agro-biotechnological applications. While previous studies indicated that plants from the *Solanaceae* family harbor a highly diverse seed microbiome, genotype-specific effects on the community composition and structure remained largely unexplored. The present study revealed *Enterobacteriaceae*-dominated seed-endophytic communities in four *Nicotiana tabacum* L. cultivars originating from Brazil, China, and the USA. When the dissimilarity of bacterial communities was assessed, none of the cultivars showed significant differences in microbial community composition. Various unusual endophyte signatures were represented by *Spirochaetaceae* family members and the genera *Mycobacterium*, *Clostridium*, and *Staphylococcus*. The bacterial fraction shared by all cultivars was dominated by members of the phyla *Proteobacteria* and *Firmicutes*. In total, 29 OTUs were present in all investigated cultivars and accounted for 65.5% of the combined core microbiome reads. Cultivars from the same breeding line were shown to share a higher number of common OTUs than more distant lines. Moreover, the Chinese cultivar Yunyan 87 contained the highest number (33 taxa) of unique signatures. Our results indicate that a distinct proportion of the seed microbiome of *N. tabacum* remained unaffected by breeding approaches of the last century, while a substantial proportion co-diverged with the plant genotype. Moreover, they provide the basis to identify plant-specific endophytes that could be addressed for upcoming biotechnological approaches in agriculture.

Submitted to "Computational and Structural Biotechnology Journal"

REFERENCES

- Abell, G.C.J., and Bowman, J.P. (2005). Colonization and community dynamics of class *Flavobacteria* on diatom detritus in experimental mesocosms based on Southern Ocean seawater. *FEMS Microbiol. Ecol.* *53*, 379–391.
- Adam, E., Müller, H., Erlacher, A., and Berg, G. (2016). Complete genome sequences of the *Serratia plymuthica* strains 3Rp8 and 3Re4-18, two rhizosphere bacteria with antagonistic activity towards fungal phytopathogens and plant growth promoting abilities. *Stand. Genomic Sci.* *11*, 61.
- Adams, T.B., Doull, J., Feron, V.J., Goodman, J.I., Marnett, L.J., Munro, I.C., Newberne, P.M., Portoghese, P.S., Smith, R.L., Waddell, W.J., et al. (2002). The FEMA GRAS assessment of pyrazine derivatives used as flavor ingredients. Flavor and Extract Manufacturers Association. *Food Chem. Toxicol. Int. J. Publ. Br. Ind. Biol. Res. Assoc.* *40*, 429–451.
- Afi, L., Metzger, P., Largeau, C., Connan, J., Berkloff, C., and Rousseau, B. (1996). Bacterial degradation of green microalgae: incubation of *Chlorella emersonii* and *Chlorella vulgaris* with *Pseudomonas oleovorans* and *Flavobacterium aquatile*. *Org. Geochem.* *25*, 117–130.
- Aichner, M., Oberauner, L., Liebminger, S., Fürnkranz, M., Klein, T., Khinast, J., and Berg, G. (2013). Volatile organic compounds from bacterial antagonists for controlling microbial growth.
- Altschul, S.F., Gish, W., Miller, W., Myers, E.W., and Lipman, D.J. (1990). Basic local alignment search tool. *J. Mol. Biol.* *215*, 403–410.
- Amaral-Zettler, L.A., McCliment, E.A., Ducklow, H.W., and Huse, S.M. (2009). A Method for Studying Protistan Diversity Using Massively Parallel Sequencing of V9 Hypervariable Regions of Small-Subunit Ribosomal RNA Genes. *PLOS ONE* *4*, e6372.
- Amavizca, E., Bashan, Y., Ryu, C.-M., Farag, M.A., Bebout, B.M., and de-Bashan, L.E. (2017). Enhanced performance of the microalga *Chlorella sorokiniana* remotely induced by the plant growth-promoting bacteria *Azospirillum brasilense* and *Bacillus pumilus*. *Sci. Rep.* *7*, 41310.
- Amin, S.A., Green, D.H., Hart, M.C., Küpper, F.C., Sunda, W.G., and Carrano, C.J. (2009). Photolysis of iron–siderophore chelates promotes bacterial–algal mutualism. *Proc. Natl. Acad. Sci.* *106*, 17071–17076.
- Amin, S.A., Parker, M.S., and Armbrust, E.V. (2012a). Interactions between Diatoms and Bacteria. *Microbiol. Mol. Biol. Rev. MMBR* *76*, 667–684.
- Amin, S.A., Green, D.H., Gärdes, A., Romano, A., Trimble, L., and Carrano, C.J. (2012b). Siderophore-mediated iron uptake in two clades of *Marinobacter* spp. associated with phytoplankton: the role of light. *Biometals Int. J. Role Met. Ions Biol. Biochem. Med.* *25*, 181–192.

- Amin, S.A., Hmelo, L.R., van Tol, H.M., Durham, B.P., Carlson, L.T., Heal, K.R., Morales, R.L., Berthiaume, C.T., Parker, M.S., Djunaedi, B., et al. (2015). Interaction and signalling between a cosmopolitan phytoplankton and associated bacteria. *Nature* **522**, 98–101.
- Anesio, A.M., and Laybourn-Parry, J. (2012). Glaciers and ice sheets as a biome. *Trends Ecol. Evol.* **27**, 219–225.
- Arndt, D., Xia, J., Liu, Y., Zhou, Y., Guo, A.C., Cruz, J.A., Snelnikov, I., Budwill, K., Nesbø, C.L., and Wishart, D.S. (2012). METAGENassist: a comprehensive web server for comparative metagenomics. *Nucleic Acids Res.* **40**, W88–95.
- Arora, M., Anil, A., Delany, J., Rajarajan, N., Emami, K., and Mesbahi, E. (2012). Carbohydrate-degrading bacteria closely associated with *Tetraselmis indica*: influence on algal growth. *Aquat. Biol.* **15**, 61–71.
- Atkin, C.L., Neilands, J.B., and Phaff, H.J. (1970). Rhodotorulic Acid from Species of *Leucosporidium*, *Rhodospiridium*, *Rhodotorula*, *Sporidiobolus*, and *Sporobolomyces*, and a New Alanine-Containing Ferrichrome from *Cryptococcus melibiosum*. *J. Bacteriol.* **103**, 722–733.
- Aziz, R.K., Bartels, D., Best, A.A., DeJongh, M., Disz, T., Edwards, R.A., Formsma, K., Gerdes, S., Glass, E.M., Kubal, M., et al. (2008). The RAST Server: rapid annotations using subsystems technology. *BMC Genomics* **9**, 75.
- Bajguz, A., and Piotrowska-Niczyporuk, A. (2014). Interactive effect of brassinosteroids and cytokinins on growth, chlorophyll, monosaccharide and protein content in the green alga *Chlorella vulgaris* (*Trebouxiophyceae*). *Plant Physiol. Biochem. PPB* **80**, 176–183.
- Balczun, C., and Scheid, P.L. (2018). Lyophilisation as a simple and safe method for long-term storage of free-living amoebae at ambient temperature. *Parasitol. Res.* **117**, 3333–3336.
- Bankevich, A., Nurk, S., Antipov, D., Gurevich, A.A., Dvorkin, M., Kulikov, A.S., Lesin, V.M., Nikolenko, S.I., Pham, S., Prjibelski, A.D., et al. (2012). SPAdes: a new genome assembly algorithm and its applications to single-cell sequencing. *J. Comput. Biol. J. Comput. Mol. Cell Biol.* **19**, 455–477.
- Bao, E., Jiang, T., and Girke, T. (2014). AlignGraph: algorithm for secondary de novo genome assembly guided by closely related references. *Bioinforma. Oxf. Engl.* **30**, i319–i328.
- Barberán, A., Bates, S.T., Casamayor, E.O., and Fierer, N. (2012). Using network analysis to explore co-occurrence patterns in soil microbial communities. *ISME J.* **6**, 343–351.
- de-Bashan, L.E., and Bashan, Y. (2010). Immobilized microalgae for removing pollutants: review of practical aspects. *Bioresour. Technol.* **101**, 1611–1627.
- de-Bashan, L., Antoun, H., and Bashan, Y. (2008). Involvement of indole-3-acetic acid produced by the growth-promoting bacterium *Azospirillum* spp. In promoting growth of *Chlorella vulgaris*. *J. Phycol.* **44**, 938–947.
- Beck, H.C., Hansen, A.M., and Lauritsen, F.R. (2003). Novel pyrazine metabolites found in polymyxin biosynthesis by *Paenibacillus polymyxa*. *FEMS Microbiol. Lett.* **220**, 67–73.
- Benemann, J.R., and Oswald, W.J. (1996). Systems and economic analysis of microalgae ponds for conversion of CO₂ to biomass. Final report (California Univ., Berkeley, CA (United States). Dept. of Civil Engineering).

- Berg, G. (2009). Plant–microbe interactions promoting plant growth and health: perspectives for controlled use of microorganisms in agriculture. *Appl. Microbiol. Biotechnol.* *84*, 11–18.
- Berg, G., Zachow, C., Müller, H., Philipps, J., and Tilcher, R. (2013). Next-Generation Bio-Products Sowing the Seeds of Success for Sustainable Agriculture. *Agronomy* *3*, 648–656.
- Berg, G., Rybakova, D., Grube, M., and Köberl, M. (2016). The plant microbiome explored: implications for experimental botany. *J. Exp. Bot.* *67*, 995–1002.
- Berg, G., Köberl, M., Rybakova, D., Müller, H., Grosch, R., and Smalla, K. (2017). Plant microbial diversity is suggested as the key to future biocontrol and health trends. *FEMS Microbiol. Ecol.* *93*.
- Bidigare, R.R., Ondrusek, M.E., Kennicutt, M.C., Iturriaga, R., Harvey, H.R., Hoham, R.W., and Macko, S.A. (1993). Evidence a Photoprotective for Secondary Carotenoids of Snow Algae1. *J. Phycol.* *29*, 427–434.
- Bínová, J., Tichý, V., Lívanský, K., and Zahradník, J. (1998). Bacterial contamination of microalgal biomass during outdoor production and downstream processing. *Algol. Stud. Für Hydrobiol. Suppl. Vol.* *151–158*.
- Bisalputra, T., and Weier, T.E. (1963). The Cell Wall of *Scenedesmus quadricauda*. *Am. J. Bot.* *50*, 1011.
- Bold, H.C. (1949). The Morphology of *Chlamydomonas chlamydogama*, Sp. Nov. *Bull. Torrey Bot. Club* *76*, 101–108.
- Borowitzka, M.A. (2013). High-value products from microalgae—their development and commercialisation. *J. Appl. Phycol.* *25*, 743–756.
- Bramwell, F.A., Burrell, K.J.W., and Riezebos, G. (1969). Characterisation of pyrazines in Galbanum oil. | Article Information | J-GLOBAL. *Tetrahedron Lett* *3215–3216*.
- Brennan, L., and Owende, P. (2010). Biofuels from microalgae—A review of technologies for production, processing, and extractions of biofuels and co-products. *Renew. Sustain. Energy Rev.* *14*, 557–577.
- Brown, S.P., Olson, B.J.S.C., and Jumpponen, A. (2015). Fungi and Algae Co-Occur in Snow: An Issue of Shared Habitat or Algal Facilitation of Heterotrophs? *Arct. Antarct. Alp. Res.* *47*, 729–749.
- Buttery, R.G., Seifert, R.M., Guadagni, D.G., and Ling, L.C. (1969). Characterization of some volatile constituents of bell peppers. *J. Agric. Food Chem.* *17*, 1322–1327.
- Buzzini, P., Branda, E., Goretti, M., and Turchetti, B. (2012). Psychrophilic yeasts from worldwide glacial habitats: diversity, adaptation strategies and biotechnological potential. *FEMS Microbiol. Ecol.* *82*, 217–241.
- Calatrava, V., Hom, E.F.Y., Llamas, Á., Fernández, E., and Galván, A. (2018). OK, thanks! A new mutualism between *Chlamydomonas* and methylobacteria facilitates growth on amino acids and peptides. *FEMS Microbiol. Lett.* *365*.
- Callahan, B.J., McMurdie, P.J., Rosen, M.J., Han, A.W., Johnson, A.J.A., and Holmes, S.P. (2016). DADA2: High-resolution sample inference from Illumina amplicon data. *Nat. Methods* *13*, 581–583.

- Caporaso, J.G., Kuczynski, J., Stombaugh, J., Bittinger, K., Bushman, F.D., Costello, E.K., Fierer, N., Peña, A.G., Goodrich, J.K., Gordon, J.I., et al. (2010). QIIME allows analysis of high-throughput community sequencing data. *Nat. Methods* 7, 335–336.
- Caporaso, J.G., Lauber, C.L., Walters, W.A., Berg-Lyons, D., Lozupone, C.A., Turnbaugh, P.J., Fierer, N., and Knight, R. (2011). Global patterns of 16S rRNA diversity at a depth of millions of sequences per sample. *Proc. Natl. Acad. Sci.* 108, 4516–4522.
- Carney, L.T., and Lane, T.W. (2014). Parasites in algae mass culture. *Front. Microbiol.* 5.
- Cassat, J.E., and Skaar, E.P. (2013). Iron in Infection and Immunity. *Cell Host Microbe* 13, 509–519.
- Cernava, T., Aschenbrenner, I.A., Grube, M., Liebming, S., and Berg, G. (2015). A novel assay for the detection of bioactive volatiles evaluated by screening of lichen-associated bacteria. *Front. Microbiol.* 6, 398.
- Chisti, Y. (2007). Biodiesel from microalgae. *Biotechnol. Adv.* 25, 294–306.
- Cho, D.-H., Ramanan, R., Heo, J., Lee, J., Kim, B.-H., Oh, H.-M., and Kim, H.-S. (2015). Enhancing microalgal biomass productivity by engineering a microalgal–bacterial community. *Bioresour. Technol.* 175, 578–585.
- Cole, J.J. (1982). Interactions Between Bacteria and Algae in Aquatic Ecosystems. *Annu. Rev. Ecol. Syst.* 13, 291–314.
- Compant, S., Samad, A., Faist, H., and Sessitsch, A. (2019). A review on the plant microbiome: Ecology, functions, and emerging trends in microbial application. *J. Adv. Res.* 19, 29–37.
- Cooper, M.B., and Smith, A.G. (2015). Exploring mutualistic interactions between microalgae and bacteria in the omics age. *Curr. Opin. Plant Biol.* 26, 147–153.
- Cornelis, P., and Matthijs, S. (2002). Diversity of siderophore-mediated iron uptake systems in fluorescent pseudomonads: not only pyoverdines. *Environ. Microbiol.* 4, 787–798.
- Croft, M.T., Lawrence, A.D., Raux-Deery, E., Warren, M.J., and Smith, A.G. (2005). Algae acquire vitamin B12 through a symbiotic relationship with bacteria. *Nature* 438, 90–93.
- Croft, M.T., Warren, M.J., and Smith, A.G. (2006). Algae Need Their Vitamins. *Eukaryot. Cell* 5, 1175–1183.
- Darwin, C. (1915). *Works of Charles Darwin: Journal of researches into the natural history and geology of the countries visited during the voyage of H.M.S. Beagle round the world* (D. Appleton and company).
- Davey, M.P., Norman, L., Sterk, P., Huete-Ortega, M., Bunbury, F., Loh, B.K.W., Stockton, S., Peck, L.S., Convey, P., Newsham, K.K., et al. (2019). Snow algae communities in Antarctica: metabolic and taxonomic composition. *New Phytol.* 222, 1242–1255.
- Dawidziuk, A., Popiel, D., Lubońska, M., Grzebyk, M., Wisniewski, M., and Koczyk, G. (2017). Assessing contamination of microalgal astaxanthin producer *Haematococcus cultures* with high-resolution melting curve analysis. *J. Appl. Genet.* 58, 277–285.
- Edgar, R.C. (2010). Search and clustering orders of magnitude faster than BLAST. *Bioinforma. Oxf. Engl.* 26, 2460–2461.

- Eevers, N., Van Hamme, J.D., Bottos, E.M., Weyens, N., and Vangronsveld, J. (2015). Draft Genome Sequence of *Methylobacterium radiotolerans*, a DDE-Degrading and Plant Growth-Promoting Strain Isolated from *Cucurbita pepo*. *Genome Announc.* *3*.
- Effmert, U., Kalderás, J., Warnke, R., and Piechulla, B. (2012). Volatile mediated interactions between bacteria and fungi in the soil. *J. Chem. Ecol.* *38*, 665–703.
- Eigemann, F., Hilt, S., Salka, I., and Grossart, H.-P. (2013). Bacterial community composition associated with freshwater algae: species specificity vs. dependency on environmental conditions and source community. *FEMS Microbiol. Ecol.* *83*, 650–663.
- Enzing, C., Ploeg, M., Barbosa, M., and Sijtsma, L. (2014). Microalgae-based products for the food and feed sector: an outlook for Europe (Publications Office of the European Union).
- Essén, S.A., Johnsson, A., Bylund, D., Pedersen, K., and Lundström, U.S. (2007). Siderophore production by *Pseudomonas stutzeri* under aerobic and anaerobic conditions. *Appl. Environ. Microbiol.* *73*, 5857–5864.
- Fall, R., and Benson, A.A. (1996). Leaf methanol — the simplest natural product from plants. *Trends Plant Sci.* *1*, 296–301.
- Faust, K., and Raes, J. (2016). CoNet app: inference of biological association networks using Cytoscape. *F1000Research* *5*, 1519.
- Felsenstein, J. (1985). Confidence limits on phylogenies: an approach using the bootstrap. *Evol. Int. J. Org. Evol.* *39*, 783–791.
- Finet, C., and Jaillais, Y. (2012). AUXOLOGY: When auxin meets plant evo-devo. *Dev. Biol.* *369*, 19–31.
- Fu, H., Jiang, P., Zhao, J., and Wu, C. (2018). Comparative Genomics of *Pseudomonas* sp. Strain SI-3 Associated With Macroalga *Ulva prolifera*, the Causative Species for Green Tide in the Yellow Sea. *Front. Microbiol.* *9*, 1458.
- Fulbright, S.P., Robbins-Pianka, A., Berg-Lyons, D., Knight, R., Reardon, K.F., and Chisholm, S.T. (2018). Bacterial community changes in an industrial algae production system. *Algal Res.* *31*, 147–156.
- Fürnkranz, M., Lukesch, B., Müller, H., Huss, H., Grube, M., and Berg, G. (2012). Microbial diversity inside pumpkins: microhabitat-specific communities display a high antagonistic potential against phytopathogens. *Microb. Ecol.* *63*, 418–428.
- Goecke, F., Labes, A., Wiese, J., and Imhoff, J.F. (2010). Chemical interactions between marine macroalgae and bacteria. *Mar. Ecol. Prog. Ser.* *409*, 267–299.
- Goecke, F., Thiel, V., Wiese, J., Labes, A., and Imhoff, J.F. (2013). Algae as an important environment for bacteria – phylogenetic relationships among new bacterial species isolated from algae. *Phycologia* *52*, 14–24.
- Gómez-Pereira, P.R., Schüler, M., Fuchs, B.M., Bennke, C., Teeling, H., Waldmann, J., Richter, M., Barbe, V., Bataille, E., Glöckner, F.O., et al. (2012). Genomic content of uncultured Bacteroidetes from contrasting oceanic provinces in the North Atlantic Ocean. *Environ. Microbiol.* *14*, 52–66.
- Gonzalez, L.E., and Bashan, Y. (2000). Increased Growth of the Microalga *Chlorella vulgaris* when Coimmobilized and Cocultured in Alginate Beads with the Plant-Growth-Promoting Bacterium *Azospirillum brasilense*. *Appl. Environ. Microbiol.* *66*, 1527–1531.

- Gordon, S.A., and Weber, R.P. (1951). Colorimetric Estimation of Indoleacetic Acid. *Plant Physiol.* 26, 192–195.
- Grant, M.A., Kazamia, E., Cicuta, P., and Smith, A.G. (2014). Direct exchange of vitamin B12 is demonstrated by modelling the growth dynamics of algal–bacterial cocultures. *ISME J.* 8, 1418–1427.
- Gray, D.W., Lewis, L.A., and Cardon, Z.G. (2007). Photosynthetic recovery following desiccation of desert green algae (*Chlorophyta*) and their aquatic relatives. *Plant Cell Environ.* 30, 1240–1255.
- Grossart, H.-P., Levold, F., Allgaier, M., Simon, M., and Brinkhoff, T. (2005). Marine diatom species harbour distinct bacterial communities. *Environ. Microbiol.* 7, 860–873.
- Gupta, S., Pawar, S.B., and Pandey, R.A. (2019). Current practices and challenges in using microalgae for treatment of nutrient rich wastewater from agro-based industries. *Sci. Total Environ.* 687, 1107–1126.
- Hagen, C., Siegmund, S., and Braune, W. (2002). Ultrastructural and chemical changes in the cell wall of *Haematococcus pluvialis* (*Volvocales*, *Chlorophyta*) during aplanospore formation. *Eur. J. Phycol.* 37, 217–226.
- Hamilton, T.L., and Havig, J. (2017). Primary productivity of snow algae communities on stratovolcanoes of the Pacific Northwest. *Geobiology* 15, 280–295.
- Hardin, G. (1960). The Competitive Exclusion Principle. *Science* 131, 1292–1297.
- Harding, T., Jungblut, A.D., Lovejoy, C., and Vincent, W.F. (2011). Microbes in High Arctic Snow and Implications for the Cold Biosphere. *Appl. Environ. Microbiol.* 77, 3234–3243.
- Hernandez, J.-P., de-Bashan, L.E., Rodriguez, D.J., Rodriguez, Y., and Bashan, Y. (2009). Growth promotion of the freshwater microalga *Chlorella vulgaris* by the nitrogen-fixing, plant growth-promoting bacterium *Bacillus pumilus* from arid zone soils. *Eur. J. Soil Biol.* 45, 88–93.
- Hom, E.F.Y., Aiyar, P., Schaeme, D., Mittag, M., and Sasso, S. (2015). A Chemical Perspective on Microalgal–Microbial Interactions. *Trends Plant Sci.* 20, 689–693.
- Hopkinson, B.M., and Morel, F.M.M. (2009). The role of siderophores in iron acquisition by photosynthetic marine microorganisms. *BioMetals* 22, 659–669.
- Huo, S., Shang, C., Wang, Z., Zhou, W., Cui, F., Zhu, F., Yuan, Z., and Dong, R. (2017). Outdoor Growth Characterization of an Unknown Microalga Screened from Contaminated *Chlorella* Culture. *BioMed Res. Int.* 2017, 1–7.
- Ignatova, L.V., Brazhnikova, Y.V., Berzhanova, R.Z., and Mukasheva, T.D. (2015). Plant growth-promoting and antifungal activity of yeasts from dark chestnut soil. *Microbiol. Res.* 175, 78–83.
- Jerney, J., and Spilling, K. (2018). Large Scale Cultivation of Microalgae: Open and Closed Systems. *Methods Mol. Biol.* Clifton NJ.
- Johnston, M.D., Lawson, S., and Otter, J.A. (2005). Evaluation of hydrogen peroxide vapour as a method for the decontamination of surfaces contaminated with *Clostridium botulinum* spores. *J. Microbiol. Methods* 60, 403–411.
- Joint, I., Tait, K., Callow, M.E., Callow, J.A., Milton, D., Williams, P., and Cámara, M. (2002). Cell-to-Cell Communication Across the Prokaryote-Eukaryote Boundary. *Science* 298, 1207–1207.

- Katoh, K., and Standley, D.M. (2013). MAFFT Multiple Sequence Alignment Software Version 7: Improvements in Performance and Usability. *Mol. Biol. Evol.* *30*, 772–780.
- Kazamia, E., Aldridge, D.C., and Smith, A.G. (2012a). Synthetic ecology – A way forward for sustainable algal biofuel production? *J. Biotechnol.* *162*, 163–169.
- Kazamia, E., Czesnick, H., Nguyen, T.T.V., Croft, M.T., Sherwood, E., Sasso, S., Hodson, S.J., Warren, M.J., and Smith, A.G. (2012b). Mutualistic interactions between vitamin B12-dependent algae and heterotrophic bacteria exhibit regulation. *Environ. Microbiol.* *14*, 1466–1476.
- Kazamia, E., Riseley, A.S., Howe, C.J., and Smith, A.G. (2014). An Engineered Community Approach for Industrial Cultivation of Microalgae. *Ind. Biotechnol.* *10*, 184–190.
- Khan, M.I., Shin, J.H., and Kim, J.D. (2018). The promising future of microalgae: current status, challenges, and optimization of a sustainable and renewable industry for biofuels, feed, and other products. *Microb. Cell Factories* *17*.
- Kim, B.-H., Ramanan, R., Cho, D.-H., Oh, H.-M., and Kim, H.-S. (2014). Role of *Rhizobium*, a plant growth promoting bacterium, in enhancing algal biomass through mutualistic interaction. *Biomass Bioenergy* *69*, 95–105.
- Kim, J., Lyu, X.M., Lee, J.J.L., Zhao, G., Chin, S.F., Yang, L., and Chen, W.N. (2018). Metabolomics analysis of *Pseudomonas chlororaphis* JK12 algicidal activity under aerobic and micro-aerobic culture condition. *AMB Express* *8*, 131.
- Klapes, N.A., and Vesley, D. (1990). Vapor-phase hydrogen peroxide as a surface decontaminant and sterilant. *Appl. Environ. Microbiol.* *56*, 503–506.
- Kouzuma, A., and Watanabe, K. (2015). Exploring the potential of algae/bacteria interactions. *Curr. Opin. Biotechnol.* *33*, 125–129.
- Krohn-Molt, I., Alawi, M., Förstner, K.U., Wiegandt, A., Burkhardt, L., Indenbirken, D., Thieß, M., Grundhoff, A., Kehr, J., Tholey, A., et al. (2017). Insights into Microalga and Bacteria Interactions of Selected Phycosphere Biofilms Using Metagenomic, Transcriptomic, and Proteomic Approaches. *Front. Microbiol.* *8*.
- Krug, L., Erlacher, A., Berg, G., and Cernava, T. (2019). A novel, nature-based alternative for photobioreactor decontaminations. *Sci. Rep.* *9*, 2864.
- Kumar, S., Stecher, G., Li, M., Nnyaz, C., and Tamura, K. (2018). MEGA X: Molecular Evolutionary Genetics Analysis across Computing Platforms. *Mol. Biol. Evol.* *35*, 1547–1549.
- Kusstascher, P., Cernava, T., Liebming, S., and Berg, G. (2017). Replacing conventional decontamination of hatching eggs with a natural defense strategy based on antimicrobial, volatile pyrazines. *Sci. Rep.* *7*, 13253.
- Kutschera, U. (2007). Plant-Associated Methylobacteria as Co-Evolved Phytosymbionts. *Plant Signal. Behav.* *2*, 74–78.
- Kwak, M.-J., Jeong, H., Madhaiyan, M., Lee, Y., Sa, T.-M., Oh, T.K., and Kim, J.F. (2014). Genome information of *Methylobacterium oryzae*, a plant-probiotic methylotroph in the phyllosphere. *PLoS One* *9*, e106704.

- Le Chevanton, M., Garnier, M., Bougaran, G., Schreiber, N., Lukomska, E., Bérard, J.-B., Fouilland, E., Bernard, O., and Cadoret, J.-P. (2013). Screening and selection of growth-promoting bacteria for *Dunaliella* cultures. *Algal Res.* *2*, 212–222.
- Letcher, P.M., Lopez, S., Schmieder, R., Lee, P.A., Behnke, C., Powell, M.J., and McBride, R.C. (2013). Characterization of *Amoebophilidium protococcarum*, an Algal Parasite New to the *Cryptomycota* Isolated from an Outdoor Algal Pond Used for the Production of Biofuel. *PLoS ONE* *8*, e56232.
- Levy, J.L., Stauber, J.L., Wakelin, S.A., and Jolley, D.F. (2009). The effect of bacteria on the sensitivity of microalgae to copper in laboratory bioassays. *Chemosphere* *74*, 1266–1274.
- Lian, J., Wijffels, R.H., Smidt, H., and Sipkema, D. (2018). The effect of the algal microbiome on industrial production of microalgae. *Microb. Biotechnol.* *11*, 806–818.
- Liu, J., Qiu, W., and Song, Y. (2016). Stimulatory effect of auxins on the growth and lipid productivity of *Chlorella pyrenoidosa* and *Scenedesmus quadricauda*. *Algal Res.* *18*, 273–280.
- Loos, E., and Meindl, D. (1982). Composition of the cell wall of *Chlorella fusca*. *Planta* *156*, 270–273.
- Lozupone, C., and Knight, R. (2005). UniFrac: a New Phylogenetic Method for Comparing Microbial Communities. *Appl Env. Microbiol* *71*, 8228–8235.
- Lugtenberg, B., and Kamilova, F. (2009). Plant-growth-promoting rhizobacteria. *Annu. Rev. Microbiol.* *63*, 541–556.
- Lundberg, D.S., Yourstone, S., Mieczkowski, P., Jones, C.D., and Dangl, J.L. (2013). Practical innovations for high-throughput amplicon sequencing. *Nat. Methods* *10*, 999–1002.
- Lutz, S., Anesio, A.M., Field, K., and Benning, L.G. (2015). Integrated ‘Omics’, Targeted Metabolite and Single-cell Analyses of Arctic Snow Algae Functionality and Adaptability. *Front. Microbiol.* *6*, 1323.
- Ma, M., Yuan, D., He, Y., Park, M., Gong, Y., and Hu, Q. (2017). Effective control of *Poteroiochromonas malhamensis* in pilot-scale culture of *Chlorella sorokiniana* GT-1 by maintaining CO₂-mediated low culture pH. *Algal Res.* *26*, 436–444.
- Mallick, N., and Mohn, F.H. (2000). Reactive oxygen species: response of algal cells. *J. Plant Physiol.* *157*, 183–193.
- Mata, T.M., Martins, A.A., and Caetano, N.S. (2010). Microalgae for biodiesel production and other applications: A review. *Renew. Sustain. Energy Rev.* *14*, 217–232.
- McClellan, K.H., Winson, M.K., Fish, L., Taylor, A., Chhabra, S.R., Camara, M., Daykin, M., Lamb, J.H., Swift, S., Bycroft, B.W., et al. (1997). Quorum sensing and *Chromobacterium violaceum*: exploitation of violacein production and inhibition for the detection of N-acylhomoserine lactones. *Microbiol. Read. Engl.* *143 (Pt 12)*, 3703–3711.
- Miethke, M., and Marahiel, M.A. (2007). Siderophore-based iron acquisition and pathogen control. *Microbiol. Mol. Biol. Rev. MMBR* *71*, 413–451.
- Miller, M.J. (1989). Syntheses and therapeutic potential of hydroxamic acid based siderophores and analogs. *Chem. Rev.* *89*, 1563–1579.

- Morohoshi, T., Kato, M., Fukamachi, K., Kato, N., and Ikeda, T. (2008). N-Acylhomoserine lactone regulates violacein production in *Chromobacterium violaceum* type strain ATCC 12472. *FEMS Microbiol. Lett.* *279*, 124–130.
- Murray, K.E., and Whitfield, F.B. (1975). The occurrence of 3-alkyl-2-methoxypyrazines in raw vegetables. *J. Sci. Food Agric.* *26*, 973–986.
- Nikolaeva, E.V., Usov, A.I., Sinitsyn, A.P., and Tambiev, A.H. (1999). Degradation of agarophytic red algal cell wall components by new crude enzyme preparations. *J. Appl. Phycol.* *11*, 385.
- Noh, S.Y., Jung, S.W., Kim, B.H., Katano, T., and Han, M.-S. (2017). Algicidal activity of the bacterium, *Pseudomonas fluorescens* SK09, to mitigate *Stephanodiscus hantzschii* (Bacillariophyceae) blooms using field mesocosms. *J. Freshw. Ecol.* *32*, 477–488.
- Ortega, R.A., Mahnert, A., Berg, C., Müller, H., and Berg, G. (2016). The plant is crucial: specific composition and function of the phyllosphere microbiome of indoor ornamentals. *FEMS Microbiol. Ecol.* *92*.
- Overbeek, R., Begley, T., Butler, R.M., Choudhuri, J.V., Chuang, H.-Y., Cohoon, M., de Crécy-Lagard, V., Diaz, N., Disz, T., Edwards, R., et al. (2005). The subsystems approach to genome annotation and its use in the project to annotate 1000 genomes. *Nucleic Acids Res.* *33*, 5691–5702.
- Ozioko, F.U., Chiejina, N.V., and Ogbonna, J.C. (2015). Effect of Some Phytohormones on Growth Characteristics of *Chlorella sorokiniana* IAM-C212 under Photoautotrophic Conditions. *Afr. J. Biotechnol.* *14*, 2367-2376–2376.
- Philippot, L., Raaijmakers, J.M., Lemanceau, P., and van der Putten, W.H. (2013). Going back to the roots: the microbial ecology of the rhizosphere. *Nat. Rev. Microbiol.* *11*, 789–799.
- Plaza, M., Herrero, M., Cifuentes, A., and Ibáñez, E. (2009). Innovative Natural Functional Ingredients from Microalgae. *J. Agric. Food Chem.* *57*, 7159–7170.
- Price, M.N., Dehal, P.S., and Arkin, A.P. (2010). FastTree 2 – Approximately Maximum-Likelihood Trees for Large Alignments. *PLOS ONE* *5*, e9490.
- Pulz, O. (2001). Photobioreactors: production systems for phototrophic microorganisms. *Appl. Microbiol. Biotechnol.* *57*, 287–293.
- Pulz, O., and Gross, W. (2004). Valuable products from biotechnology of microalgae. *Appl. Microbiol. Biotechnol.* *65*, 635–648.
- Quast, C., Pruesse, E., Yilmaz, P., Gerken, J., Schweer, T., Yarza, P., Peplies, J., and Glöckner, F.O. (2013). The SILVA ribosomal RNA gene database project: improved data processing and web-based tools. *Nucleic Acids Res.* *41*, D590–D596.
- Ramanan, R., Kang, Z., Kim, B.-H., Cho, D.-H., Jin, L., Oh, H.-M., and Kim, H.-S. (2015). Phycosphere bacterial diversity in green algae reveals an apparent similarity across habitats. *Algal Res.* *8*, 140–144.
- Reich, K., and Spiegelstein, M. (1964). Fishtoxins in *Ochromonas* (*Chrysomonadina*). *Isr. J. Zool.* *13*, 141–141.
- Remias, D., Lütz-Meindl, U., and Lütz, C. (2005). Photosynthesis, pigments and ultrastructure of the alpine snow alga *Chlamydomonas nivalis*. *Eur. J. Phycol.* *40*, 259–268.

- Remias, D., Jost, S., Boenigk, J., Wastian, J., and Lütz, C. (2013). Hydrurus-related golden algae (*Chrysophyceae*) cause yellow snow in polar summer snowfields. *Phycol. Res.* *61*, 277–285.
- Renuka, N., Guldhe, A., Prasanna, R., Singh, P., and Bux, F. (2018). Microalgae as multi-functional options in modern agriculture: current trends, prospects and challenges. *Biotechnol. Adv.* *36*, 1255–1273.
- Rivas, M.O., Vargas, P., and Riquelme, C.E. (2010). Interactions of *Botryococcus braunii* Cultures with Bacterial Biofilms. *Microb. Ecol.* *60*, 628–635.
- Rognes, T., Flouri, T., Nichols, B., Quince, C., and Mahé, F. (2016). VSEARCH: a versatile open source tool for metagenomics. *PeerJ* *4*, e2584.
- Rooney-Varga, J.N., Giewat, M.W., Savin, M.C., Sood, S., LeGresley, M., and Martin, J.L. (2005). Links between Phytoplankton and Bacterial Community Dynamics in a Coastal Marine Environment. *Microb. Ecol.* *49*, 163–175.
- Ross, S.J. (1819). *A Voyage of Discovery: Made Under the Orders of the Admiralty, in His Majesty's Ships Isabella and Alexander, for the Purpose of Exploring Baffin's Bay, and Inquiring Into the Probability of a North-west Passage* (J. Murray).
- Ruisi, S., Barreca, D., Selbmann, L., Zucconi, L., and Onofri, S. (2007). Fungi in Antarctica. *Rev. Environ. Sci. Biotechnol.* *6*, 127–141.
- Rybakova, D., Cernava, T., Köberl, M., Liebming, S., Shalamzari, M.E., and Berg, G. (2016). Endophytes-assisted biocontrol: novel insights in ecology and the mode of action of *Paenibacillus*. *Plant Soil* *405*, 125–140.
- Rybakova, D., Rack-Wetzlinger, U., Cernava, T., Schaefer, A., Schmuck, M., and Berg, G. (2017). Aerial Warfare: A Volatile Dialogue between the Plant Pathogen *Verticillium longisporum* and Its Antagonist *Paenibacillus polymyxa*. *Front. Plant Sci.* *8*, 1294.
- Saitou, N., and Nei, M. (1987). The neighbor-joining method: a new method for reconstructing phylogenetic trees. *Mol. Biol. Evol.* *4*, 406–425.
- Sapp, M., Schwaderer, A.S., Wiltshire, K.H., Hoppe, H.-G., Gerds, G., and Wichels, A. (2007a). Species-Specific Bacterial Communities in the Phycosphere of Microalgae? *Microb. Ecol.* *53*, 683–699.
- Sapp, M., Wichels, A., and Gerds, G. (2007b). Impacts of Cultivation of Marine Diatoms on the Associated Bacterial Community. *Appl. Environ. Microbiol.* *73*, 3117–3120.
- Schäfer, H., Servais, P., and Muyzer, G. (2000). Successional changes in the genetic diversity of a marine bacterial assemblage during confinement. *Arch. Microbiol.* *173*, 138–145.
- Schöck, M., Liebming, S., Berg, G., and Cernava, T. (2018). First evaluation of alkylpyrazine application as a novel method to decrease microbial contaminations in processed meat products. *AMB Express* *8*, 54.
- Schulz-Bohm, K., Martín-Sánchez, L., and Garbeva, P. (2017). Microbial Volatiles: Small Molecules with an Important Role in Intra- and Inter-Kingdom Interactions. *Front. Microbiol.* *8*.
- Seckbach, J. (2007). *Algae and Cyanobacteria in Extreme Environments* (Springer Science & Business Media).

- Segawa, T., Matsuzaki, R., Takeuchi, N., Akiyoshi, A., Navarro, F., Sugiyama, S., Yonezawa, T., and Mori, H. (2018). Bipolar dispersal of red-snow algae. *Nat. Commun.* *9*, 3094.
- Seymour, J.R., Amin, S.A., Raina, J.-B., and Stocker, R. (2017). Zooming in on the phycosphere: the ecological interface for phytoplankton-bacteria relationships. *Nat. Microbiol.* *2*, 17065.
- Shannon, P., Markiel, A., Ozier, O., Baliga, N.S., Wang, J.T., Ramage, D., Amin, N., Schwikowski, B., and Ideker, T. (2003). Cytoscape: a software environment for integrated models of biomolecular interaction networks. *Genome Res.* *13*, 2498–2504.
- Sharma, P., and Sharma, N. (2017). Industrial and Biotechnological Applications of Algae: A Review. *J. Adv. Plant Biol.* *1*, 01.
- Shurtz, B.K., Wood, B., and Quinn, J.C. (2017). Nutrient resource requirements for large-scale microalgae biofuel production: Multi-pathway evaluation. *Sustain. Energy Technol. Assess.* *19*, 51–58.
- Singh, R.N., and Sharma, S. (2012). Development of suitable photobioreactor for algae production – A review. *Renew. Sustain. Energy Rev.* *16*, 2347–2353.
- Singh, P., Singh, S.M., Tsuji, M., Prasad, G.S., and Hoshino, T. (2014). *Rhodotorula svalbardensis* sp. nov., a novel yeast species isolated from cryoconite holes of Ny-Ålesund, Arctic. *Cryobiology* *68*, 122–128.
- Spolaore, P., Joannis-Cassan, C., Duran, E., and Isambert, A. (2006). Commercial applications of microalgae. *J. Biosci. Bioeng.* *101*, 87–96.
- Spribille, T., Tuovinen, V., Resl, P., Vanderpool, D., Wolinski, H., Aime, M.C., Schneider, K., Stabentheiner, E., Toome-Heller, M., Thor, G., et al. (2016). Basidiomycete yeasts in the cortex of ascomycete macrolichens. *Science* *353*, 488–492.
- Sriram, R., Shoff, M., Booton, G., Fuerst, P., and Visvesvara, G.S. (2008). Survival of *Acanthamoeba* Cysts after Desiccation for More than 20 Years. *J. Clin. Microbiol.* *46*, 4045–4048.
- Stibal, M., Elster, J., Šabacká, M., and Kaštovská, K. (2007). Seasonal and diel changes in photosynthetic activity of the snow alga *Chlamydomonas nivalis* (*Chlorophyceae*) from Svalbard determined by pulse amplitude modulation fluorometry. *FEMS Microbiol. Ecol.* *59*, 265–273.
- Stoeck, T., Bass, D., Nebel, M., Christen, R., Jones, M.D.M., Breiner, H.-W., and Richards, T.A. (2010). Multiple marker parallel tag environmental DNA sequencing reveals a highly complex eukaryotic community in marine anoxic water. *Mol. Ecol.* *19 Suppl 1*, 21–31.
- Tamura, K., Nei, M., and Kumar, S. (2004). Prospects for inferring very large phylogenies by using the neighbor-joining method. *Proc. Natl. Acad. Sci. U. S. A.* *101*, 11030–11035.
- Tanabe, Y., Shitara, T., Kashino, Y., Hara, Y., and Kudoh, S. (2011). Utilizing the Effective Xanthophyll Cycle for Blooming of *Ochromonas smithii* and *O. itoi* (*Chrysophyceae*) on the Snow Surface. *PLOS ONE* *6*, e14690.
- Tani, A., Ogura, Y., Hayashi, T., and Kimbara, K. (2015). Complete Genome Sequence of *Methylobacterium aquaticum* Strain 22A, Isolated from *Racomitrium japonicum* Moss. *Genome Announc.* *3*.

- Terashima, M., Umezawa, K., Mori, S., Kojima, H., and Fukui, M. (2017). Microbial Community Analysis of Colored Snow from an Alpine Snowfield in Northern Japan Reveals the Prevalence of Betaproteobacteria with Snow Algae. *Front. Microbiol.* *8*, 1481.
- Thompson, L.R., Sanders, J.G., McDonald, D., Amir, A., Ladau, J., Locey, K.J., Prill, R.J., Tripathi, A., Gibbons, S.M., Ackermann, G., et al. (2017). A communal catalogue reveals Earth's multiscale microbial diversity. *Nature* *551*, 457–463.
- Ugwu, C.U., Aoyagi, H., and Uchiyama, H. (2008). Photobioreactors for mass cultivation of algae. *Bioresour. Technol.* *99*, 4021–4028.
- Van Dien, S., Marx, C., O'Brien, B., and Lidstrom, M. (2004). Genetic Characterization of the Carotenoid Biosynthetic Pathway in *Methylobacterium extorquens* AM1 and Isolation of a Colorless Mutant. *Appl. Environ. Microbiol.* *69*, 7563–7566.
- Vander Meer, R.K., Preston, C.A., and Choi, M.-Y. (2010). Isolation of a pyrazine alarm pheromone component from the fire ant, *Solenopsis invicta*. *J. Chem. Ecol.* *36*, 163–170.
- Verginer, M., Siegmund, B., Cardinale, M., Müller, H., Choi, Y., Míguez, C.B., Leitner, E., and Berg, G. (2010). Monitoring the plant epiphyte *Methylobacterium extorquens* DSM 21961 by real-time PCR and its influence on the strawberry flavor. *FEMS Microbiol. Ecol.* *74*, 136–145.
- Villa, J.A., Ray, E.E., and Barney, B.M. (2014). *Azotobacter vinelandii* siderophore can provide nitrogen to support the culture of the green algae *Neochloris oleoabundans* and *Scenedesmus* sp. BA032. *FEMS Microbiol. Lett.* *351*, 70–77.
- Wang, B., Lan, C.Q., and Horsman, M. (2012). Closed photobioreactors for production of microalgal biomasses. *Biotechnol. Adv.* *30*, 904–912.
- Wang, H., Zhang, W., Chen, L., Wang, J., and Liu, T. (2013). The contamination and control of biological pollutants in mass cultivation of microalgae. *Bioresour. Technol.* *128*, 745–750.
- Wang, K., Sipilä, T.P., and Overmyer, K. (2016a). The isolation and characterization of resident yeasts from the phylloplane of *Arabidopsis thaliana*. *Sci. Rep.* *6*, 39403.
- Wang, L., Yuan, D., Li, Y., Ma, M., Hu, Q., and Gong, Y. (2016b). Contaminating microzooplankton in outdoor microalgal mass culture systems: An ecological viewpoint. *Algal Res.* *20*, 258–266.
- Wang, S.-B., Hu, Q., Sommerfeld, M., and Chen, F. (2004). Cell wall proteomics of the green alga *Haematococcus pluvialis* (*Chlorophyceae*). *PROTEOMICS* *4*, 692–708.
- Wang, X.-X., Zhang, T.-Y., Dao, G.-H., and Hu, H.-Y. (2018). Tolerance and resistance characteristics of microalgae *Scenedesmus* sp. LX1 to methylisothiazolinone. *Environ. Pollut. Barking Essex* *1987* *241*, 200–211.
- Waters, C.M., and Bassler, B.L. (2005). QUORUM SENSING: Cell-to-Cell Communication in Bacteria. *Annu. Rev. Cell Dev. Biol.* *21*, 319–346.
- Wayama, M., Ota, S., Matsuura, H., Nango, N., Hirata, A., and Kawano, S. (2013). Three-Dimensional Ultrastructural Study of Oil and Astaxanthin Accumulation during Encystment in the Green Alga *Haematococcus pluvialis*. *PLoS ONE* *8*, e53618.
- Werner, P. (2007). *Roter Schnee: oder Die Suche nach dem färbenden Prinzip* (Berlin: De Gruyter Akademie Forschung).

-
- White, T.J., Bruns, T., Lee, S., and Taylor, J. (1990). Amplification and direct sequencing of fungal ribosomal RNA genes for phylogenetics. In *PCR Protocols*, (San Diego: Academic Press), pp. 315–322.
- Wieners, P.C., Mudimu, O., and Bilger, W. (2018). Survey of the occurrence of desiccation-induced quenching of basal fluorescence in 28 species of green microalgae. *Planta* 248, 601–612.
- Wijffels, R.H., and Barbosa, M.J. (2010). An outlook on microalgal biofuels. *Science* 329, 796–799.
- Xie, B., Bishop, S., Stessman, D., Wright, D., Spalding, M.H., and Halverson, L.J. (2013). *Chlamydomonas reinhardtii* thermal tolerance enhancement mediated by a mutualistic interaction with vitamin B12-producing bacteria. *ISME J.* 7, 1544–1555.
- Xin, G., Glawe, D., and Doty, S.L. (2009). Characterization of three endophytic, indole-3-acetic acid-producing yeasts occurring in *Populus* trees. *Mycol. Res.* 113, 973–980.
- Yu, Z., Song, M., Pei, H., Jiang, L., Hou, Q., Nie, C., and Zhang, L. (2017). The effects of combined agricultural phytohormones on the growth, carbon partitioning and cell morphology of two screened algae. *Bioresour. Technol.* 239, 87–96.

CURRICULUM VITAE

CONTACT



e-mail: lisa.krug@gmx.at

SKILLS

ambitious – diligent – stress resistant –
inventive – communicative – flexible –
energetic – determined

LANGUAGES

| | | |
|---------|-----------|--------|
| German | ● ● ● ● ● | native |
| English | ● ● ● ● | B2 |
| Italian | ● ● ● | A2 |

INTERESTS

cooking – hiking – gardening – photography

EXPERIENCE

2014 – 2015

Warehouse worker
Kwizda pharmaceutical trade

2014

Internship
Austrian Agency for Health and Food Safety

EDUCATION

2016 – 2019

Junior Scientist and PhD Candidate

Austrian Centre of Industrial Biotechnology (ACIB); Institute of Environmental Biotechnology, University of Technology Graz

2015 – 2016

Master studies of Biotechnology

University of Technology Graz / Institute of Environmental Biotechnology
Master's Thesis – Microalgae in an industrial-scale process: analyzing the co-microbiome dynamics

2011 – 2015

Baccalaureate studies of Molecular Biology

University of Technology Graz

2003 – 2011

Secondary School

Stiftsgymnasium Admont

1999 – 2003

Elementary School

Volksschule Ardning

LIST OF PUBLICATIONS

Krug L, Erlacher A, Berg G, Cernava T. A novel, nature-based alternative for photobioreactor decontaminations. *Sci Rep.* 2019;9:2864.

Cernava T, Erlacher A, Aschenbrenner IA, **Krug L**, Lassek C, Riedel K, *et al.*, Deciphering functional diversification within the lichen microbiota by meta-omics. *Microbiome.* 2017;5.
doi:10.1186/s40168-017-0303-5.

Cernava T, Chen X, **Krug L**, Li H, Yang M, Berg G. The tea leaf microbiome shows specific responses to chemical pesticides and biocontrol applications. *Sci Total Environ.* 2019;667:33–40.

LIST OF PRESENTATIONS

Krug L: The algal microbiome: structure, biocontrol and biotechnology, 22. Jahrestagung des Arbeitskreises Biologischer Pflanzenschutz, 2019, Bielefeld, Germany

Krug L, Erlacher A, Berg G: The microbiome in spotlight: improving microalgae cultivation processes, esib - European Summit of Industrial Biotechnology, 2017, Graz, Austria

LIST OF POSTERS

Krug L, Cernava T, Erlacher A, Berg G: Harnessing the microalgae microbiome for biotechnology, 5th Theodor Escherich Symposium, 2018, Graz, Austria

Krug L, Cernava T, Berg G: Deciphering microbiome-algae associations on red, green and orange colored snowfields in the Austrian Alps for biotechnology, International Society for Microbial Ecology (ISME), 2018, Leipzig, Germany

Krug L, Erlacher A, Berg G: The microbiome in spotlight: improving microalgae cultivation processes, esib - European Summit of Industrial Biotechnology, 2017, Graz, Austria

Krug L, Erlacher A, Cernava T, Berg G: Profiling and controlling the microbiome of microalgae in mass cultivation processes, 7th Congress of European Microbiologists – FEMS, 2017, Valencia, Spain